GENERATION OF COMPLETE SOURCE SAMPLES FROM THE SLEW SURVEY

IN-89-CR
77023
P-85

NASA Grant NAG5-1746

Semiannual Report No. 1

For the Period 15 August 1991 through 14 February 1992

Principal Investigator
Dr. Jonathan Schachter

February 1992

Prepared for:

National Aeronautics and Space Administration
Goddard Space Flight Center
Greenbelt, Maryland 20771

Smithsonian Institution
Astrophysical Observatory
Cambridge, Massachusetts 02138

The Smithsonian Astrophysical Observatory
is a member of the
Harvard-Smithsonian Center for Astrophysics

The NASA Technical Officer for this grant is Dr. Donald K. West, NASA, Code 684.1, Laboratory for Astronomy and Solar Physics, Space Sciences Directorate, Goddard Space Flight Center, Greenbelt, Maryland 20771.

This report describes the status for the period 15 August 1991 to 14 February 1992 of Astrophysics Data Program contract NAG5–1746 to the Smithsonian Astrophysical Observatory ("Generation of Complete Source Samples from the Slew Survey").

1 Identifications

We had proposed to establish well–defined samples of bright X–ray sources with the *Einstein* Slew Survey, via identifications with optical counterparts. The Slew Survey, which was 44% identified at the outset of the grant, is now 78% identified. These identifications have come from a thorough search of existing X–ray and optical catalogs, SIMBAD, and the NASA Extragalactic Database. For sources not previously known to be X–ray sources, nearly all ($\geq$ 90%) of the proposed identifications are consistent with X–ray to optical flux ratios from the *Einstein* Extended Medium Sensitivity Survey. Only a small amount of optical observing is needed to confirm these identifications, since 80% of the unidentified sources are expected be brighter than $V = 17$.

We have searched radio catalogs (from the 6 cm 87GB and 90GB, the Green Bank 20 cm, and the University of Texas 327 MHz surveys) to find possible BL Lac candidates. These identifications will be confirmed by 22 hours of VLA snapshot observations, which provide ~2 orders of magnitude improvement in radio flux sensitivity over radio catalogs, and few arcsecond positional accuracy. To help find optical counterparts, we have also searched digitized archives (the Hubble Guide Star Catalog, the ROE/NRL UK Schmidt database, and the University of Minnesota POSS plates).

We are developing statistical techniques to separate the correct counterpart from confusing foreground sources. Since X–ray sources are often much bluer than field stars, we are using the MIT/SAO HEAO–A1 $U - B$ plates, and new multiband UBV observations at Las Campanas (with M. Donahue). In a ROSAT AO2 collaboration with J. Truemper of MPE, we obtained positions, fluxes, and hardness ratios for all Slew Survey sources with ROSAT survey counterparts. The factor of 3–10 improvement in positional accuracy over the Slew Survey will greatly aid our identification effort, while the PSPC to IPC flux ratios provide important variability and spectral information.

2 Data Products and Community Interest

Over 100 members of the community have expressed interest in using the Slew Survey data. We continue to receive requests monthly, and have made the Slew Survey data products available in a variety of ways. A CD–ROM issued by SAO (Plummer et al. 1991) contains the full data on the individual photons in the Slew Survey and the aspect solution file for each slew. (The CD–ROM was funded not by this contract, but by the *Einstein* data center grant.) This enables a user to derive fluxes and upper limits for any position on the sky covered by the Slew Survey. The CD–ROM also contains more information on the source detections.

The CD–ROM has also been incorporated into the *Einstein* On-line Service, *einline*, which is accessible via modem or internet. In addition to the CD–ROM, users can search the Slew Survey source list at specified positions directly in *einline*. The Slew Survey source list can also be accessed and searched by the NASA High Energy Astrophysics Archive Research Center (HEASARC). Updated information on the Slew Survey is described in the semiannual HEAO Newsletter, published by the SAO *Einstein* data center.

3 Scholarly Dissemination of Results

The basic techniques used to construct the Slew Survey are given in Elvis et al. 1992 (see attached preprint). This paper also contains a catalog of positions and optical and X–ray identifications. Our ongoing work is studying Slew Survey source samples, and comparing to other existing complete samples. For example, the Slew Survey AGN are 3 magnitudes fainter in M_V than AGN in the Palomar Green Survey (Schachter et al. 1992; see attached). Low–luminosity are thought to be the dominant contributor to the 2 keV X–ray background.

4 Slew Survey Bibliography and Discography

Elvis, M., Plummer, D., Schachter, J., & Fabbiano, G. 1992, ApJS, in press (May issue).

Plummer D., Schachter J., Garcia M., & Elvis M., 1991, CD-ROM issued by Smithsonian Astrophysical Observatory, Cambridge, MA.

Schachter, J. F., Elvis, M., Plummer, D., & Remillard, R. 1992, "Extragalactic Counterparts to *Einstein* Slew Survey Sources," in Proc. X–ray Emission from Active Galactic Nuclei and the Cosmic X–ray Background, in press.

EXTRAGALACTIC COUNTERPARTS TO

Einstein SLEW SURVEY SOURCES

JONATHAN F. SCHACHTER, MARTIN ELVIS, AND DAVID PLUMMER
Harvard–Smithsonian Center for Astrophysics, MS 4
60 Garden St. Cambridge MA 02138, USA

RON REMILLARD
Massachusetts Institute of Technology
Center for Space Research, Room 37–595
Cambridge, MA 02139, USA

Abstract

The *Einstein* Slew Survey consists of 819 bright X–ray sources, of which 636 (or 78%) are identified with counterparts in standard catalogs. We argue for the importance of bright X–ray surveys, and compare the Slew Survey to the ROSAT all–sky survey. Also, we discuss statistical techniques for minimizing confusion in arcminute error circles in digitized data. We describe the 238 Slew Survey AGN, clusters, and BL Lac objects identified to date and their implications for *logN-logS* and source evolution studies.

1 Introduction

1.1 Wanted: a Soft X–ray All–sky Survey

Before the ROSAT all–sky survey (RASS), no all–sky survey in soft X–rays was ever performed. For example, the well–known *Einstein* Extended Medium Survey (Stocke et al. 1992; see also Maccacaro in these proceedings) covers only ~2% of sky. All–sky surveys preferentially detect bright sources, owing to the large observed solid angle and the rarity of bright sources. The lack of survey information means that in the soft X–ray band we paradoxically know more about faint sources than bright ones.

This has hampered our understanding of extragalactic X–ray sources. At present it is necessary to compare Medium Survey results with those of the *HEAO–A2* Piccinotti *et al.* (1982) sample in order to reach AGN with high fluxes and low redshifts. Yet the normalizations of the soft X–ray and hard X–ray *logN-logS* are known to be in disagreement from a *Ginga* fluctuations analysis (Warwick & Stewart 1989).

1.2 Benefits of Soft X–ray Surveys

The steep luminosity function of AGN (meaning emission-line objects only) means that low luminosity AGN (e.g. Seyfert nuclei) are likely to provide a major part of the AGN contribution to the diffuse X-ray background (Schmidt & Green 1986). Yet optical color-selected samples (e.g. the Palomar Bright Quasar Survey; Schmidt & Green 1983) are incomplete at low luminosities ($M_V \geq -23$) because of dilution by host galaxy starlight. New X-ray–selected samples can be far more complete down to significantly lower luminosities ($M_V \sim -18$).

The second most important component in the 2 keV background is thought to be clusters of galaxies. Clusters have recently been observed in X–ray surveys to undergo negative luminosity evolution with redshift, i.e. there appear to be few high–redshift, high L_X clusters in hard X–ray samples (Edge et al. 1990). and the Medium Survey (Henry et al. 1991, preprint). The uniformly selected, unbiased cluster samples of a soft X–ray all–sky survey can be used to compute a luminosity function to compare with existing data.

1.3 IPC Surveys vs. the ROSAT Survey (RASS)

For a decade now X-ray *logN-logS* studies have been dominated by results from the *Einstein* IPC, a well understood instrument studied at the Deep (Primini et al. 1991) and Medium Survey flux limits. The energy range of the ROSAT PSPC is significantly lower than that of *Einstein* so that obscuration, both Galactic and intrinsic, is even more significant; thus, the population of sources *ROSAT* will detect will be biased toward softer spectra. These difficulties will enlarge the ambiguities in explaining the diffuse x-ray background since its spectrum is only well determined at energies well above the ROSAT energy range.

A tremendous effort is going on to identify ROSAT survey sources with optical counterparts. A master list of ~50,000 X–ray sources and positions has been prepared, but identification of all Medium Survey flux limit sources will require, plausibly, several years of optical observing and data analysis (see, for example, Bade in these proceedings). In the interim before the ROSAT survey becomes available, we need a survey to answer the important questions outlined above. For these reasons, we used IPC data to construct an all–sky survey: The *Einstein* Slew Survey (see below). Of course, when the ROSAT all–sky survey is fully identified, it will become a treasure for X–ray astronomy into the 21st century.

Figure 1: Spectrum of the serendipitous $V = 16$ Slew Survey CV 1ES1113+432, obtained at MDM 1.3 m. Shows strong Hα and weaker Hβ.

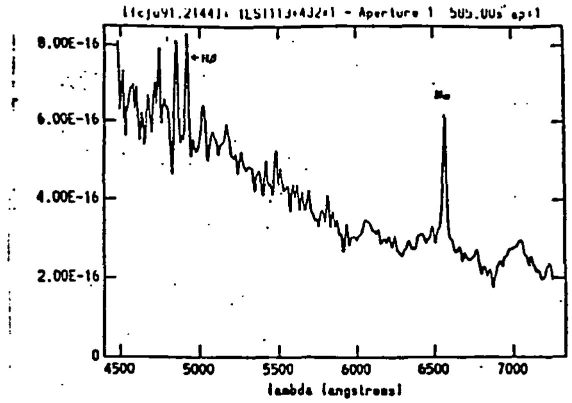

2 The Slew Survey

2.1 Overview and Source List Revisions

The *Einstein* Slew Survey is an all-sky survey constructed from 2799 individual slews of the IPC, and covering 50% of sky at an exposure of 6 s (Elvis et al. 1992). [1] It contains 819 bright soft X-ray sources ($\gtrsim 3 \times 10^{-12}$ erg cm^{-2} s^{-1}, 0.2 – 4.0 keV) with a positional accuracy of 1.2′ (90% confidence radius), of which 317 were not previously known to emit X-rays. The flux limit is ~10–20 times higher than the Medium Survey. All the Slew Survey photon data, useful lists, and software tools are available either on CD–ROM (from the *Einstein* Data Products Office at CfA; email: edpo@cfa.harvard.edu) or via *einline* (telnet zahpod.harvard.edu, or 128.103.40.204; login as "einline").

Sources were detected by a percolation algorithm, which is more efficient than traditional methods (e.g., sliding box) for a spatially sparse data set. For each detection, we calculated a Poisson probability that the distribution of photons is produced randomly (P_{rand}). Initially we adopted $\log P_{rand} = -3.95$ as a threshold, which gave the list of 1067 sources on the CD–ROM. A much lower than expected percentage (60%; expected 80%–90%) of Slew Survey sources with RASS counterparts (with J. Truemper, T. Fleming, and W. Voges) led to a careful Slew Survey data re–analysis. The Slew/RASS comparison also provides important variability and spectral information, as will be detailed in a future paper. We subsequently have rejected as unreliable ~25% of sources, mainly with high P_{rand} and low numbers of counts (3–5; details in Elvis et al. 1992).

2.2 New X–ray Identifications of Catalogued AGN and Clusters

Almost 80% (636) of the Slew Survey sources now have counterparts in standard catalogs, from *positional coincidences only.* There are 136 new identified X–ray sources (catalog counterparts with new Slew X–ray detections), which we have begun confirming via optical observations. We have independently checked the assigned optical counterpart type (e.g. AGN, BL Lac) of the new identified sources by comparing their X-ray to optical flux ratios with those expected from the Medium Survey (Stocke et al 1992). Most (84%) of the proposed counterparts have acceptable values of

[1] Due to the imminent publication of the Slew Survey Ap.J. Supplement paper, we will focus here on results not discussed there.

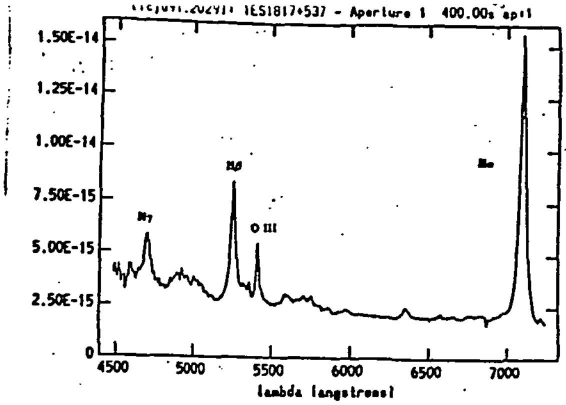

Figure 2: Redshifted MDM 1.3 m spectrum of the serendipitous Slew Survey AGN 1ES1817+537 ($z = 0.08$). Exhibits Balmer emission (Hα, Hβ, Hγ) and weaker O III $\lambda\lambda$4959, 5007.

f_X / f_{opt}; the apparent disagreement for the remainder is may be caused by stars flaring in the Slew Survey, and AGN previously catalogued as normal galaxies.

Spectroscopy at the MDM 1.3 m has confirmed 17 counterparts and ruled out 8 others. The brightest Slew Survey source, at 10 IPC cts s^{-1} (or $\sim 3.26 \times 10^{-10}$ ergs cm^{-2} s^{-1}, 0.2–4.0 keV), is a serendipitous $V = 16$ CV (Figure 1). We also find 2 serendipitous AGN (1ES2137+241 at $z = 0.05$, and 1ES1817+537 at $z = 0.08$; Figure 2), and reclassify the catalogued normal galaxy ESO 509−14 as an AGN ($z = 0.05$). Echelle work by S. Saar at the McMath 2.5 m has discovered stellar activity in bright, previously catalogued normal stars.

There are 124 Slew Survey sources with counterparts in catalogs of AGN, of which 9 are new X-ray sources. We expect to get a total sample of 240–250 AGN when the Slew Survey is fully identified. To date, the highest redshift AGN in the Slew Survey is 4C 71.07 (= S5 0836+710; $z = 2.2$), a ROSAT AO2 PSPC target. The identified Slew Survey AGN to date are compared with the Palomar Bright Quasar Survey sample in Figure 3. Clearly, the Slew Survey can detect sources at least 3 magnitudes fainter in M_V, showing the efficiency of detecting low-luminosity AGN. Plotting the Slew Survey and the Medium Survey AGN on a similar graph (not shown) shows that the two samples can be readily combined to sample a large range of luminosity-redshift space.

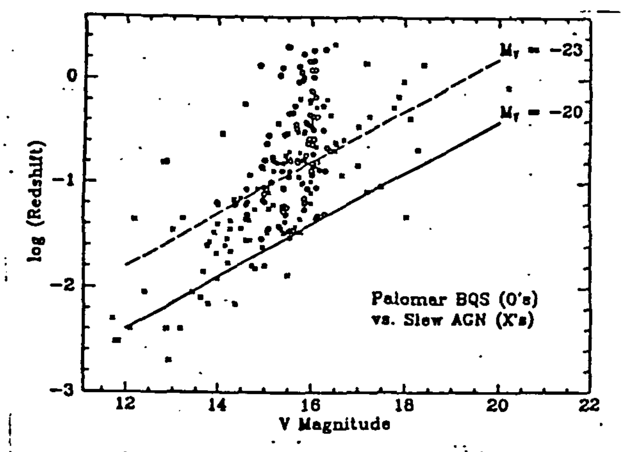

Figure 3: Redshift-V magnitude distribution for the Palomar Bright Quasar Survey (O's), and for identified Slew Survey AGN to date (X's). The broader distribution in V magnitude for the Slew Survey AGN is a consequence of the X-ray selection. The Slew Survey AGN are seen to be intrinsically 3 magnitudes fainter in M_V.

We find 11 new X-ray clusters, of a total of 79 identified clusters; we expect 160–170 clusters in the completely identified Slew Survey. The new X-ray clusters are all high z (or large D), i.e. $z \gtrsim 0.1$, and also high L_X, $\gtrsim 10^45$ ergs s^{-1}. If this trend continues for the entire new X–ray cluster sample, it would contradict the negative evolution found in other surveys, suggesting that the apparent evolution is due instead to selection effects.

3 AGN Identifications from Digitized Plate Data

3.1 Expected Optical Magnitudes

Most of the 183 sources with no counterparts in standard optical catalogs are expected to be relatively bright. Using the known f_X/f_{opt} values and expected source distribution (Stocke et al. 1992), we can divide the sources into 3 groups by expected V-magnitude range: (i) $V \leq 15$. This group, containing 37% of the unidentified sources, is dominated by KM stars. (ii) $15 < V \leq 17$. This group is dominated by AGN with some clusters as well. It accounts for 43% of the unidentified subset. (iii) $17 < V \leq 19$. The smallest of the three groups (20%), this has arguably the most interesting objects—BL Lacs and faint clusters. It is necessary to search digitized plate data to find possible counterparts of these sources.

The digitized plate data we considered are the Hubble Guide Star Catalog (GSC; $m_V \leq 15$), the POSS plates ($m_E \leq 22$, $m_O \leq 21$), and the southern UK Schmidt plates ($m_{B(J)} \leq 22$). We concentrated on the GSC, since 90% of the sources with no counterparts in standard optical catalogs have GSC counterparts. This concentration also reflects issues of timing. As of 1991 October, the POSS plates are in the process of being scanned at the University of Minnesota, while querying the UK Schmidt database is an ongoing project at NRL.

3.2 Likelihood Techniques

To compensate for confusion ($\sim 7 \times 10^2$/sq. deg. at the GSC limit), we calculate the likelihood of a positional coincidence relative to background—the likelihood ratio (e.g., de Ruiter, Willis, & Arp 1977)—using source count estimates (Bahcall & Soneira 1980 and Tyson & Jarvis 1979). We are testing likelihood techniques to identify sources in the Hubble Guide Star Catalog (GSC), using a subset of known identified X–ray sources in the Slew Survey (mainly AGN and stars). Only 50%–60% of the known sources match the GSC (i.e. within 1 mag). Intrinsic source variability, and poor handling in the GSC of extended objects is probably to blame (e.g., Garnavitch 1991). However, we can study the number of known sources which do not match at all as a function of likelihood. From these, a threshold likelihood of 3 was adopted.

Applying the likelihood technique to the GSC, we find 57 new optical identifications of Slew Survey sources The dominant counterpart types are M stars (20, or $\sim$ 35%) and AGN (16), which if confirmed spectroscopically bring the total AGN count to 140. We have begun to apply similar likelihood techniques to 103 digitized UK Schmidt (ROE/NRL) and 20 digitized POSS (U. Minn.) fields.

4 BL Lacs and Future Work

We have identified 32 BL Lacertae objects to date, with 82 expected in the survey when fully identified. In addition, we have isolated 62 possible BL Lacs, from X-ray to optical and optical to radio flux ratios (Stocke et al. 1992). These will be observed in short 3.5 min exposures (to ~0.2 mJy) during a January, 1992 VLA run, where the greatly improved positions will confirm or deny the proposed optical counterparts. We will also search the new southern 6 cm, 25 mJy survey (the PMN survey, currently being reduced; A. Wright, priv. commun.), for BL Lac candidates. Currently, we are studying IRAS to X-ray flux ratios as a way of separating different types of sources (Green, Anderson, & Ward 1992).

To further combat confusion, we have obtained BVR photometry of 17 unidentified Slew Survey fields at the Las Campanas 40" (with M. Donahue of MWLCO). Optical counterparts of X-ray sources are often significantly bluer than field stars and galaxies (e.g., Remillard et al. 1992). We will continue this work in Spring 1992 at the CTIO Curtis-Schmidt.

This work was supported by NASA grant NAG5-1746 (ADP).

5 References

Bahcall, J. N., & Soneira, R. M. 1980, ApJS, 44, 73.

de Ruiter, H. R., Willis, A. G., & Arp, H. C. 1977, AJ, 28, 211.

Edge, A. C., Stewart, G. C., Fabian, A. C., & Arnaud, K. A., 1990, MNRAS, 245, 559.

Elvis, M., Plummer, D., Schachter, J., & Fabbiano, G. 1992, ApJS, in press (April issue).

Green, P.J., Anderson, S.F., & Ward, M.J. 1992, MNRAS, in press.

Garnavitch, P. 1991, Ph.D. Thesis, Univ. of Washington.

Piccinoti et al. 1982, ApJ, 253, 485.

Primini F.A., Murray S.S., Huchra J., Schild R., Burg R., & Giacconi R., 1991, ApJ, 374, 440.

Remillard R., *et al.* 1992, in preparation.

Schmidt M., & Green R.F., 1983, ApJ, 269, 352.

Schmidt M., & Green R.F., 1986, ApJ, 305, 68.

Stocke, J. T., Morris, S. L., Fleming, T. A., & Henry, J. P. 1992, ApJS, in press.

Tyson, J. A. & Jarvis, J. F. 1979, ApJ, 230, L153.

Warwick, R.S., & Stewart, G.C. 1989, in *X-ray Astronomy*, Proc. 23rd ESLAB Symposium, ed. N.E. White (Noordwijk: ESA).

Harvard-Smithsonian
Center for Astrophysics

Preprint Series

No. 3297
(Received September 3, 1991)

THE EINSTEIN SLEW SURVEY

Martin Elvis, David Plummer, Jonathan Schachter, and G. Fabbiano
Harvard-Smithsonian Center for Astrophysics

To appear in
The Astrophysical Journal, Supplement Series
1992

HARVARD COLLEGE OBSERVATORY
Sesquicentennial Year 1989

SMITHSONIAN ASTROPHYSICAL OBSERVATORY
Centennial Year 1990

Center for Astrophysics
Preprint Series No. 3297

The Einstein Slew Survey

Martin Elvis, David Plummer, Jonathan Schachter, G. Fabbiano
Harvard-Smithsonian Center for Astrophysics

To appear in The Astrophysical Journal, Supplement Series, 1992.

Received: 31 May 1991; Accepted: 15 August 1991.

Running Title: The Einstein Slew Survey

ABSTRACT

A catalog of 1075 sources detected in the Einstein IPC Slew Survey of the X-ray sky is presented; 554 of the sources were not previously known as X-ray sources. Typical count rates are 0.1 IPC count/s, roughly equivalent to a flux of 3×10^{-12} $erg\ cm^{-2}\ s^{-1}$. The sources have positional uncertainties of 1.2 arcmin (90% confidence) radius, based on a subset of 452 sources identified with previously known point-like X-ray sources (*i.e.* extent less than 3′).

Identifications based on a number of existing catalogs of X-ray and optical objects are proposed for 689 of the sources, $\frac{2}{3}$ of the survey, (within a 3′ error radius) including 170 identifications of new X-ray sources. A public identification data base for the Slew Survey sources will be maintained at CfA, and contributions to this data base are invited.

Subject headings: surveys – catalogs – X-rays:general – X-rays:stars – quasars:general – BL Lacertae objects:general

1. INTRODUCTION

Sky surveys have always played a major role in astronomy. In the present era in astronomy we are rapidly accumulating new sky surveys across the whole spectrum. The advent of imaging telescopes has made X-ray surveys possible that are comparable in sensitivity to those at other wavelengths. The ***Einstein Observatory*** (Giacconi ***et al.*** 1979a) was the first imaging X-ray astronomy satellite and many papers have reported on surveys of restricted regions of the sky made using pointed observations taken with the Imaging Proportional Counter (IPC, Gorenstein ***et al.*** 1981) on-board ***Einstein***. (The 'Medium Survey' ***e.g.*** Gioia ***et al.*** 1990; the 'Deep Survey' ***e.g.*** Primini ***et al.*** 1991; Table 1). As a result we are in the peculiar position in the soft X-ray band covered by ***Einstein*** (~0.2–3.5 keV), of knowing more about the faint sources than about the bright sources. The limited sky coverage of the Medium and Deep Surveys results in their having effective ***upper*** limits to their sensitivity as well as lower limits since bright sources are rare on the sky (figure 1; table 1). This limitation complicates ***logN-logS*** and source evolution studies (Figure 1) since for bright source counts we have to refer to the hard x-ray surveys, usually to the Piccinotti ***et al.*** (1982) HEAO-A2 survey which covered the 2–10 keV energy band. For example, Schmidt (1990) has emphasized how the Piccinotti ***et al.*** and the Medium Survey source counts are in contradiction for AGN and clusters of galaxies (although evolution may explain these problems, Gioia ***et al.*** 1990). What is needed is a ***logN-logS*** with the same instrument over the whole x-ray flux range. A survey of the bright sources in the soft x-ray range is thus important and only a survey covering most of the sky can find the relatively rare bright sources. A survey using the same instrument as used for the ***Einstein*** Medium and Deep Surveys would greatly simplify interpretation. Samples of bright sources selected uniformly by their X-ray properties are also valuable for follow-up detailed work with other instruments, ***e.g.*** ROSAT, ASTRO-D.

We have constructed a survey of the sky with the ***Einstein*** IPC using the 'Slew' data taken when the satellite was moving ('slewing') from one target to the next. By co-adding all these slews we have achieved a useful sensitivity over a large solid angle, some 50% of the sky. The main properties of the ***Einstein*** IPC Slew Survey are given in table 2. Because it was not clear that this survey could be constructed successfully it was not attempted earlier. The resources needed to process the data were large, making the effort too large for the uncertain payoff. Computer processing power and on-line storage capacity have grown by orders of magnitude in the last few years so that it is now possible for projects of this size to be carried out experimentally by a small team relatively quickly, and thus at low risk. This paper describes the ***Einstein*** Slew Survey and presents the resulting catalog of X-ray sources.

The complete information content of the Slew Survey is more than the source catalog. A CD-ROM issued by SAO (Plummer *et al.* 1991) contains the full data on the individual photons in the Slew Survey and the aspect solution file for each slew. This enables a user to derive fluxes and upper limits for any position on the sky covered by the Slew Survey. The CD-ROM also contains more information on the source detections. (see 'lists/unix/srcs.lis', 'lists/vms/srcs.lis' etc.). The CD-ROM is available from SAO (send requests by e-mail to the *Einstein* Data Products Office, edpo@cfa.harvard.edu), or *via* the Einstein On-Line Information System, *einline* (Harris *et al.* 1991).

2. DATA SELECTION

For the survey we selected all the data taken while the *Einstein* satellite was slewing with the IPC at the focus ('SLEW' mode data- hence the survey name). Only the IPC data is valuable for this survey. Table 3 compares a 'figure of merit' for this type of work for the four focal plane instruments on *Einstein*. The combination of wide field of view, high quantum efficiency, and large fraction of time in the focal plane combine to make the IPC over 100 times more valuable than the next most useful instrument, the HRI. Only slews for which IPC targets lay at each end were used (*i.e.* no instrument changes during the slew). Also only slews in which which data dropouts were small (< 1 major frame, 40.96 s) were included. This gave 2799 useful slews with a total instrument on-time of 1.0 million seconds of data, and 2.6 million photons.

All photon events were accepted: unlike the processing of the pointed data no Sun/Earth angle or pulse height event (PHA) screening was made. Screening proved unnecessary for most of the survey since its purpose is to reduce the background, which is negligible for the short exposures in the Slew Survey. In processing we omitted photons from regions near the IPC 'ribs' (features produced by the window support structure of the IPC, Harnden *et al.* 1984), and near to the edges of the detector. Edge photons are not processed in the standard, pointed, data either.

Figure 2 shows the exposure map for the Slew Survey. The concentration of exposure near the ecliptic poles is clear. This concentration occurs for all Earth-orbiting satellites with fixed solar panels since one axis must point toward the Sun and the satellite lies in the ecliptic plane. The spacecraft is then only free to rotate along arcs of ecliptic longitude. There is lower than average exposure in parts of the Galactic plane, because the IPC was turned off if it was expected to slew across the brightest few sources, and these are concentrated in the Galactic plane. This was a protection against detector gas breakdown that could be induced by too many counts being detected in a small region. The Slew Survey thus has zero exposure on the Crab Nebula. This policy was not always successfully followed and we do have exposure on GX5-1, which was fortunate for our purposes since it allowed a 'proof-of-concept' at an early stage (figure 3).

Figure 4 is an exposure histogram showing the fraction of the sky covered to a given exposure depth. From this, and the ***logN-logS*** of the Medium Survey (Gioia *et al.* 1990) one can predict that the Slew Survey will contain of order 1000 sources, which in fact is a quite accurate prediction.

3. ASPECT SOLUTION

The key to producing a Slew Survey is to solve for the pointing position of the satellite with time as it slews across the sky (the 'aspect' or 'aspect solution'). To determine the *Einstein* aspect during slews it was necessary to use the on-board gyroscope rate data ('gyro data'). The on-board star trackers, which are the primary means of providing the aspect solution for the pointed observations, could not be used since the satellite moved some 5–6 $'$ during a single readout interval (1 minor frame = 0.32 s, the standard minimum read-out interval for a NASA mission), while the star trackers could only follow stars at rates of <2 arcminutes s^{-1} (Koch *et al.* 1978).

At any time during the mission three of the six gyros in the gyro assembly were operating. Each gyro yields a spin rate every minor frame, and the gyros are oriented so that any set of three will give sufficient information to determine rotations about the three spacecraft axes. The existing calibration of the gyro rates to rotation rates was designed only to be accurate enough to bring the spacecraft to a direction where the star trackers, with their $\sim 2°$ field of view, could acquire a field. Accurate pointing depended on the star trackers.

To use the gyros alone for deriving a Slew aspect required that the existing calibration be checked, and modified to give solutions accurate at the arcminute level anywhere during a slew. Two things made this possible: (1) the level of accuracy required is of order 1′—similar to the IPC point spread function—which is some 30 times less demanding than for pointed observations; and (2) enough well-positioned X-ray sources are known which are bright enough to be detected in a single slew. These sources give us an internal check on the quality of our aspect solution on several hundred individual slews, thus allowing a reliable Slew aspect solution to be developed.

Figure 5 shows the initial offsets between the slew derived position and the accurate positions for known X-ray sources in the HEAO-1 A3 (Remillard *et al.* 1991) and pointed IPC catalogs (2E; Harris et al. 1991) detected in individual slews. The coordinates are oriented along and perpendicular to the slew direction. Several features can be seen: There is a concentration of points near the origin, implying that a good fraction of the time the gyro system does give good aspect during slews; this concentration is however offset along the slew direction by ~3–5 ′ ; there is a 'tail' of poorly positioned sources along the slew direction; and there is a 'halo' of poorly positioned sources extending to large distances from the central cluster near the origin.

The offset of the central cluster is due to an ambiguity in the documentation of the timing information. We determined empirically that the aspect data and photon data sent in a single data packet (minor frame) refer to different times: the photon data to the current minor frame and the aspect data to the preceding minor frame. This is negligible in pointed mode but in Slew mode leads to the observed offset.

The 'tail' of poor aspect slews we found to be due to the quality of the pointed aspect at the start of the slew. The 'MAPMODE' star tracker aspect (where the trackers send back the positions of all stars in the field) is not sufficiently reliable (*e.g.* Harris, Stern and Biretta 1990a) and it is essential to go back into the pointed observation until 'LOCKED' star tracker aspect is found. (In LOCKED aspect the tracker records only the position of the chosen guide star.) Errors of a few arcseconds in the starting position extrapolate to large errors when the spacecraft slews through tens of degrees.

The cause of much of the spread seen in figure 5 is seen in figure 6a. This shows the offset perpendicular to the slew direction as a function of position along the slew path. The clear 'bow' shape arises naturally from a displacement of the gyro assembly from its assumed orientation with respect to the spacecraft axes. This offset can be illustrated by imagining a vector rotating 180° within a given plane. This represents the actual rotation of the satellite. Now consider a second vector parallel to the first vector at its original position. Rotate the second vector within a second plane tilted slightly from the first plane such that they intersect along the line of the vectors' original direction. The second vector represents the rotation of the satellite as reported by the displaced gyros. The two vectors will be coincident at the start and end of the 180° rotation, but will be offset in between, reaching a maximum at 90°. The offset at 90° exactly equals the relative offset of the two planes, and therefore the offset of the gyro assembly. By rotating the gyro assembly axes according to the maximum observed offset the 'bow' distortions in the derived positions can be virtually eliminated (figure 6b). A separate set of corrections is needed for each set of gyros which indicates that the rotations are not of the gyro assembly as a whole but of the individual gyros mounted in the assembly. Errors in the assumed gyro orientations of a few arcminutes are entirely negligible for pointed observations. The rotations for each set of gyros were fixed and are given in table 4.

In addition the conversion from gyro spin rate to angular rotation is only calibrated to a level sufficient for pointed operation. In the Slew Survey this conversion is critical, and leads to errors when extrapolating the gyro solution over large slew angles. We calculate the initial offset between the known, star-tracker-derived, pointing position and the gyro-extrapolated position at the end of the each slew. Each offset is measured as a small difference, δ, in R.A., Dec. and Roll angle. Since we measure three δ's and can adjust the scale factors for three gyros there is sufficient information to force this offset to be zero for each slew. The corrections needed are of order $3'$. We used the following procedure: using the initial offsets we guess an appropriate trial scale factor for each gyro in turn. This leads to a change in the three δ's for each of the three gyros. The resulting 3×3 matrix forms a set of simultaneous equations which can be solved to give scale factors for each gyro that will exactly set the δ's to zero. This procedure produces a sufficiently accurate aspect solution, as determined, ***post facto*** by the identification process (see §6). The scale factors, however, are mostly not systematic. This suggests that there is a residual aspect error that could, if corrected, improve the Slew Survey aspect. The solution may lie in treating the orientation of each gyro separately instead of 'rotating' the whole gyro assembly.

Finally slews having scale factor corrections larger than 2% were found to introduce greater errors in position. In very short slews, for example, the aspect became so bad that sources were distorted into smears that were not detected at all. We simply excluded any slews for which we derived scale factor corrections larger than 2% (8.6% of the total), leaving the total of 2799 useful slews.

The offsets of the Slew positions from the accurate positions of known X-ray sources in the HEAO-1 A3 catalog (Remillard ***et al.*** 1991) and the Bright Star Catalog (Hoffleit and Jaschek 1982) for the final set of corrected aspect slews gave the offset diagram seen in figure 7a. The true reliability of the Slew Survey aspect solution is better than is immediately apparent from figure 7a since false identifications produce a significant 'background' at radii $>3'$. Figure 7b shows the distribution of offsets from a false set of Slew Survey sources obtained by shifting all the Slew Survey sources by 1° in R.A. Figure 7c shows a plot of the average background due to false identifications plotted against the radial histogram of figure 7a. Subtracting this background rate implies a 90% confidence radius of order an arcminute for the Slew Survey aspect. Figure 7d shows an integrated histogram with the background subtracted which allows the derivation of confidence radii of the reader's choice. We derive a 90% confidence radius of $1.2'$ and a 95% radius of $3'$from figure 7d.

4. SOURCE DETECTION

The short exposures of the Slew Survey over most of the sky lead to an expectation value of 0.1 photons in a standard 2.4′ square IPC detection cell. Since we expect ~1000 sources over the sky, approximately 99.996% of the 2.58×10^7 detection cells would be empty of sources. The 'sliding box' detection algorithm used for the pointed data (Harnden *et al.* 1984) is thus highly inefficient for the slew survey.

4.1 Percolation Algorithm

Instead we have developed a 'percolation' algorithm that tests each photon for the presence of unusual numbers of near neighbors. Since there are only $\sim 3 \times 10^6$ photons in the survey this takes a factor of ~ 50 fewer operations than the sliding box method. The percolation algorithm is exactly analogous to the method described by Huchra and Geller (1984) for the selection of groups of galaxies from the CfA Redshift Survey (Bright galaxies, like Slew Survey photons, are sparsely distributed on the sky) except that the Slew Survey contains only the two dimensions of R.A. and Dec., and has no equivalent of the redshift dimension. The Slew Survey percolation algorithm loops through every photon in the field and searches for other photons within the percolation length. If another photon is found it is added to the group and subsequently searched for neighbors. The process continues until no more photons lie within a percolation length. Figure 8 describes the process in a flowchart. These groups constitute our candidate sources for the Slew Survey. This algorithm has the advantage of not being biased against extended sources as is a sliding box (by subtracting a source-enhanced background). It does, of course, have a surface brightness limit when the mean distance between source photons exceeds the percolation length. A percolation length of 2′ (~ double the FWHM of the IPC point spread function) produced good results except in regions of high exposure where the background began to become important (see below). All groups detected by the percolation algorithm with fewer than three photons were automatically rejected.

4.2 Exposure Map

It was then necessary to determine which photon groupings constituted significant sources. This significance is highly dependent on the local background and the distribution of exposure time around a source. Figure 9 illustrates some of the difficulties. The contours are iso-exposure levels. Each field covers $30 \times 30'$ and the exposure map has a resolution of 1′. Detailed structure on the few arcminute scale is evident. Because of the random nature of the slew paths there is no predictable structure to the exposure maps. Figure 9 also shows the individual photons in the regions. Each frame is centered on a Slew Survey source which illustrates that the size of the point spread function is comparable with the exposure map structure. It is clear that the detailed exposure distribution in the surrounding region must be calculated in order to compare the background from this region with the number of counts detected in the 'source' region defined by the percolation detect algorithm.

The exposure maps were generated from the aspect solution and the timing gap records ('.tgr' files) for each slew ('HUT'). A template of the relative exposure within the one degree IPC field of view was made including corrections for vignetting and window support features ('ribs', Harnden *et al.* 1984) at the full 8″ resolution of the detector. The vignetting is a radial function which reaches 46% at the midpoint of the side of the IPC; the regions affected by the ribs (which are 4′ wide and roughly 20′ from the center, parallel to the sides, see Harnden *et al.* 1984 for details) are set to zero exposure. This map was then moved across the sky at the rate determined by the aspect solution and effective exposure time assigned to one arcminute square bins on the sky accordingly. For convenience the sky was divided into a set of 6.5° square bins on 6° centers. No exposure was accumulated during times when the detector was off, or data was not received for other reasons (*e.g.* telemetry dropout).

4.3 Source Probabilities

The Poisson probability of a collection of 'source' photons arising by chance inside a source region centered on the percolation centroid can be calculated given a local background. Source counts were derived by taking all counts within a 6′ on a side box centered on the centroid given by the percolation algorithm. Background was estimated from two 'square annuli' of inner side 6′ outer side 12′ and inner side 12′ outer side 30′ (background regions 1 and 2). The mean exposure times in the source and the background regions were derived by averaging the one arcminute bins of the exposure map. In the case where there were no background counts we calculated the probabilities by assuming one background count. Otherwise, we used background region 2 for background subtraction. The probability, P_{rand}, was determined for each candidate source. (On the CD-ROM P_{rand} is called Prob2; Prob1, the same probability using the background region 1, was also calculated and is listed on the CD-ROM.) The values of P_{rand} order the candidate sources according to their likely reality (small probabilities being more likely real). P_{rand} does not by itself tell us which sources to accept. For this we must define a threshold value of P_{rand}.

4.4 Setting the Threshold Probability

Setting a threshold probability for source acceptance is a balance between excluding too many real sources and including too many false sources. We adopted two methods for determining an appropriate threshold. The first predicts the expected number of sources based on Poisson statistics; the second checks the reliability of the sources by the distribution of positional offsets for identifications with optical counterparts.

We can predict the expected number of false sources. We first used the distribution of single photon 'source candidates' since these are the least likely to be real sources. Figure 10 shows a histogram of the number of single photon candidates as a function of P_{rand}. The histogram peaks at a probability of 0.5 where the number of 'source' photons equals the number of background photons, which is the most likely case. (Above a probability of 0.5 our sample will necessarily always be incomplete because the percolation algorithm cannot include candidates with zero counts in the source box.) If the probability calculation is appropriate to the data then we should find that the number of candidate sources drops linearly with probability. We show a straight line of slope 1 in figure 10 which was normalized by setting the area under the line equal to the area under the histogram up to a probability of 0.5. This normalization assures that the line intersects the histogram at $P_{rand} \sim 0.5$. Since the line fits the data well for about four decades in probability we conclude that the Poisson probability is a good description of the data. This is a conservative approach because we are assuming that the percentage of 'true' sources within the total sample is essentially zero, whereas some single photon 'sources' will indeed come from real sources.

We can then use this predicted distribution of false sources with the list of 'candidate sources' (those with three photons or more) to determine the number of false sources as a function of P_{rand}. The histogram of figure 11 shows the number of sources detected as a function of P_{rand}. The solid line was normalized as for the single photon candidate sources to give the same area under the curve as the histogram, up to P_{rand}=0.5. The line then predicts the number of 'false' sources included as a function of P_{rand}. A convenient representation is given in figure 12 which shows the percentage of false sources as a function of the P_{rand} threshold.

We selected a value of $log(P_{rand}) = 3.95$ as our threshold. This criterion yields a list of 1085 prospective sources with 21 false sources expected to be included, $\sim 2\%$ (see figure 12). If the statistics were Gaussian this would correspond to a 3.3σ threshold; but the highly asymmetric nature of the Poisson distribution for such small numbers of counts makes the detections more significant that common experience with 3σ results would suggest.

Figure 11 shows an excess of candidate sources even above our threshold probability, implying the existence of many real sources up to quite high P_{rand}, as one would expect. Some of these sources may be extractable by searching the original Slew Survey data at a predefined set of positions such as those of an optical catalog. This is possible given the software and data on the CD-ROM (Plummer *et al.* 1991).

The source list (see §6) gives the values of P_{rand} for each source so that readers may set more stringent thresholds if they wish. We believe that our visual check (below) has probably removed of order half of the false sources.

An independent check on the level of confidence we can place in the final list of sources is given by the following procedure. We have made identifications of all the candidates against two catalogs of known X-ray sources that have positions known to better than one arcminute– the ***Einstein*** IPC Catalog (2E, Harris *et al.* 1991) and the HEAO-A3 Catalog (Remillard *et al.* 1991). Figure 13 shows the offset of the Slew position from the known position in arcminutes for sources matched in this way, against the probability of the source being a chance congregation of photons, P_{rand} . Extended sources, (clusters of galaxies, supernova remnants and all other IPC sources with 'extent parameter' $> 3'$) were excluded from this comparison.

It is clear from figure 13 that for small probabilities ($P_{rand} < 10^{-6}$) almost all the sources must be real since they are clustered at offsets of order the aspect accuracy derived from individual slews. Similarly at large probabilities ($P_{rand} > 10^{-3}$) there are a great number of false sources since they are distributed nearly uniformly in offset. Our threshold P_{rand} for accepting a candidate source as real is clearly at a level where the fraction of identified sources lying within $2'$ of the optical position begins to decrease rapidly, as one would expect from figure 11 where the fraction of false sources is low (>90%) until $P_{rand} \sim 10^{-4}$, and then rises rapidly.

As a final check, two of us (M. E. and J. S.) visually inspected each of the proposed sources for cases of dubious detections. A total of 10 sources were eliminated in this manner. Of these 8 were rejected because photons from the outer fringes of a bright source caused a spurious second detection; 2 were rejected because the exposure gradients across the region were extreme and an isolated region of high exposure led to a 'source'. A reliability index (1, 2, 3; 3 best) was compiled based on the visual inspection (see §6).

In Figure 14, the fraction of objects within $2'$ of the correct position is plotted against the probability of a source arising by chance. Note that the figure contains an excess of sources near to zero offset even at $P_{rand} > 10^{-3}$ which is consistent with figure 12. This implies that other real sources exist in the data. Searches of the Slew Survey data base at given positions, defined *a priori* by *e.g.* a optical catalog may give significant detections even if no source appears in this catalog. (Since the number of trials is small a lower significance threshold can be used.)

4.5 High Background and Extended Sources

As noted above in regions of high exposure the percolation algorithm did not produce sensible results because the mean distance between background photons became similar to the percolation length. Thus large areas of background were included with sources, leading to large extended 'sources'. This tends to merge sources together and leads to their systematic undercounting in these regions. We dealt with this problem by selecting all sources with a maximum photon distance from the percolation centroid of $> 9'$. We then reran the percolation algorithm with a smaller percolation length, which normally resolved the problem. Figure 15 shows how the galaxies M81 and M82 were initially included in a single source, but were resolved by using a shorter percolation length.

We found that when Probl/Prob2 (defined in §4.3) is large ($> 10^3$) the source is extended, or that there are multiple sources within 15 arcmin. A visual inspection of all cases with Probl/Prob2 $> 10^3$ was made (M. E. and J. S.). For all such sources an 'Image Code' was assigned which notes extended sources larger than $\sim 15'$ (E), regions with multiple sources within $15'$ (M), and sources which are a part of a larger extended source (P). Sources with acceptable Probl/Prob2 are assigned the code 'A'.

Some sources are truly extended on this scale. Each extended source was inspected visually, which we found to be an effective, but unfortunately subjective, means of discriminating real sources from confusion with background. This procedure added 33 sources and improved the positions of 78. A more automatic means of changing the percolation length with the exposure to match the mean free path between background photons needs to be developed. Some few sources have extent of order degrees (*e.g.* the Cygnus Loop, Puppis A). Although these are not included in our source catalog the data is on the CD-ROM. These sources will be treated fully in a later paper (Schachter *et al.* 1991, see also §7).

5. SOURCE PROPERTIES

Having produced a list of reliable sources we need to determine their properties. The IPC gives information on positions, count rates, structure, and pulse height (energy).

The reliability of the positions was established using known X-ray sources, as described above (§3, figure 7c).

Count rates were derived from the $6'$ diameter box used for the probability calculation with background from background region 2 (see §4.3).

For extended sources (*e.g.* clusters of galaxies, supernova remnants, and those labled 'E' in the source table) the count rates will clearly not be accurate. For most of these a better count rate can be derived using the counts and exposure in the 6′-12′ 'square annulus' surrounding the central detection cell (background region 1). This information is available on the CD-ROM version of the Slew Survey (see 'lists/unix/readme.txt', 'lists/vms/readme.txt.' etc.).

The count rates were checked for accuracy by comparing the Slew Survey rates with those derived from the pointed IPC data for sources in common. In figure 16a we plot the Slew Survey count rates as listed in this catalog versus the pointed IPC count rates from the 2E catalog (Harris *et al.* 1991). There is a strong correlation with a slight offset (a factor 1.19) toward higher count rates in the Slew Survey. This is due primarily to our use of all 15 PI bins in the Slew Survey, compared with the standard 2–10 used in pointed data. (The restricted range for pointed data is used to minimize background, which is unnecessary in the Slew Survey.) When we restrict the Slew Survey source count rates to the same PI bins the offset is reduced to a factor 1.03, as shown in figure 16b. The source of this residual offset is still under investigation. The errors on these count rates are non-trivial to determine since both the background and the source counts are not in the Gaussian limit and so do not add in quadrature. The problem of calculating these uncertainties in the Poisson case has recently been investigated by Kraft *et al.* (1991) and we have used their methods with software routines which they kindly supplied to us. (Note that the uncertainties on the CD-ROM assumed Gaussian statistics. Updated values can be obtained using ***einline***, Harris *et al.* 1991)

Several measures of source extent were attempted. Large sources, >9′ diameter, are readily selected using the maximum distance of a source photon from the percolation centroid. Smaller extended sources are clearly seen on the maps but are not so easily characterized. We are continuing a search for an objective means of classifying the size of sources.

The mean pulse height bin for each source was calculated from the photons in the 6′ box. The 'pulse height invariant' (PI) bins were used since they have a first order correction to remove the effects of the variable gain of the IPC (Harnden *et al.* 1984). (This variation changes the mapping of photon energy to pulse height bin.) That an extreme ultraviolet source from the Wide Field Camera on ROSAT (1ES1631+781) has a mean PI bin of 2 (on a scale from 1, low energy, to 15, high energy) shows that the PI data carries useful information.

6. SOURCE LIST

The Slew Survey source catalog contains 1075 sources. [1] Table 5 gives a summary of the identifications made.

6.1 Table of Objects

Table 6 is the Slew Survey source catalog. The identifications suggested in table 6 are discussed in the next section (§7). Table 6 has the following entries:

Column 1: SOURCE NAME. '1ES' stands for first ***Einstein*** Slew Survey source. Coordinate names are based on the B1950.0 position constructed from hours,minutes±degrees,tenths of degrees, truncated according to the IAU convention.

Columns 2 and 3: POSITION. In B1950.0 coordinates, based on the percolation algorithm centroid. Where noted positions have been refined by changing the percolation length as discussed in §4.5. Errors on position are primarily systematic, arising from the aspect solution. A 90% error radius of 1.2′ and a 95% radius of 3.0′ are estimated from figure 7d.

Column 4: COUNT RATE. Mean count rate in all PI bins (1—15). This is on average a factor 1.19 larger than the standard IPC 'broad band' count rate (based on PI channels 2—10) used in the 2E catalog (see §5). Counts are taken from a 6′ on a side box centered on the percolation algorithm centroid. Background counts scaled for exposure and area from a 30′ on a side box (background region 2) have been subtracted. Errors represent a 1 σ confidence interval. When total source plus background in the source box had $\leq$100 counts the error bars are based on a Poisson probability, distribution as computed in Kraft *et al.* (1991), which gives asymmetric error bars. For sources with a larger number of photons a Gaussian approximation was used.

Column 5: NUMBER OF PHOTONS (NP) in the 6′ on a side box and NUMBER OF SLEWS (NS) that contribute photons to the object. Other slews may have passed over the source positions but yielded no photons.

Column 6: PROBABILITY, P_{rand}. Probability of finding the number of photons listed in column 5 relative to background region 2. Small numbers indicate a higher chance that the source is real. Values of $P_{rand} < 1 \times 10^{-10}$ are listed as equal to 1×10^{-10}. A threshold of $log(P_{rand}) = -3.95$ was used to generate the list of accepted sources.

[1]The CD-ROM contains 8 fewer sources due to a software bug which omitted a thin slice of R.A. near 24^h.

Column 7: EXPOSURE. Total Slew Survey exposure time averaged over the $6'$ on a side box used in column 3.

Column 8: MEAN PULSE HEIGHT bin. The average of the 'pulse invariant' (PI, Harnden *et al.* 1984) channel numbers (1–15) for each photon, which coarsely indicates the source spectrum.

Column 9: QUALITY CONTROL INDEX (Q) and IMAGE CODE (I). The Q (1, 2, or 3; 3 being highest quality) value is a visual estimate of the reliability of the source. The IMAGE CODE highlights cases where Prob1/Prob2 (defined in §4.3) is large ($> 10^3$), and which a visual inspection shows to be extended, or to have multiple sources within 15 arcmin (see §4.5). The IMAGE CODE has the following values:
A — Generally acceptable Prob1/Prob2;
E — Extended source ($>$ 15 arcmin);
M — Multiple sources within 15 arcmin;
P — Part of source (extended source existing in more than one field).

Columns 10 and 11: EOSCAT NUMBER, ***Einstein*** MEDIUM SURVEY MEMBERSHIP (noted by m), and OFFSET FROM EOSCAT POSITION (Δ2E). For sources with counterparts in the 2E Catalog (Harris et al. 1991), we provide the EOSCAT number and the difference between the Slew Survey and catalog positions, in arc minutes. In addition, Medium Survey (Gioia *et al.* 1990, Stocke *et al.* 1991) sources are noted with a letter m preceding the EOSCAT number.

Columns 12 and 13: ***HEAO—1*** A3 COUNTERPART, ***EXOSAT*** DETECTIONS (noted by x), and OFFSET FROM HEAO—A3 POSITION (Δ1H). For sources with counterparts in the ***HEAO—1*** A3 catalog (Remillard *et al.*1991), we provide the '1H' name and the difference between the Slew Survey and catalog positions, in arc minutes. In addition, ***EXOSAT*** sources are noted with a letter x preceding the 1H name.

Columns 14—17: OPTICAL CATALOG (Cat.), OBJECT CLASSIFICATION (Class.), COUNTERPART NAME (Name), and OFFSET FROM CATALOG POSITION (ΔC). For sources with counterparts in (mainly) optical catalogs searched to date (see below for catalog list and references), we provide the name of the catalog, the classification (e.g., AGN), the counterpart name, and the difference between the Slew Survey and catalog positions, in arc minutes. If the redshift or stellar spectral type is known, it is listed after the object classification in column 15.

Composite spectral types in table 6 indicate a binary (or other multiple star system). In general, we have tried to use the most common names of objects. For cases in which two objects (most commonly an SAO star and an extragalactic object) were found in the same error box we compared their f_x/f_o ratios with those for the Medium Survey sources (Maccacaro *et al.*1988). In most cases only one of the objects was a plausible counterpart given these ratios. Cases in which more than one object is a likely counterpart are indicated with asterisks, and noted below (§7.3).

If the counterpart name is the same as the Slew name in column 1, and the catalog is well known, only the catalog designator is listed in column 16 (e.g., PG, EXO, 2E). Woolley names with letters A, B, ... indicate multi-star systems (e.g., WLY 127AB). For each of the newly discovered X-ray sources, we list all the names known to us in Table 7.

Abbreviations for names of catalogs are:
2E—Second *Einstein* IPC Catalog ('EOSCAT', Harris *et al.* 1991);
A3—*HEAO—A3* Catalog (Remillard *et al.* 1991);
ABL—Abell Catalog Abell Catalog (1958, Struble and Rood 1987) and Southern Abell Catalog (Abell, Corwin, and Olowin 1989);
BMC—Bradt and McClintock (1983);
BSC—Bright Star Catalog (Hoffleit and Jaschek 1982);
EXO—*EXOSAT* Database of optical and other astronomical catalogs;
GCV—General Catalog of Variable Stars (Kholopov et al. 1985-1988);
HB—Hewitt and Burbidge (1986);
HD—Henry Draper Catalog (Cannon and Pickering 1918–1924);
MCS—McCook and Sion (1986);
MS—*Einstein* Extended Medium Sensitivity Survey (Gioia *et al.* 1990);
RNG—Revised NGC Catalog (Sulentic and Tifft 1973);
WFC—ROSAT Wide Field Camera (Cooke *et al.* 1991);
SAO—SAO Catalog (SAO Staff 1966);
SBD—SIMBAD database;
SHA—Shara (1990);
UGC—Uppsala General Catalogue of Galaxies (Nilsson 1973);
VV—Veron-Cetty and Veron (1987);
WLY—Woolley Catalog (Woolley et al. 1970); [2];
ZCT—CfA Redshift Catalog, Huchra (1990).

Abbreviations for object classification are:
AC—active star,
AGN—active galactic nucleus,
BL—BL Lac object,
CG—cluster of galaxies,

[2]This is an extended version of the Gleise catalog, using the same numbering scheme as Gleise

CV—cataclysmic variable,
GAL—normal galaxy,
P—pulsar,
S—normal star,
SNR—supernova remnant,
WD–white dwarf,
XRB–X-ray binary,
(XRB-Be)—X-ray binary (with Be star secondary).

6.2 Notes On Individual Objects

1ES0013+195: The error box also contains G 32 −7 (S:M4.5), but at $V = 14$ (cf. 13 for G 32 −6) it is an unlikely counterpart based on f_x/f_{opt} (Maccacaro et al. 1984).

1ES0100+405: The stars G132 −51B and G132 −51C are in the error box and have acceptable f_x/f_o ratios, although both (at $V = 13.01$) are 2.2 magnitudes fainter than G 132 −51A.

1ES0120+004: Besides the star, the error box contains MCG +00-04-103, a 16th magnitude galaxy which may be an AGN.

1ES0122+084A and B: Besides the cluster, the error box also includes the galaxy UGC 977, which may be a previously unknown AGN.

1ES0237−531: The error box also contains SAO 232842 (S:K5), which at $V = 8.3$ is 0.9 magnitudes fainter than HD 16699.

1ES0255+128: Besides the cluster, the error box also contains the galaxy UGC 2438, another possible AGN.

1ES0305−284: The error box also contains LTT 1477 (S:M3), but this source has $V = 14.0$, and can be ruled out by f_x/f_{opt} arguments.

1ES0315+681: The error box also contains SAO 12702 (S:M0).

1ES0316+413: Besides the cluster, the error box also contains the AGN NGC 1275, a known X-ray source.

1ES0429+130: The error box also contains HD 286839 (S:K0).

1ES0538−019: In addition to HD 37742, the brightest in the field ($V = 1.75$), the field also has HD 37743 (S: B0III; $V = 4.2$) and BD−02 1338C ($V = 10.0$).

1ES0702+646: Other than the AGN, the error box contains SAO 14073 (S: G0).

1ES0716−248: The error box contains a substantial portion of the globular cluster

N2362, of which HD 57061 is the brightest star (at $V = 4.32$). There are more than 30 other possible counterparts, ranging from $V = 8.12$ to $V = 13$, with known spectral types B2−A0.

1ES0924+232: In addition to the galaxy, there are at least 3 other galaxies in the error box. One of these, 0924+2312, has similar redshift (GAL:0.021) to U5037. The others are IC 0538, MCG +04-22-055, MCG +04-22-059, and MCG +04-22-260.

1ES0953+693: The error box also contains 0953+6917, a $B = 13.7$ galaxy which may have an active nucleus.

1ES1035−268: Error box contains the compact group HCG 048, which includes the galaxy counterpart.

1ES1101+384: The error box contains two identifications based on the 2E catalog: Mkn 421 (BL), and 51 UMA (S: A3), but the latter is 2.1′ from the 1ES position. Mkn 421 is a well known source at high energies (REF) and is clearly the preferred identification based on an HRI position (from *einline*)).

1ES1215+039: The source is a double galaxy.

1ES1254−172: The error box also contains 1254-1711 GAL:0.049), a possible AGN.

1ES1259+289: The error box also contains 1259+2857 (GAL:0.030), a possible AGN.

1ES1301−239: Error box also contains A3541 (CG).

1ES1351+695: Error box also includes MCG12.13.24 (AGN: 0.031). With $V = 17$ MCG12.13.24 is a marginally acceptable candidate based on f_x/f_{opt} (Maccacaro *et al.* 1984). Mkn 279 is the preferred identification based on an HRI position (in *einline*).

1ES1503+017: The counterpart, N5486, is part of a galaxy pair with the fainter N5486A (GAL: 0.007).

1ES1507−076: Error box also contains MKN 1394, a possible AGN.

1ES1549+203: There are two acceptable identifications: LB 906 (AGN), and SAO 084044 (S: G0), but the latter is 1.6′ from the 1ES position.

1ES1602+178: The UGC counterpart is a galaxy pair. In addition, the error box contains an NGC pair at $z \sim 0.035$ and a Zwicky triple at $z = 0.038$.

1ES1702+457: The error box also contains two galaxies—1702+4544A (GAL:0.061) and 1701+4544B (GAL:0.007).

1ES1704+545: Triple system (with WLY 9584B, F6V; Wool 9584C).

1ES1706+787: The error box also contains a Zwicky triple (1706+7842), and another Zwicky galaxy.

1ES1714+574: Error box also includes NGC 6345 (GAL), 2.7′ from the 1ES position.

1ES1731-325: Error box also includes HD 159176 (S:O6V+O6V), possibly a member of the globular cluster.

1ES1753−290: The error box also contains HD 163247 (S:FOV).

1ES1821+643: Error box also includes K1-16 (WD: DOZ1), which had an EXOSAT detection, (1.2′ from the 1ES position). However, the PI bin value (= 6) suggests that the AGN is the correct identification, since white dwarfs typically have a mean PI bin of 2 (Schachter *et al.*1991, in preparation).

1ES1914+092: Error box also includes SAO 124466 (S: F0).

1ES1928+233: Other then the infrared source, the field contains HD 344462 (S:F5) and HD 344461 (S:A0).

1ES2247+106: Other than the cluster, the error box also contains MCG 2-58-21, a 16th magnitude galaxy which is possibly an AGN.

1ES2311-430: The error box also contains 2311-4300 (GAL:0.056), with the same redshift as the cluster, a possible AGN.

7. IDENTIFICATIONS

Identifications of Slew Survey sources with known X-ray sources have played an important role in producing this catalog (as detailed in §3). Identifications with other, primarily optical, catalogs are also useful in providing a final check on the reality of the sources and the accuracy of the derived positions. All the identifications with counterparts presented here come from searching 3′ fields centered on the Slew Survey positions, based on the 95% confidence radius estimated in Figure 7d. 554 (52%) of the Slew Survey sources are new as X-ray sources, and 689 (66%) have been identified with optical catalog sources, including 170 (16%) of the new X-ray sources. Few of these are likely to be chance coincidences since a 3′ radius search circle gives $\sim 5 \times 10^6$ independent bins on the sky. Thus, assuming that all the objects are randomly distributed, for the ~1000 Slew Survey sources only about one in 5000 objects will accidentally associated with a catalog object. Most catalogs contain fewer sources than this, so one chance coincidence or less per catalog is expected. The SAO catalog (with ~100,000 entries) is an exception. A detailed examination of the identifications and their reliability will be presented in a forthcoming paper (Schachter *et al.* 1991).

In the case of extended objects, especially supernova remnants and clusters of galaxies, this technique may fail to identify some objects. A solution to this problem is to increase the search radius systematically while also checking for any duplicate counterpart identifications. A preliminary analysis suggests that increasing the radius to $\sim$ 5–15′ gives $\sim$ 20%–30% more supernova remnant and cluster candidates.

We are presently extending the identification program to handle the extended sources in more detail, and also to include the IRAS survey (including both the Point Source Catalog and the Faint Source Catalog), the HST Guide Star Selection System catalog, and the radio 87GB and UT 327 MHz surveys. Optical magnitudes for candidate identifications in all fields are being obtained from digitizations of the Palomar and UK Schmidt surveys. An on-line data base of identifications will be maintained at CfA, accessible remotely through the *einline* system . To allow for detailed follow-up, we will make available an on-line ascii version of the source identification list, which will be updated periodically. We welcome contributions to this identification list, which will be referenced in the database.

7.2 New Identified X-ray sources

Table 7 contains a list of the 170 new X–ray sources with optical identifications by object class. By a new X-ray source, we mean a Slew Survey source undetected in the EXOSAT, pointed IPC (Harris et al. 1991), or *HEAO-A3* (Remillard 1991) catalogs within 3′ of the Slew position. Some sources may not be in these catalogs, yet be detected in other X–ray missions (e.g., *HEAO-A2*, *Uhuru*, *Ariel V*). Therefore, we inspected other comprehensive X-ray source compilations (e.g., Bradt and McClintock 1983 ; Kowalski et al. 1984). Three ($\sim$3%) of the candidate new identified X-ray sources were eliminated in this manner: the X-ray binaries 4U1755-338 and AQL X-1 (4U1908+005), and the cluster A2315 (a *HEAO-A2* source).

The entries in Table 7 are grouped by object type—AGN, galaxies, clusters, white dwarfs, and stars—while the stars are further subdivided as in Table 5 [active, binaries, early type (OBA), late type ($\geq F$), unknown type]. The first column gives the 1ES (First *Einstein* Slew Survey) name of the object. If the redshift or stellar spectral type is known, it is indicated in column 2. We list in column 3 the common name of each object, including only a catalog designator such as PG for common catalogs, if the coordinate name is the same as in the 1ES name. An asterisk following the object name signifies an uncertain identification (see §6.2). Column 4 lists alternate names of the object, if any.

Based on their f_X/f_{Opt} ratios in comparison with the values given for Medium Survey sources by Maccacaro *et al.*, we expect that the new 'galaxies' are previously unknown active galaxies, primarily Seyfert galaxies.

8. PROPERTIES OF THE SLEW SURVEY

The Slew Survey contains 1075 sources, which are concentrated toward the ecliptic poles (figure 17). Half of these sources are newly discovered as X-ray sources. This is the largest list of sources from any 'all-sky' x-ray survey to date.

The range of source fluxes complements well that of the Medium Survey (Gioia *et al.* 1990, figure 1): there are similar numbers of sources in each survey; they each cover about a decade of flux with excellent statistics; and the Slew Survey sources are on average ten times brighter. The uniform selection of the Slew Survey sources by soft x-ray emission will allow the formation of well-defined samples of most classes of x-ray emitter: Stars, CVs, AGN, clusters of galaxies, and BL Lacs.

Some regions of the sky have especially favorable coverage. The Cygnus Loop has ~150 s exposure, which produces an image with over 100,000 photons (figure 18). Of more general interest is the North Ecliptic Pole region (figure 19) which has between 30 and 100 seconds exposure. In the region within 10 degrees of the Ecliptic Pole 21 sources can be seen, illustrating the ability of the Slew Survey to detect new 'serendipitous' sources.

Two examples of the uses of the Slew Survey samples are given below, one for quasars the other for BL Lacs:

(1) The steep luminosity function of AGN means that low luminosity AGN (*i.e.* Seyfert galaxies) are likely to make up a major part of the AGN contribution to the diffuse x-ray background. Yet most optical studies cannot treat these AGN because the host galaxy leads to fuzzy images and dilutes the AGN colors, both of which effects produce uncertain levels of incompleteness in the samples. Thus Schmidt and Green (1983), for example, could not extend their luminosity function fainter than $M_V = -23$. The Slew Survey will give a bright AGN survey, similar to the Palomar Bright Quasar Survey (BQS, 'PG', Schmidt and Green 1983), but with the advantage that it is free from the problem of galaxy starlight contamination. AGN will be seen down to $M_V \sim -20$ up to z~0.1, complementing the Medium Survey which reaches a similar absolute magnitude but has few AGN at z<0.1. The Slew Survey may also be a good means of finding high luminosity quasars of moderate redshift since, being rare, they require large sky coverage to be detected. Another problem, the dependence of AGN evolution on the unknown spectrum of the sources (Elvis *et al.* 1986, Tananbaum *et al.* 1986), can be removed empirically by using the Slew/A-2 flux ratios.

(2) There is a peculiar break in the x-ray ***logN-logS*** for BL Lac objects, which may be related to relativistic beaming in these sources (Giommi *et al.* 1991) or to cosmological evolution (Wolter *et al.* 1991, Morris *et al.* 1991). The flux region of the break is not presently well-sampled. This is the range covered by the Slew

Survey. Recent x-ray surveys (Stocke ***et al.*** 1989) have clearly demonstrated that x-ray selection is currently the best method of discovering BL Lacertae objects. For the flux limit of the IPC Slew Survey a uniform, x-ray selected, sample of ~100 objects will be detected (and identified through our ongoing program to identify all Slew Survey sources) in the high Galactic latitude sky. This compares with a ***total*** of 87 BL Lac objects, selected by all methods, in the Hewitt and Burbidge (1987) Catalog. There are about 40 known x-ray selected BL Lacs. All x-ray selected BL Lacs are radio-loud (Stocke ***et al.*** 1989) and have well-defined and distinct x-ray/optical/radio flux ratios (Giommi ***et al.***, 1991). This tight α_{RO}/α_{OX} distribution implies that the BL Lacs in the Slew Survey will have radio flux densities in the range 50–80 mJy. This, when combined with the correlation between radio and optical fluxes, gives an expected m_V in the range 18–19 for the faintest objects. The three fluxes alone are sufficient to select a large sample of BL Lac objects for further study.

Identification of the unidentified Slew Survey sources should be relatively easy since they are all bright. We can estimate their optical magnitudes using the nomogram constructed for Medium Survey sources (Maccacaro ***et al.*** 1988). The typical AGN will be at V $\sim$ 16^m and the faintest M dwarfs will be at $\sim$ 14^m. This is 2–3 magnitudes brighter than the the Medium Survey identifications and our error circles have only ~5 times their area, so the typical number of possible optical candidates, and possible spurious counterparts, will be few. Many of the new sources will also show up in the IRAS (IRAS 1988) and Green Bank (Condon and Broderick 1989) surveys. We will use the Minnesota POSS (Humphries 1988) and Edinburgh UK Schmidt digitizations to derive the bulk of our optical magnitudes. In this way relatively few new optical observations will be needed to make the remaining identifications.

We have not constructed a ***logN-logS*** for the Slew Survey in this paper. This obvious step is in practice quite difficult to do properly. The uncertainty on the count rates in the survey are mostly large, so that the 'Eddington Bias' is large. This is the effect by which sources below the formal flux threshold are detected while sources above the threshold are missed due to flux measurement errors. A simple flux threshold thus cannot be readily defined. Since the ***logN-logS*** is steep (Gioia ***et al.*** 1991) more sources will enter the survey than will drop out, systematically distorting and steepening the observed ***logN-logS*** at low fluxes. A proper treatment requires detailed simulations of the procedures used to produce the survey source list and we defer this to a later paper.

9. CONCLUSIONS

We have presented a survey of the sky in soft (~0.1–3.5 keV) X-rays containing 1075 sources. New, well-defined, samples of bright X-ray sources can be derived from this survey for many object types. The survey has a limiting flux a few times fainter than the largest previous all sky survey in X-rays (HEAO-A1, Wood *et al.*, 1984) which took place in the ~2–10 keV band, and a factor ~10 brighter than the typical sensitivity of the ROSAT survey which covers the 0.1–2 keV band.

It is fair to ask what the value of the Slew Survey is in the context of the much larger and more sensitive ROSAT survey (Trümper 1991). This question has several answers: first the Slew Survey makes available rapidly a large number of new bright X-ray sources suitable for follow-up study with ROSAT (and, in a few years, with ASTRO-D); second virtually all of the existing faint source X-ray work has been carried out with IPC-selected sources as part of the *Einstein* Medium Survey (Maccacaro *et al.* 1988, Gioia *et al.* 1990) and the Deep Survey (Giacconi *et al.* 1979b, Primini *et al.* 1991), so that a comparison sample of bright identified sources selected with the same instrument can be put to use at once for source count and evolution work, without ambiguities due to different detector characteristics; thirdly a comparison of Slew Survey sources with ROSAT survey sources will allow the selection of unusual objects having extreme variability and/or extreme spectra; and finally the energy band of the *Einstein* IPC extends to significantly higher energies than that of the ROSAT survey, so that it will continue to be valuable (*e.g.* for the selection of hard X-ray sources) even when the ROSAT survey is published.

The large amplitude variations in exposure on a few arcminute scale in the Slew Survey mean that it is not possible to derive upper limits for arbitrary positions on the sky from the present catalog. We are preparing two methods to allow this – an on-line service will be added to *einline* (the *Einstein* On-line Service, Harris *et al.* 1990); and the original, aspect corrected, slew data is available on a CD-ROM as part of the SAO CD-ROM series of *Einstein* Data Products (Fabbiano 1990). This CD-ROM also allows timing, spectral and structural information to be extracted from the Slew Survey via standard X–ray data reduction packages (*e.g.* IRAF/PROS, MIDAS).

The Slew Survey presently has only coarsely known completeness as a function of source flux. A program to derive accurate sky coverage and source detection efficiencies as a function of source flux and extent is being initiated. This will allow the derivation of statistical population properties such as luminosity functions from the Slew Survey.

We are pursuing a program of identifications for all Slew Survey sources. This is initially based on existing archival data and catalogs in an attempt to minimize the amount of optical observing needed. A first paper on these identifications is in preparation (Schachter *et al.* 1991). We shall maintain a data base of these identifications as part of the on-line *einline* system for general use. We welcome any contributions to these identifications. The on-line data base will include a reference for the source of each identification. We ask that any publication using this information reference its source as listed in the on-line system.

We have received many requests for information on sources in the Slew Survey. As a result we are forming working groups for astronomers interested in pursuing an interest in the active galaxies and quasars, and for the BL Lacs in the survey. The aim of these groups is to exchange information and prevent unnecessary duplication of effort, not to direct anyone's research. Anyone interested in joining one of these groups or in forming another should send e-mail to the Slew Survey Project (slew@cfa.harvard.edu, cfa::slew). The *Einstein* Slew Survey data are part of the *Einstein* data bank. As such they are part of the NASA Astrophysics Data Program and are available to all interested parties.

There exists some 50% more slew data in the *Einstein* data bank than was used for the present survey. These were originally rejected because it had problems that would have complicated this first analysis, primarily long data dropouts that make the extrapolation of the gyro aspect solution less certain. Our experience now suggests that this problem can be overcome and we hope to include this data in constructing a second 'definitive' Slew Survey, which should have roughly double the number of sources.

ACKNOWLEDGMENTS

We thank John McSweeney and the *Einstein* data center team for assistance with data handling; Ron Remillard, Jonathan McDowell, Paolo Giommi, John Stocke and Nick White for their assistance with the identifications, and John Stocke for a careful reading of the manuscript. This research has made use of the Simbad database, operated at CDS, Strasbourg, France. This research has also made use of the NASA/IPAC Extragalactic Database (NED) which is operated by the Jet Propulsion Laboratory, California Institute of Technology, under contract with NASA. This work was supported by NASA contract NAS8-30751 (*Einstein*), and NASA grant NAG5-1201 (ADP).

TABLES

Table 1: *Einstein* Surveys

	Area[a]	f_{lim}^{b}(upper[c])	f_{lim}^{b}(lower)	no. sources	ref.
Deep	2.3	$\sim 7 \times 10^{-14}$	$\sim 4 \times 10^{-14}$	25	Primini *et al.* 1991
Medium	780	$\sim 5 \times 10^{-12}$	$\sim 2 \times 10^{-13}$	835	Gioia *et al.* 1990
Slew	35,060[d]	$\sim 1 \times 10^{-9}$	$\sim 3 \times 10^{-12}$	1075	this paper

a. Square degrees (sq°).

b. erg cm^{-2} s^{-1}.

c. Defined as the flux below which 90% of the sources lie.

d. Defined by the minimum exposure (1.0s) at which a source was detected.

Table 2: *Einstein* IPC Slew Survey Properties

Observing time	0.99×10^6s
Effective exposure[a]	$0.47 \times 10^6 s$
Total no. of photons	2.6×10^6
Mean background	~0.7 photons/source box[b]
Min. no. of photons/source (for mean background)	5 ($P_{Rand} \sim 1 \times 10^{-4}$)
Mean exposure	12 s
Mean limiting count rate	0.45 ct s^{-1}
Mean limiting flux[c]	14×10^{-12} erg cm^{-2} s^{-1}
No. sources	1075
Identifications[d]	Stars: m_V <7
	AGN: m_V <17

a. including corrections for vignetting and excluding the 'ribs' regions.

b. $6' \times 6'$ box.

c. 0.2–4.0 keV, for a conversion factor of 3.26×10^{-11} *ergs/count* appropriate for an a power law energy index of 0.5 and a Galactic N_H of 2.0×10^{20} atoms cm^{-2} as used in the *Einstein* Medium Survey (Gioia *et al.* 1984)

d. based on Medium Survey nomogram (Maccacaro *et al.* 1988).

Table 3: Relative value of *Einstein* instruments for slew surveying

	(FOV×% time×QE)[a]	figure of merit
IPC	1800× ∼0.5×0.7	630
HRI	216× ∼0.2×0.1	4.3
SSS	9× ∼0.15×0.9	1.2
FPCS	≤90× ∼0.15×0.01	0.14

a. FOV= field of view in square arcminutes; %time = fraction of time in focal plane; QE = quantum efficiency.

Table 4: Offsets for each set of gyros (in arcminutes)

gyro combination[a]	gyros in use			ΔX	ΔY
A	1	2	3	0.0	0.0
B	2	3	5	3.2	0.0
C	2	3	4	4.25	1.25
D	2	4	6	6.0	0.0
E	3	5	6	6.0	1.75
G	3	4	6	4.75	1.75

a. gyro combination F did not contribute usable slews to the survey.

Table 5: **Identified Sources to Date**

Class	Num. New X-ray Src.	Total Num. IDs.	% Survey Det.	% Survey Pred. (MS)
AGN	10	131	19	30
BL Lacs	0	33	5	10
Clusters	12	80	11	20
CVs	0	23	3	6
Stars	121	274	40	20
Known Active	2	48	...	...
Binaries	4	19	...	...
Wind Cand. (OBA)	18	38	...	...
Coronal Cand. ($\geq$F)	89	149	...	...
Unk., Pecul.	8	20	...	...
X-ray binaries and Pulsars	0	41	6	6
Other:	27	109	16	8
Galaxies	22	42	...	...
SN Remnants	0	28	...	...
White Dwarfs	1	6	...	...
2E Sources	0	25	...	...
SIMBAD Sources	4	6	...	...
EXOSAT Sources	0	2	...	...

TABLE 6
The First Einstein Slew Survey Catalog

Slew Desig.	RA 1950	DEC 1950	IPC Rate (cts s^{-1})	NP/NS	P_{rand}	Exp. (s)	PI	QI	EOS # EMSS	Δ2E (′)	A3 EXO	Δ1H (′)	Cat.	Class.: Type/z	Name	ΔC (′)
1ES0002+166	00 02 51	+16 38 40	$0.25^{+0.14}_{-0.10}$	5/3	3.46E−05	18.4	5	3A	...	...	...	...	...	...	...	...
1ES0003+158	00 03 23	+15 52 55	$0.09^{+0.03}_{-0.03}$	20/3	7.03E−05	145.0	6	3A	12	0.6	...	...	HB	AGN:0.112	PHL 656	0.5
1ES0003+199	00 03 48	+19 55 15	$1.63^{+0.35}_{-0.31}$	26/3	1.00E−10	15.4	4	3A	...	...	x1H0003+200	0.8	HB	AGN:0.025	MKN 335	0.7
1ES0004+287	00 04 04	+28 44 18	$0.29^{+0.07}_{-0.06}$	26/4	1.00E−10	77.2	5	3A	m15	0.4	...	...	WLY	S:K0V	WLY 5	0.8
1ES0005+159	00 05 17	+15 59 01	$0.12^{+0.05}_{-0.04}$	13/5	4.26E−05	79.8	11	3A	...	...	...	...	...	...	...	...
1ES0005+145	00 05 36	+14 32 48	$0.36^{+0.20}_{-0.15}$	5/4	3.44E−05	12.9	6	3A	...	...	...	...	SBD	GAL	Z 0005.5+1433	1.5
1ES0008+107	00 08 00	+10 42 03	$0.57^{+0.08}_{-0.07}$	63/4	1.00E−10	102.9	6	3A	29	0.5	x1H0014+111	0.8	HB	AGN:0.089	III ZW 2	0.8
1ES0008−025	00 08 46	−02 35 02	$0.29^{+0.14}_{-0.11}$	7/3	2.17E−05	21.1	6	3A	...	...	...	...	...	...	...	...
1ES0011+192	00 11 56	+19 17 51	$0.35^{+0.18}_{-0.14}$	6/3	4.93E−05	15.4	12	3A	...	...	...	...	...	...	...	...
1ES0013−108	00 13 16	−10 51 52	$0.60^{+0.44}_{-0.30}$	3/2	2.02E−05	4.9	13	3A	...	...	...	...	...	...	...	...
1ES0013+195	00 13 37	+19 35 38	$0.28^{+0.13}_{-0.10}$	7/5	1.04E−05	22.6	6	3A	...	...	...	...	SBD	S:M4	G 32 -6*	0.0
1ES0013−376	00 13 47	−37 36 37	$0.59^{+0.34}_{-0.25}$	5/4	9.62E−05	7.8	6	3A	...	...	...	...	...	...	...	...
1ES0021−723	00 21 39	−72 21 40	$0.09^{+0.03}_{-0.03}$	19/5	7.46E−06	143.6	5	3A	82	0.9	...	...	2E	XRB	...	...
1ES0022+638	00 22 26	+63 52 03	$9.90^{+0.65}_{-0.65}$	236/9	1.00E−10	23.5	7	3A	83	2.3	x1H0022+638	1.8	A3	SNR	TYCHO	1.7
1ES0023+310	00 23 43	+31 04 16	$0.44^{+0.25}_{-0.18}$	5/5	3.25E−05	10.6	6	3A	...	...	...	...	...	...	...	...
1ES0029+814	00 29 07	+81 26 34	$0.36^{+0.19}_{-0.14}$	6/5	5.16E−05	14.9	6	3A	...	...	...	...	...	...	...	...
1ES0031+463	00 31 03	+46 22 16	$0.41^{+0.26}_{-0.19}$	4/3	8.60E−05	9.1	7	3A	...	...	...	...	...	...	...	...
1ES0032−622	00 32 37	−62 12 52	$0.53^{+0.34}_{-0.24}$	4/2	9.54E−05	7.1	5	3A	...	...	...	...	SBD	S:K5V	HD 3221	1.5
1ES0033+595	00 33 04	+59 33 23	$0.59^{+0.22}_{-0.18}$	10/5	1.00E−10	16.2	7	3A	...	...	...	...	...	...	...	...
1ES0037+405	00 37 30	+40 33 19	$0.06^{+0.02}_{-0.02}$	29/4	1.92E−05	301.7	6	3A	113	0.2	...	...	2E	...	5C3 76	0.2
1ES0037+293	00 37 43	+29 18 26	$0.23^{+0.10}_{-0.08}$	10/3	5.14E−06	36.6	10	3A	m118	2.2	...	...	MS	CG:0.069	A77	2.2
1ES0037+272	00 37 59	+27 13 51	$0.39^{+0.24}_{-0.17}$	4/4	6.28E−05	9.8	7	3A	...	...	...	...	...	...	...	...
1ES0039−095	00 39 19	−09 34 43	$0.96^{+0.12}_{-0.11}$	83/8	1.00E−10	79.6	7	3A	136	0.4	...	...	2E	CG:0.052	A85	0.7
1ES0039+400	00 39 36	+40 03 04	$0.09^{+0.02}_{-0.02}$	48/6	1.00E−10	370.5	7	3E	141	1.0	...	...	VV	AGN:0.102	IV ZW 29	0.7
1ES0039+341	00 39 41	+34 09 22	$0.40^{+0.21}_{-0.16}$	6/4	3.45E−05	13.6	7	3A	...	...	...	...	...	...	...	...
1ES0039+409	00 39 58	+40 59 48	$0.41^{+0.05}_{-0.05}$	90/6	1.00E−10	197.5	5	3E	147	0.2	x1H0039+408	0.4	UGC	GAL:-0.001	M 31	0.4
1ES0040−260	00 40 09	−26 00 34	$0.31^{+0.19}_{-0.14}$	4/2	6.70E−05	12.4	6	3A	...	...	...	...	...	...	...	...
1ES0040+044	00 40 41	+04 26 17	$0.21^{+0.11}_{-0.08}$	6/4	1.02E−04	25.6	5	3A	...	...	...	...	...	...	...	...
1ES0041−182	00 41 09	−18 15 26	$0.88^{+0.15}_{-0.14}$	40/4	1.00E−10	43.4	4	3A	163	0.8	...	...	WLY	S:K0III	WLY 31	1.0
1ES0041+402	00 41 57	+40 16 51	$0.08^{+0.03}_{-0.03}$	19/5	6.12E−05	160.3	6	3A	...	...	...	...	...	...	...	...
1ES0043+413	00 43 00	+41 23 27	$0.07^{+0.02}_{-0.01}$	49/2	1.47E−09	464.5	5	3A	169	0.3	...	...	SBD	...	P SKHB 307	0.2
1ES0044−211	00 44 31	−21 06 21	$0.14^{+0.05}_{-0.04}$	26/3	3.87E−06	119.2	7	3A	179	2.8	...	...	2E	GAL	2E	2.5
1ES0044+239	00 44 40	+23 59 27	$0.65^{+0.09}_{-0.08}$	63/6	1.00E−10	90.8	5	3A	181	0.3	...	...	SAO	AC:K1II	ζ AND	0.4

TABLE 6—*Continued*

Slew Desig.	RA 1950	DEC 1950	IPC Rate (cts s^{-1})	NP/NS	P_{rand}	Exp. (s)	PI	QI	EOS # EMSS	Δ2E (′)	A3 EXO	Δ1H (′)	Cat.	Class.: Type/s	Name	ΔC (′)
1ES0045−255	00 45 07	−25 33 56	$0.16^{+0.03}_{-0.03}$	37/4	1.00E−10	191.9	5	3A	184	0.3	...	...	RNG	GAL:0.001	NGC 253	0.6
1ES0045+311	00 45 41	+31 09 34	$0.12^{+0.06}_{-0.04}$	8/3	4.86E−05	55.7	9	3A	...	...	...	...	...	...	...	...
1ES0048+236	00 48 16	+23 40 51	$0.43^{+0.27}_{-0.19}$	4/2	4.25E−05	8.9	9	3A	...	...	...	...	SBD	S:F8	AG+23 78	1.4
1ES0048+291	00 48 50	+29 07 15	$0.20^{+0.09}_{-0.07}$	10/1	8.34E−05	39.6	7	3A	m198	0.8	1H0043+294	0.9	VV	AGN:0.036	VV	0.9
1ES0050+124	00 50 58	+12 25 09	$0.39^{+0.09}_{-0.08}$	27/3	1.00E−10	64.2	5	3A	209	0.2	...	...	VV	AGN:0.061	I ZW 1	0.2
1ES0051−749	00 51 26	−74 55 33	$0.30^{+0.06}_{-0.06}$	36/5	1.00E−10	101.1	6	3A	214	0.2	...	...	SAO	AC:G0	CV TUC	0.1
1ES0052+251	00 52 09	+25 09 35	$0.27^{+0.08}_{-0.07}$	16/5	3.06E−10	52.5	5	3A	217	0.5	x1H0048+250	0.6	VV	AGN:0.154	PG	0.5
1ES0053+604	00 53 42	+60 27 09	$2.04^{+0.33}_{-0.30}$	45/8	1.00E−10	21.4	6	3A	...	...	x1H0053+604	0.4	A3	XRB-Be	γ CAS	0.4
1ES0054+231	00 54 32	+23 09 18	$0.20^{+0.06}_{-0.05}$	25/2	2.83E−08	93.5	4	3A	232	0.2	...	...	SAO	AC:G8IIIb	SAO 074388	0.3
1ES0054+145	00 54 38	+14 30 45	$0.15^{+0.05}_{-0.04}$	15/4	2.93E−06	78.5	6	3A	233	1.3	x	...	VV	AGN:0.171	PHL 909	1.7
1ES0054−702	00 54 48	−70 14 22	$0.40^{+0.22}_{-0.17}$	5/1	1.03E−04	11.4	2	3A	...	...	...	...	SAO	S:F8	SAO 255722	2.1
1ES0055+227	00 55 17	+22 45 02	$0.17^{+0.07}_{-0.06}$	12/3	1.08E−04	53.7	4	3A	...	...	...	...	...	...	...	...
1ES0057+315	00 57 06	+31 33 45	$0.91^{+0.12}_{-0.11}$	69/8	1.00E−10	72.2	5	3A	244	0.7	x1H0106+324	0.7	VV	AGN:0.015	MKN 352	0.7
1ES0057+655	00 57 21	+65 31 17	$0.30^{+0.23}_{-0.15}$	3/1	1.01E−04	9.5	9	3A	...	...	...	...	...	...	...	...
1ES0058+345	00 58 57	+34 31 18	$1.14^{+0.71}_{-0.51}$	4/2	1.84E−05	3.4	3	3A	...	...	...	...	EXC	CG	ZW 314	2.8
1ES0100−199	01 00 12	−19 54 26	$0.48^{+0.27}_{-0.20}$	5/3	1.44E−05	9.8	6	3A	...	...	...	...	...	...	...	...
1ES0100+644	01 00 16	+64 25 32	$0.56^{+0.31}_{-0.23}$	5/3	8.38E−06	8.5	8	3A	...	...	...	...	...	...	...	...
1ES0100+405	01 00 56	+40 35 02	$0.22^{+0.07}_{-0.06}$	17/3	4.77E−09	64.0	5	3A	254	0.9	...	...	SBD	S	G 132 -50A*	1.3
1ES0101+410	01 01 48	+41 02 52	$0.23^{+0.10}_{-0.08}$	10/2	2.16E−05	35.6	7	3A	260	1.0	...	...	GCV	S:PEC(UG)	RX AND	1.0
1ES0102−722	01 02 25	−72 17 50	$0.82^{+0.09}_{-0.09}$	106/9	1.00E−10	117.7	6	3A	261	0.4	x	...	2E	SNR	SMC	1.7
1ES0102+362	01 02 44	+36 15 00	$0.33^{+0.17}_{-0.13}$	6/4	3.78E−05	16.2	3	3A	...	...	...	...	...	...	...	...
1ES0103−726	01 03 32	−72 38 01	$0.18^{+0.05}_{-0.05}$	25/9	1.03E−07	101.7	5	3A	267	1.3	x	...	GCV	S	SZ TUC	2.2
1ES0107+085	01 07 08	+08 35 05	$0.53^{+0.33}_{-0.23}$	4/2	1.76E−06	7.3	13	3A	...	...	...	...	...	...	...	...
1ES0107−580	01 07 55	−58 02 07	$0.55^{+0.34}_{-0.24}$	4/1	3.39E−07	7.2	6	3A	...	...	...	...	...	...	...	...
1ES0108+174	01 08 25	+17 24 40	$0.06^{+0.02}_{-0.02}$	23/5	6.18E−05	230.5	7	3A	311	1.5	...	...	ABL	CG:0.066	A154	1.8
1ES0114−027	01 14 06	−02 46 03	$1.85^{+0.17}_{-0.17}$	128/3	1.00E−10	67.7	4	3A	339	0.6	...	...	BSC	AC:G5IIIe	AY CET	0.5
1ES0114+065	01 14 18	+06 33 35	$0.25^{+0.08}_{-0.07}$	15/2	5.01E−09	51.5	5	3A	340	0.6	x	...	SAO	S:G5	UV PSC	0.7
1ES0115+634	01 15 17	+63 28 26	$1.52^{+0.29}_{-0.26}$	33/5	1.00E−10	20.9	9	3A	345	0.6	1H0115+635	0.4	A3	XRB-Be	V635 CAS	0.4
1ES0115−737	01 15 45	−73 42 18	$0.18^{+0.04}_{-0.04}$	39/7	1.00E−10	160.0	7	3A	350	0.4	x1H0115−737	0.1	A3	XRB	SMC X-1	0.1
1ES0115−272	01 15 50	−27 14 37	$0.26^{+0.10}_{-0.08}$	11/3	4.64E−07	36.8	8	3A	349	0.8	...	...	ABL	CG	A2895	2.3
1ES0118+189	01 18 04	+18 55 24	$0.34^{+0.18}_{-0.14}$	6/2	4.64E−05	15.9	11	3A	...	...	...	...	...	...	...	...
1ES0119−286	01 19 31	−28 36 22	$0.61^{+0.22}_{-0.18}$	11/4	1.00E−10	17.0	4	3A	...	...	x1H0122−281.B	0.3	HB	AGN:0.117	GD 1339	0.3
1ES0120+004	01 20 16	+00 26 50	$0.34^{+0.15}_{-0.12}$	8/5	2.23E−06	21.1	5	3A	...	...	...	...	SAO	S:G0	HD 8358*	0.5

TABLE 6—*Continued*

Slew Desig.	RA 1950	DEC 1950	IPC Rate (cts s^{-1})	NP/NS	P_{rand}	Exp. (s)	PI	QI	EOS # EMSS	Δ2E (′)	A3 EXO	Δ1H (′)	Cat.	Class.: Type/z	Name	ΔC (′)
1ES0120+340	01 20 20	+34 08 43	$1.01^{+0.18}_{-0.16}$	40/2	1.00E−10	37.7	7	3A	369	1.0	...	...	2E	...	...	...
1ES0121−590	01 21 53	−59 03 48	$2.29^{+0.18}_{-0.18}$	171/3	1.00E−10	72.9	8	3A	378	0.2	x1H0122−590	0.3	HB	AGN:0.046	FAIR 9	0.3
1ES0122+084A	01 22 29	+08 29 52	$0.17^{+0.06}_{-0.05}$	15/8	6.28E−06	68.6	7	2A	...	...	...	...	SBD	CG:0.045	A193*	2.9
1ES0122+084B	01 22 33	+08 26 23	$0.21^{+0.07}_{-0.06}$	14/7	9.35E−07	55.0	7	3A	...	...	...	...	ABL	CG:0.045	A193*	0.8
1ES0122+190	01 22 52	+19 04 33	$0.12^{+0.06}_{-0.04}$	10/6	5.01E−05	63.8	8	3A	...	...	...	...	...	...	...	...
1ES0124+189	01 24 50	+18 55 36	$0.20^{+0.08}_{-0.06}$	12/2	8.01E−07	50.7	4	3A	390	0.5	...	...	VV	AGN:0.017	MKN 359	0.4
1ES0126+587	01 26 49	+58 42 09	$0.34^{+0.18}_{-0.14}$	6/4	7.92E−05	15.8	10	3A	...	...	...	...	...	...	...	...
1ES0127−372	01 27 41	−37 17 04	$0.39^{+0.24}_{-0.17}$	4/1	5.90E−05	9.8	7	3A	...	...	...	...	...	...	...	...
1ES0131+303	01 31 02	+30 23 53	$0.42^{+0.06}_{-0.05}$	72/7	1.00E−10	150.1	7	3A	409	0.5	x1H0129+303	0.9	RNG	GAL:-0.001	NGC 598	0.4
1ES0132−534	01 32 46	−53 25 13	$0.71^{+0.41}_{-0.30}$	5/3	5.86E−05	6.4	7	3A	...	...	...	...	...	...	...	...
1ES0133+484	01 33 26	+48 27 26	$0.37^{+0.18}_{-0.14}$	7/4	4.40E−05	16.5	4	3A	...	...	...	...	BSC	S:gK1	HD 9746	0.8
1ES0133−134	01 33 34	−13 29 42	$0.14^{+0.08}_{-0.06}$	6/2	8.76E−05	36.6	4	3A	...	...	...	...	...	...	...	...
1ES0133+207	01 33 42	+20 43 05	$0.14^{+0.04}_{-0.04}$	23/6	3.98E−07	121.4	6	3A	437	0.8	x	...	HB	AGN:0.425	3C47	1.0
1ES0134+527	01 34 49	+52 44 07	$0.33^{+0.19}_{-0.14}$	5/2	5.11E−05	14.1	9	3A	...	...	...	...	...	...	...	...
1ES0136−182	01 36 30	−18 12 37	$0.18^{+0.03}_{-0.03}$	64/9	1.00E−10	282.3	4	3A	455	0.7	x	...	SBD	S:M5.5V:e	LHS 9	1.2
1ES0138+391	01 38 57	+39 08 58	$0.12^{+0.05}_{-0.04}$	16/7	2.53E−05	93.5	7	2A	...	...	1H0140+393	1.0	VV	AGN:0.080	B2 0138+39B	0.9
1ES0139−472	01 39 03	−47 15 54	$0.33^{+0.19}_{-0.14}$	5/4	6.48E−05	14.0	8	3A	...	...	...	...	...	...	...	...
1ES0139−189	01 39 05	−18 54 14	$0.42^{+0.18}_{-0.14}$	8/4	1.78E−07	17.6	4	3A	...	...	...	...	...	...	...	...
1ES0139−681	01 39 39	−68 07 54	$1.38^{+0.19}_{-0.18}$	63/9	1.00E−10	43.1	3	3A	469	0.4	x1H0136−681	0.6	A3	CV	BL HYI	0.6
1ES0140+603	01 40 24	+60 19 54	$0.37^{+0.23}_{-0.17}$	4/2	8.45E−05	10.3	6	3A	...	...	...	...	...	...	...	...
1ES0142+614	01 42 51	+61 29 52	$3.37^{+0.56}_{-0.51}$	41/7	1.00E−10	12.0	7	3A	...	...	x1H0132+607	0.3	A3	XRB	X0142+614	0.4
1ES0143−253	01 43 17	−25 18 04	$0.30^{+0.12}_{-0.10}$	9/6	6.80E−08	27.3	4	3A	...	...	...	...	BSC	S:F1V	ϵ SCL	0.2
1ES0145+138	01 45 39	+13 49 52	$1.12^{+0.70}_{-0.50}$	4/2	1.86E−05	3.4	3	3A	...	...	...	...	...	...	...	...
1ES0147+153	01 47 12	+15 22 28	$0.56^{+0.41}_{-0.27}$	3/2	2.09E−05	5.3	10	3A	...	...	...	...	...	...	...	...
1ES0149+229	01 49 27	+22 57 36	$0.22^{+0.10}_{-0.08}$	8/5	2.23E−06	32.6	11	3A	...	...	...	...	...	...	...	...
1ES0149+358	01 49 42	+35 53 33	$0.29^{+0.07}_{-0.06}$	33/3	1.00E−10	90.0	7	3E	493	2.1	...	...	ABL	CG:0.016	A262	2.5
1ES0150+293	01 50 12	+29 19 29	$0.33^{+0.06}_{-0.06}$	39/5	1.00E−10	106.3	4	3A	495	0.7	...	...	WLY	S:F6IV	WLY 9062	0.7
1ES0150+574	01 50 54	+57 26 21	$0.41^{+0.22}_{-0.17}$	6/2	1.05E−04	13.0	5	3A	...	...	...	...	...	...	...	...
1ES0152+022	01 52 51	+02 13 43	$0.31^{+0.13}_{-0.10}$	9/4	1.04E−06	26.2	5	3A	...	...	...	...	...	...	...	...
1ES0154−518	01 54 00	−51 51 25	$0.45^{+0.20}_{-0.16}$	8/4	1.17E−06	16.2	3	3A	...	...	...	...	WLY	S:G5IV+	WLY 81AB	0.2
1ES0157+706	01 57 50	+70 39 01	$0.24^{+0.12}_{-0.09}$	8/6	7.39E−05	27.7	6	3A	...	...	...	...	BSC	S:A3IV	SAO 4554	0.9
1ES0158−365	01 58 00	−36 33 06	$0.19^{+0.09}_{-0.07}$	9/7	5.44E−05	38.2	6	3A	...	...	...	...	...	...	...	...
1ES0158+003	01 58 32	+00 19 29	$0.51^{+0.10}_{-0.09}$	34/5	1.00E−10	59.6	5	3A	m513	0.5	...	...	2E	...	MS	0.5

TABLE 6—*Continued*

Slew Desig.	RA 1950	DEC 1950	IPC Rate (cts s^{-1})	NP/NS	P_{rand}	Exp. (s)	PI	QI	EOS # EMSS	Δ2E (′)	A3 EXO	ΔIH (′)	Cat.	Class.: Type/z	Name	ΔC (′)
1ES0200+166	02 00 33	+16 41 12	$0.25^{+0.13}_{-0.10}$	6/3	3.92E−05	21.7	6	2A	...	...	...	...	...	...	...	...
1ES0201+645	02 01 48	+64 35 39	$0.33^{+0.16}_{-0.12}$	7/5	3.09E−05	18.8	7	3A	518	0.6	...	...	2E	SNR	3C58	0.4
1ES0202−482	02 02 30	−48 16 00	$0.42^{+0.24}_{-0.17}$	5/3	2.66E−05	11.1	10	3A	...	...	...	...	...	...	...	...
1ES0203+158	02 03 36	+15 51 15	$0.12^{+0.05}_{-0.04}$	17/3	3.43E−05	95.0	6	3A	...	...	...	...	...	...	...	...
1ES0204+150	02 04 11	+15 03 29	$0.53^{+0.06}_{-0.06}$	105/7	1.00E−10	180.3	7	3A	m522	0.3	x1H0157+142	0.3	A3	CV	TT ARI	0.3
1ES0204+482	02 04 37	+48 14 24	$0.81^{+0.46}_{-0.34}$	5/2	3.59E−05	5.7	6	3A	...	...	...	...	...	...	...	...
1ES0205+024	02 05 14	+02 29 43	$0.20^{+0.07}_{-0.06}$	15/3	4.83E−07	61.3	6	3A	526	1.0	...	...	HB	AGN:0.155	MKN 586	1.0
1ES0205+492	02 05 35	+49 12 37	$0.30^{+0.16}_{-0.12}$	6/3	1.03E−04	17.5	7	3A	...	...	...	...	SBD	GAL	G 173 -39	0.6
1ES0206+522	02 06 19	+52 12 18	$0.62^{+0.21}_{-0.17}$	12/6	1.00E−10	18.6	6	3A	534	0.3	1H0203+513	0.6	VV	AGN:0.049	GPX 002	0.7
1ES0207−013	02 07 01	−01 22 46	$0.37^{+0.21}_{-0.16}$	5/2	7.70E−05	12.4	7	3A	...	...	...	...	...	...	...	...
1ES0209+300	02 09 29	+30 04 50	$0.46^{+0.10}_{-0.09}$	30/3	1.00E−10	60.7	5	3A	544	0.7	...	...	BSC	AC:G5III+F5V	ζ TRI	0.6
1ES0212−010	02 12 00	−01 00 09	$1.02^{+0.12}_{-0.12}$	78/4	1.00E−10	73.9	6	3A	548	0.3	x1H0215−007	0.2	VV	AGN:0.027	MKN 590	0.2
1ES0212+735	02 12 54	+73 33 32	$0.17^{+0.07}_{-0.06}$	10/2	8.90E−07	50.0	7	3A	549	2.2	...	...	HB	AGN:2.367	S5 0212+735	2.2
1ES0213+070	02 13 02	+07 02 11	$0.54^{+0.34}_{-0.24}$	4/3	4.63E−05	7.1	12	3A	...	...	...	...	...	...	...	...
1ES0215−021	02 15 02	−02 08 16	$0.27^{+0.13}_{-0.10}$	7/2	1.97E−05	22.8	10	3A	...	...	...	...	...	...	...	...
1ES0219+428	02 19 30	+42 48 27	$0.29^{+0.03}_{-0.03}$	156/11	1.00E−10	453.8	6	3A	558	0.2	x	...	VV	BL:0.444	3C 66A	0.1
1ES0221+323	02 21 55	+32 20 21	$0.23^{+0.11}_{-0.09}$	8/4	9.39E−05	28.7	10	3A	...	...	...	...	...	...	...	...
1ES0224+307	02 24 32	+30 45 04	$0.45^{+0.08}_{-0.07}$	43/3	1.00E−10	88.2	5	3A	569	0.2	x	...	SBD	S	BD+30 397AB	1.1
1ES0225+310	02 25 18	+31 05 29	$0.35^{+0.07}_{-0.06}$	38/4	1.00E−10	96.5	8	3A	573	0.1	x1H0218+304	0.7	VV	AGN:0.016	MKN 1040	0.4
1ES0226+115	02 26 24	+11 34 16	$0.90^{+0.66}_{-0.45}$	3/2	8.76E−05	3.2	11	3A	...	...	...	...	...	...	...	...
1ES0226−615	02 26 54	−61 32 41	$0.58^{+0.23}_{-0.19}$	9/5	3.07E−08	14.4	4	3A	...	...	...	...	SAO	S:F8	SAO 248569	1.1
1ES0227+156	02 27 47	+15 38 16	$0.33^{+0.17}_{-0.13}$	6/2	2.68E−05	16.6	5	2A	...	...	...	...	...	...	...	...
1ES0229+200	02 29 58	+20 04 18	$0.51^{+0.16}_{-0.13}$	14/5	1.00E−10	25.9	7	3A	...	...	...	...	...	...	...	...
1ES0232−090	02 32 10	−09 00 53	$0.66^{+0.11}_{-0.10}$	44/5	1.00E−10	62.6	6	3A	590	0.6	x1H0227−094	0.5	VV	AGN:0.043	NGC 985	0.5
1ES0232−440	02 32 25	−44 01 08	$1.47^{+0.51}_{-0.41}$	11/4	1.00E−10	7.3	5	3A	592	1.1	x1H0226−448	0.8	SBD	AC:M0Vp	HD 16157	0.7
1ES0235+016	02 35 48	+01 40 50	$0.63^{+0.30}_{-0.24}$	7/4	1.03E−05	9.9	6	3A	617	1.0	...	...	VV	AGN:0.024	NGC 1019	1.3
1ES0235+164	02 35 54	+16 24 15	$0.04^{+0.01}_{-0.01}$	35/6	7.97E−06	450.4	7	3E	618	0.2	...	...	HB	BL:0.940	OD 160	0.4
1ES0236−524	02 36 43	−52 24 22	$0.41^{+0.21}_{-0.16}$	7/6	1.03E−04	14.6	6	3A	...	...	x1H0235−525	0.5	A3	AGN	WARD	0.4
1ES0236+610	02 36 46	+61 00 07	$0.26^{+0.10}_{-0.09}$	12/4	7.25E−06	37.1	7	3A	627	1.1	x	...	GCV	S:B1EIB:	LS I +61 303	1.0
1ES0236−002	02 36 51	−00 14 19	$0.18^{+0.07}_{-0.06}$	11/5	3.02E−07	51.8	6	3A	628	0.8	...	...	2E	...	...	...
1ES0237−531	02 37 05	−53 10 24	$0.64^{+0.24}_{-0.20}$	10/4	2.40E−09	14.5	4	3A	...	...	x	...	SBD	S:F8IV/V+	HD 16699*	0.4
1ES0238−009	02 38 43	−00 54 23	$0.26^{+0.12}_{-0.09}$	9/3	1.39E−05	29.0	3	3A	...	...	x	...	SAO	S:F7IV	SAO 130055	0.6
1ES0238+057	02 38 52	+05 45 46	$0.22^{+0.10}_{-0.08}$	8/6	5.01E−05	31.3	5	3A	...	...	...	...	SBD	S:M	BD+05 378	1.4

TABLE 6—*Continued*

Slew Desig.	RA 1950	DEC 1950	IPC Rate (cts s^{-1})	NP/NS	P_{rand}	Exp. (s)	PI	QI	EOS # EMSS	Δ2E (′)	A3 EXO	Δ1H (′)	Cat.	Class.: Type/z	Name	ΔC (′)
1ES0238+069	02 38 55	+06 58 40	$0.17^{+0.04}_{-0.04}$	29/5	1.00E−10	134.7	8	3A	646	0.3	...	...	VV	AGN:0.028	MKN 595	0.3
1ES0240−002	02 40 08	−00 13 50	$0.53^{+0.06}_{-0.06}$	85/4	1.00E−10	148.8	5	3A	649	0.5	x1H0244+001	0.4	VV	AGN:0.003	NGC 1068	0.4
1ES0241+622	02 41 02	+62 15 37	$0.19^{+0.07}_{-0.06}$	13/2	2.65E−06	53.9	8	3A	653	0.1	x1H0240+621	0.2	VV	AGN:0.044	4U 0241+61	0.2
1ES0241−381	02 41 26	−38 06 21	$2.19^{+1.18}_{-0.87}$	5/2	1.57E−07	2.2	2	2A	...	...	1H0247−370	2.0	SBD	AC:G6V+	SAO 193879	2.0
1ES0242−675	02 42 29	−67 33 30	$0.36^{+0.17}_{-0.13}$	8/4	1.48E−05	19.4	7	3A	...	...	...	...	...	...	...	...
1ES0242+532	02 42 40	+53 14 10	$0.38^{+0.22}_{-0.16}$	5/3	5.62E−05	12.1	11	3A	...	...	...	...	...	...	...	...
1ES0244+694	02 44 21	+69 26 27	$0.62^{+0.24}_{-0.19}$	10/3	8.78E−09	14.9	5	3A	663	0.9	...	...	SAO	S:A3V	SAO 012445	0.7
1ES0244+191	02 44 38	+19 09 57	$0.29^{+0.10}_{-0.09}$	13/3	7.30E−08	39.0	6	3A	664	0.1	...	...	SAO	S:G0	SAO 093105	0.1
1ES0245+120	02 45 32	+12 03 17	$0.54^{+0.30}_{-0.22}$	5/2	3.34E−05	8.7	10	3A	...	...	...	...	...	...	...	...
1ES0245+309	02 45 42	+30 54 16	$0.96^{+0.19}_{-0.17}$	32/5	1.00E−10	31.6	5	3A	669	0.4	...	...	WLY	S:G9	VY ARI	0.3
1ES0247−253	02 47 16	−25 20 03	$0.18^{+0.09}_{-0.07}$	7/1	1.04E−05	35.5	8	3A	...	...	...	...	...	...	...	...
1ES0249−251	02 49 09	−25 08 09	$0.18^{+0.06}_{-0.05}$	14/4	7.24E−08	67.0	6	3A	673	1.0	...	...	ABL	CG:0.116	A389	1.3
1ES0250−129	02 50 06	−12 58 07	$0.17^{+0.07}_{-0.06}$	13/2	1.06E−05	57.9	4	3A	674	0.9	...	...	BSC	S:K2V	HD 17925	0.0
1ES0250−618	02 50 41	−61 50 01	$0.35^{+0.15}_{-0.12}$	9/5	2.98E−07	23.1	4	3A	...	...	1H0256−617	0.6	SBD	AC:K1Vp	SAO 248669	0.6
1ES0252−085	02 52 34	−08 30 59	$0.31^{+0.20}_{-0.14}$	4/3	6.31E−05	12.2	12	3A	...	...	...	...	...	...	...	...
1ES0254−467	02 54 56	−46 44 45	$0.23^{+0.12}_{-0.09}$	7/5	9.69E−05	25.8	4	3A	...	...	...	...	...	...	...	...
1ES0255+139	02 55 06	+13 56 13	$0.16^{+0.08}_{-0.06}$	8/2	9.40E−05	40.9	8	2A	...	...	...	...	...	...	...	...
1ES0255+128	02 55 08	+12 50 34	$0.26^{+0.04}_{-0.04}$	75/3	1.00E−10	235.2	7	3A	682	0.3	...	...	ABL	CG:0.072	A399*	1.8
1ES0256+133	02 56 06	+13 21 56	$0.26^{+0.07}_{-0.06}$	28/3	1.00E−10	85.2	8	3E	687	1.6	1H0253+138	1.9	ABL	CG:0.075	A401	1.8
1ES0257+442	02 57 22	+44 15 24	$0.73^{+0.38}_{-0.28}$	6/4	8.04E−06	7.5	6	3A	...	...	...	...	UGC	GAL	U02468	1.5
1ES0303+067	03 03 35	+06 44 59	$0.30^{+0.15}_{-0.11}$	7/4	1.79E−05	20.8	10	3A	...	...	...	...	...	...	...	...
1ES0304+407	03 04 56	+40 45 05	$2.68^{+0.70}_{-0.60}$	18/3	1.00E−10	6.6	5	3A	724	0.8	x	...	BSC	S:B8V	β PER	0.9
1ES0305−284	03 05 50	−28 24 24	$0.33^{+0.15}_{-0.12}$	9/3	2.62E−05	22.8	7	3A	...	...	...	...	SBD	S:K7V	CD-28 1030*	0.2
1ES0308−055	03 08 09	−05 33 58	$0.39^{+0.21}_{-0.16}$	6/5	4.91E−05	13.8	7	3A	...	...	...	...	SAO	S:K0	SAO 130323	1.0
1ES0309+479	03 09 48	+47 55 20	$0.16^{+0.08}_{-0.06}$	7/2	3.24E−05	38.6	7	3A	736	0.9	...	...	SAO	AC:G0IV+KIV	LX PER	1.0
1ES0309−291	03 09 58	−29 11 02	$1.02^{+0.25}_{-0.21}$	22/6	1.00E−10	20.5	4	3A	...	...	...	...	WLY	S:F8IV+	WLY 127AB	0.2
1ES0310−568	03 10 04	−56 49 43	$0.23^{+0.10}_{-0.08}$	9/9	2.29E−05	32.7	7	2A	...	...	...	...	...	...	...	...
1ES0310−640	03 10 10	−64 05 01	$0.23^{+0.09}_{-0.07}$	11/9	3.88E−07	41.0	6	2A	...	...	...	...	...	...	...	...
1ES0311−227	03 11 59	−22 46 44	$1.27^{+0.13}_{-0.13}$	108/7	1.00E−10	82.1	5	3A	740	0.3	x1H0311−227	0.2	A3	CV	EF ERI	0.2
1ES0313−770	03 13 00	−77 03 18	$0.14^{+0.05}_{-0.04}$	17/2	4.47E−06	89.2	6	3A	746	0.3	...	...	HB	AGN:0.223	PKS	0.4
1ES0315+681	03 15 42	+68 08 46	$0.59^{+0.36}_{-0.26}$	4/3	1.20E−05	6.6	9	1A	...	...	...	...	SBD	S:F0	AG+68 165*	1.3
1ES0316−444	03 16 11	−44 24 39	$0.97^{+0.45}_{-0.35}$	7/4	1.15E−06	6.7	7	3A	...	...	x1H0315−445	0.4	ABL	CG:0.070	A3112	0.4
1ES0316+413	03 16 31	+41 19 48	$7.25^{+0.15}_{-0.15}$	2420/6	1.00E−10	316.4	7	3A	751	0.2	x1H0316+413.AB	0.2	VV	BL:0.017	A426*	0.3

TABLE 6—*Continued*

Slew Desig.	RA 1950	DEC 1950	IPC Rate (cts s^{-1})	NP/NS	P_{rand}	Exp. (s)	PI	QI	EOS # EMSS	Δ2E (′)	A3 EXO	Δ1H (′)	Cat.	Class.: Type/z	Name	ΔC (′)
1ES0316+031	03 16 44	+03 11 20	$0.28^{+0.10}_{-0.08}$	11/4	1.20E−05	36.1	4	3A	782	0.8	x	...	WLY	S:G5V	WLY 137	0.0
1ES0323+285	03 23 32	+28 32 16	$3.49^{+0.22}_{-0.22}$	252/4	1.00E−10	70.7	5	3A	770	0.2	x1H0334+291	0.3	SBD	AC:G5IV+K0	UX ARI	0.3
1ES0323+022	03 23 39	+02 14 37	$0.80^{+0.24}_{-0.20}$	15/6	1.00E−10	17.6	7	3A	771	0.3	x1H0323+022	0.2	VV	BL:0.147	H 0323+022	0.3
1ES0324+098	03 24 26	+09 33 42	$0.54^{+0.21}_{-0.17}$	9/4	9.51E−09	15.7	7	3A	...	...	...	...	BSC	S:B9Vn	HD 21364	0.3
1ES0325+042	03 25 17	+04 13 13	$0.29^{+0.12}_{-0.10}$	10/5	2.85E−06	29.4	6	3A	...	...	...	...	...	...	...	...
1ES0327−242	03 27 11	−24 16 15	$0.19^{+0.06}_{-0.05}$	22/3	8.24E−08	87.5	3	3A	m783	0.7	...	...	SAO	S:K5	SAO 168581	0.4
1ES0328+054	03 28 14	+05 27 48	$0.45^{+0.17}_{-0.14}$	12/5	8.52E−08	23.0	6	3A	...	...	...	...	...	...	...	...
1ES0330−621	03 30 08	−62 07 17	$0.42^{+0.20}_{-0.16}$	8/5	3.76E−05	16.2	7	3A	...	...	...	...	...	...	...	...
1ES0334+004	03 34 14	+00 25 24	$4.02^{+0.11}_{-0.11}$	1349/9	1.00E−10	331.8	4	3A	804	0.3	x1H0327+000	0.2	SBD	AC:G9V	V711 TAU	0.3
1ES0339−214	03 39 52	−21 24 12	$0.75^{+0.12}_{-0.11}$	46/4	1.00E−10	57.9	6	3A	m826	0.1	...	...	MS	AGN:0.015	MS	0.2
1ES0341−538	03 41 40	−53 49 14	$0.37^{+0.16}_{-0.13}$	9/4	1.92E−05	20.6	7	3A	845	1.9	1H0341−537	1.3	ABL	CG:0.059	A3158	1.3
1ES0342−293	03 42 39	−29 21 59	$0.26^{+0.15}_{-0.11}$	5/2	7.27E−05	17.7	7	3A	...	...	...	...	...	...	...	...
1ES0346−277	03 46 07	−27 44 38	$0.62^{+0.35}_{-0.26}$	5/2	5.77E−05	7.4	6	3A	...	...	...	...	...	...	...	...
1ES0347−121	03 47 02	−12 08 33	$1.47^{+0.28}_{-0.25}$	34/7	1.00E−10	22.4	5	3A	...	...	...	...	...	...	...	...
1ES0347+170	03 47 33	+17 05 31	$0.47^{+0.09}_{-0.08}$	38/3	1.00E−10	75.9	5	3A	894	0.3	x	...	MCS	WD:DA2	BD+16 516	0.9
1ES0348+084	03 48 05	+08 24 02	$0.29^{+0.18}_{-0.13}$	4/3	8.20E−05	13.2	6	3A	...	...	...	...	...	...	...	...
1ES0350+556	03 50 09	+55 38 02	$0.23^{+0.12}_{-0.09}$	6/4	1.06E−04	22.8	7	3A	...	...	...	...	...	...	...	...
1ES0352+308	03 52 14	+30 53 54	$2.07^{+0.38}_{-0.34}$	36/5	1.00E−10	16.9	8	3A	906	0.5	x1H0352+308	0.2	A3	XRB-Be	ξ PER	0.3
1ES0352−686	03 52 52	−68 40 15	$0.49^{+0.12}_{-0.11}$	22/14	1.00E−10	40.9	6	3A	...	...	...	...	...	...	...	...
1ES0353−741	03 53 23	−74 10 07	$0.19^{+0.07}_{-0.06}$	17/3	5.17E−06	64.3	7	3A	m908	0.6	1H0350−735	1.7	A3	CG:0.127	MS	1.7
1ES0355−612	03 55 19	−61 12 55	$0.33^{+0.10}_{-0.09}$	18/12	2.85E−09	45.9	6	3A	...	...	...	...	...	...	...	...
1ES0356−788	03 56 05	−78 52 08	$1.14^{+0.65}_{-0.48}$	5/2	3.73E−05	4.1	3	3A	...	...	...	...	...	...	...	...
1ES0357−400	03 57 56	−40 01 50	$0.30^{+0.13}_{-0.10}$	10/6	6.64E−06	28.1	6	3A	...	...	...	...	SBD	S:K0	HD 25300	1.2
1ES0359+403	03 59 24	+40 21 56	$0.46^{+0.34}_{-0.23}$	3/3	9.48E−05	6.3	6	2A	...	...	...	...	...	...	...	...
1ES0402−362	04 02 01	−36 13 31	$0.49^{+0.28}_{-0.21}$	5/2	8.44E−05	9.4	7	3A	m931	0.8	...	...	HB	AGN:1.417	PKS	0.5
1ES0403−373	04 03 13	−37 19 12	$0.42^{+0.15}_{-0.13}$	12/6	3.97E−08	25.1	6	3A	...	...	...	...	SBD	GAL:0.055	ESO 359- 19	0.2
1ES0403+201	04 03 21	+20 10 11	$0.52^{+0.32}_{-0.23}$	4/2	2.99E−05	7.4	11	3A	...	...	...	...	...	...	...	...
1ES0404+659	04 04 11	+65 57 24	$0.52^{+0.33}_{-0.23}$	4/3	4.84E−05	7.4	5	3A	...	...	...	...	...	...	...	...
1ES0405−123	04 05 25	−12 20 06	$0.36^{+0.09}_{-0.08}$	24/1	1.00E−10	58.3	7	3A	938	0.9	1H0413−116	0.8	VV	AGN:0.574	MS	0.8
1ES0406+099	04 06 55	+09 59 33	$0.22^{+0.14}_{-0.10}$	4/2	6.72E−05	17.0	8	3A	...	...	...	...	SBD	S	HG 7-114	2.5
1ES0407−080	04 07 17	−08 01 52	$1.98^{+0.32}_{-0.29}$	46/2	1.00E−10	22.5	5	3A	943	0.5	1H0409−078	0.5	A3	AC	SAO 130994	0.6
1ES0407+163	04 07 43	+16 23 01	$0.32^{+0.18}_{-0.13}$	5/3	1.78E−05	14.5	6	3A	...	...	...	...	...	...	...	...
1ES0408−587	04 08 20	−58 47 54	$0.37^{+0.17}_{-0.14}$	7/6	2.48E−06	17.4	9	2A	...	...	...	...	...	...	...	...

TABLE 6—*Continued*

Slew Desig.	RA 1950	DEC 1950	IPC Rate (cts s^{-1})	NP/NS	P_{rand}	Exp. (s)	PI	QI	EOS # EMSS	Δ2E (′)	A3 EXO	Δ1H (′)	Cat.	Class.: Type/z	Name	ΔC (′)
1ES0410+103	04 10 37	+10 19 34	$0.79^{+0.17}_{-0.15}$	29/7	1.00E−10	34.5	6	3A	949	1.1	x1H0409+102	2.3	ABL	CG:0.090	A478	1.5
1ES0411+261	04 11 30	+26 09 35	$0.14^{+0.07}_{-0.05}$	8/2	9.65E−05	46.4	5	3A	952	0.7	...	...	SAO	S:G5	SAO 076514	1.6
1ES0412−382	04 12 09	−38 12 03	$0.64^{+0.30}_{-0.23}$	7/3	1.17E−06	10.1	6	3A	...	...	...	...	EXC	GAL:0.050	ESO(B) 303R	1.5
1ES0412+060	04 12 48	+06 04 15	$0.16^{+0.03}_{-0.03}$	41/5	1.00E−10	206.9	4	3A	956	0.2	...	...	BSC	S:G0IV	HD26923	0.5
1ES0413−625	04 13 36	−62 34 55	$0.15^{+0.05}_{-0.05}$	17/7	2.27E−06	83.6	5	3A	m958	1.2	...	...	BSC	S:G8II-III	HD27256	1.6
1ES0414+009	04 14 19	+00 57 36	$1.59^{+0.66}_{-0.52}$	8/2	7.74E−10	4.8	6	3A	959	0.8	x1H0414+009	0.6	HB	BL:0.287	1H	0.6
1ES0414−417	04 14 33	−41 47 32	$0.27^{+0.15}_{-0.11}$	5/4	1.57E−05	17.3	10	3A	...	...	...	...	...	...	...	...
1ES0414+365	04 14 49	+36 35 19	$0.30^{+0.16}_{-0.12}$	5/4	5.86E−07	16.0	9	3A	...	...	...	...	...	...	...	...
1ES0414+379	04 14 58	+37 54 33	$0.41^{+0.12}_{-0.10}$	18/4	1.00E−10	38.6	7	3A	963	0.7	1H0414+380	0.6	VV	AGN:0.048	3C 111.0	0.6
1ES0415+231	04 15 06	+23 09 27	$0.35^{+0.15}_{-0.12}$	8/4	7.50E−07	21.1	6	3A	...	...	...	...	SBD	S:K0	HD 284303	1.2
1ES0415+283	04 15 24	+28 19 50	$0.26^{+0.09}_{-0.08}$	13/5	4.34E−07	42.5	6	3A	...	...	x	...	GCV	S:K3E-K7E	V410 TAU	0.3
1ES0415+790	04 15 54	+79 02 13	$0.30^{+0.21}_{-0.14}$	3/2	2.32E−05	10.0	9	3A	...	...	...	...	...	...	...	...
1ES0418+281	04 18 51	+28 10 32	$0.26^{+0.12}_{-0.09}$	9/3	1.52E−05	29.5	6	3A	987	0.8	1H0419+280.A	0.7	SBD	AC:G2III	SAO 076567	0.6
1ES0418−550	04 18 52	−55 03 02	$0.34^{+0.07}_{-0.06}$	39/6	1.00E−10	101.2	6	3A	988	0.5	x1H0414−551	0.4	VV	AGN:0.005	NGC 1566	0.4
1ES0419−826	04 19 19	−82 40 33	$0.61^{+0.34}_{-0.25}$	5/3	1.68E−05	7.7	6	3A	...	...	...	...	...	...	...	...
1ES0419+148	04 19 36	+14 48 40	$0.07^{+0.03}_{-0.02}$	22/12	1.33E−05	197.1	6	3M	...	...	...	...	SBD	S:F8	HD 285756	2.2
1ES0419+149	04 19 57	+14 56 42	$0.09^{+0.03}_{-0.02}$	31/12	4.15E−08	240.4	5	3M	1000	0.7	...	...	SAO	S:G0	SAO 093896	0.7
1ES0421+146	04 21 22	+14 38 46	$0.17^{+0.03}_{-0.03}$	47/16	1.00E−10	221.0	5	3A	1020	0.2	...	...	SAO	S:G0	SAO 093910	0.3
1ES0422−146	04 22 03	−14 39 12	$0.87^{+0.64}_{-0.43}$	3/2	5.22E−05	3.4	10	3A	...	...	...	...	...	...	...	...
1ES0423+154	04 23 29	+15 29 54	$0.25^{+0.05}_{-0.04}$	42/13	1.00E−10	143.8	5	3A	1034	0.5	x	...	BSC	S:F0V	HD28052	0.5
1ES0423+146	04 23 51	+14 36 12	$0.11^{+0.04}_{-0.03}$	17/10	1.58E−05	112.8	10	1A	...	...	...	...	SAO	S:G7III	SAO 093935	0.9
1ES0424+177	04 24 18	+17 44 42	$0.16^{+0.07}_{-0.06}$	11/5	2.64E−05	54.6	6	3A	1043	0.4	...	...	2E	...	...	...
1ES0424+099	04 24 48	+09 54 13	$0.14^{+0.05}_{-0.04}$	15/9	5.61E−06	80.3	8	2A	...	...	...	...	...	...	...	...
1ES0424+326	04 24 49	+32 40 22	$0.47^{+0.26}_{-0.19}$	5/3	1.76E−05	10.1	6	3A	...	...	...	...	SBD	S:G8	HD 282099	1.3
1ES0425−573	04 25 03	−57 18 41	$0.67^{+0.20}_{-0.17}$	17/6	1.00E−10	22.7	5	3A	...	...	1H0419−577	0.1	A3	AGN	1H	0.1
1ES0426−131	04 26 43	−13 07 07	$0.12^{+0.05}_{-0.04}$	11/3	4.96E−05	72.1	6	3A	...	...	...	...	BSC	S:B1Vne	DU ERI	2.6
1ES0428+366	04 28 41	+36 37 49	$0.59^{+0.36}_{-0.26}$	4/2	2.29E−06	6.6	6	3A	...	...	...	...	SAO	S:G5	SAO 057285	0.8
1ES0429−537	04 29 33	−53 43 18	$0.69^{+0.22}_{-0.18}$	14/8	1.10E−10	18.5	4	3A	...	...	1H0435−531	0.4	VV	AGN:0.040	FAIR 303	0.3
1ES0429+130	04 29 36	+13 00 09	$0.20^{+0.09}_{-0.07}$	9/5	1.16E−05	38.0	4	3A	...	...	...	...	SBD	S:F8	HD 286840*	2.7
1ES0430+052	04 30 32	+05 14 57	$0.68^{+0.03}_{-0.03}$	834/32	1.00E−10	1153.3	7	3A	1087	0.1	x1H0426+051	0.1	VV	AGN:0.033	3C 120	0.1
1ES0430+179	04 30 38	+17 54 34	$0.12^{+0.04}_{-0.03}$	23/4	3.48E−07	134.1	6	3A	m1089	0.2	1H0427+177	0.3	BSC	S:B9IVn	HD28867	0.3
1ES0430−615	04 30 47	−61 31 22	$0.38^{+0.06}_{-0.05}$	75/7	1.00E−10	162.6	6	3E	1090	1.8	...	...	ABL	CG:0.055	ESO 118- 30	2.7
1ES0431−133	04 31 21	−13 22 00	$1.00^{+0.06}_{-0.06}$	315/7	1.00E−10	292.3	6	3A	1092	0.5	x1H0430−133	0.7	ABL	CG:0.032	A496	1.2

TABLE 6—*Continued*

Slew Desig.	RA 1950	DEC 1950	IPC Rate (cts s^{-1})	NP/NS	P_{rand}	Exp. (s)	PI	QI	EOS # EMSS	Δ2E (′)	A3 EXO	Δ1H (′)	Cat.	Class.: Type/s	Name	ΔC (′)
1ES0433+270	04 33 42	+27 02 15	$0.73^{+0.10}_{-0.09}$	69/3	1.00E−10	90.5	4	3A	1103	0.4	...	...	SAO	S:K2	SAO 076672	0.2
1ES0435−472	04 35 54	−47 17 14	$0.50^{+0.23}_{-0.18}$	8/5	5.27E−06	14.1	4	3A	...	...	...	...	...	...	...	...
1ES0437−046	04 37 02	−04 41 30	$0.50^{+0.16}_{-0.14}$	14/6	1.95E−10	25.3	8	3A	...	...	...	...	GCV	S	BF ERI	0.6
1ES0437+444	04 37 21	+44 25 55	$2.78^{+0.95}_{-0.78}$	11/1	1.00E−10	3.9	10	3A	...	...	...	...	GCV	S	OU PER	1.9
1ES0437+035	04 37 22	+03 32 42	$0.27^{+0.14}_{-0.11}$	6/3	4.03E−05	19.7	9	3A	...	...	...	...	...	...	...	...
1ES0439−085	04 39 30	−08 32 20	$0.21^{+0.10}_{-0.08}$	8/4	6.02E−05	32.1	5	3A	...	...	...	...	...	...	...	...
1ES0439−682	04 39 56	−68 14 44	$0.20^{+0.08}_{-0.07}$	13/11	1.39E−05	50.8	2	3A	...	...	...	...	...	...	...	...
1ES0441−107	04 41 22	−10 46 31	$0.12^{+0.04}_{-0.04}$	20/4	9.93E−07	117.6	8	3A	1142	0.7	...	...	SAO	S:A5	RZ ERI	0.7
1ES0444−704	04 44 32	−70 24 51	$0.20^{+0.08}_{-0.06}$	11/5	3.26E−08	48.5	3	3A	...	...	...	...	HD	S:K7	HD270712	0.8
1ES0445−291	04 45 57	−29 11 20	$0.99^{+0.61}_{-0.43}$	4/1	4.84E−06	3.9	5	3A	...	...	...	...	...	...	...	...
1ES0446+449	04 46 12	+44 56 08	$0.15^{+0.04}_{-0.04}$	30/4	2.06E−06	128.1	8	3E	...	...	...	...	...	...	...	...
1ES0447+068	04 47 10	+06 51 40	$0.77^{+0.33}_{-0.26}$	8/1	2.14E−07	9.6	4	3A	...	...	...	...	SAO	S:F6V	SAO 112106	1.0
1ES0452−559	04 52 25	−55 55 54	$0.27^{+0.08}_{-0.07}$	17/3	1.00E−10	55.1	5	3A	1177	1.2	x1H0451−560	1.0	A3	AC	1H	1.0
1ES0453−685	04 53 50	−68 33 40	$0.16^{+0.07}_{-0.06}$	12/8	7.09E−05	54.9	6	3A	1184	0.6	...	...	2E	SNR	...	...
1ES0454−220	04 54 00	−22 03 30	$0.17^{+0.07}_{-0.06}$	14/2	5.87E−06	62.1	8	3A	1185	0.3	...	...	HB	AGN:0.534	PKS	0.7
1ES0456−632	04 56 06	−63 17 36	$0.26^{+0.14}_{-0.10}$	6/4	5.16E−05	20.8	6	3A	...	...	...	...	...	...	...	...
1ES0457+017	04 57 00	+01 42 29	$0.39^{+0.06}_{-0.06}$	50/2	1.00E−10	117.1	5	3A	1191	0.1	x	...	WLY	S:M1EV	WLY 182	0.3
1ES0459+034	04 59 31	+03 27 38	$0.45^{+0.11}_{-0.10}$	24/2	1.00E−10	48.0	7	3A	m1208	0.3	1H0510+031	0.1	VV	AGN:0.016	GHIGO	0.1
1ES0459−753	04 59 47	−75 21 49	$0.44^{+0.16}_{-0.13}$	12/6	2.34E−08	24.0	8	3A	...	...	x1H0502−755	0.8	SBD	AC:K1IIIp	HD32918	0.9
1ES0501+589	05 01 50	+58 57 06	$0.35^{+0.11}_{-0.09}$	16/3	1.00E−10	41.0	6	3A	1213	0.3	1H0501+592	0.2	A3	AC	BM CAM	0.2
1ES0502+675	05 02 42	+67 34 03	$0.59^{+0.33}_{-0.24}$	5/3	2.34E−05	7.9	7	3A	...	...	...	...	SBD	GAL	Z 0502.3+6735	2.6
1ES0504−575	05 04 40	−57 32 10	$0.76^{+0.26}_{-0.21}$	12/7	1.00E−10	14.7	4	3A	...	...	...	...	WLY	S:F8V	WLY 189	0.3
1ES0505−054	05 05 01	−05 28 03	$0.35^{+0.07}_{-0.07}$	33/5	1.00E−10	82.4	8	3A	m1220	0.1	...	...	MS	AC	MS	1.1
1ES0505−679	05 05 48	−67 56 28	$0.71^{+0.16}_{-0.14}$	28/9	1.00E−10	35.6	5	3A	1222	0.3	...	...	2E	SNR	DEM 17	0.8
1ES0505−546	05 05 58	−54 38 09	$0.47^{+0.20}_{-0.16}$	8/6	6.29E−08	16.0	6	3A	...	...	...	...	...	...	...	...
1ES0506−680	05 06 11	−68 05 36	$0.28^{+0.11}_{-0.09}$	15/7	2.18E−05	39.6	7	3M	1223	0.7	...	...	2E	SNR	N23 (LMC)	0.9
1ES0507−040	05 07 15	−04 04 52	$0.35^{+0.15}_{-0.12}$	9/5	1.91E−06	22.6	6	3A	...	...	x1H0506−039	1.4	A3	BL	EXO	1.4
1ES0509−687	05 09 15	−68 47 13	$0.81^{+0.12}_{-0.10}$	62/14	1.00E−10	71.6	5	3A	1232	0.2	x	...	2E	SNR	N103B (LMC)	0.5
1ES0509−675	05 09 28	−67 34 54	$0.26^{+0.04}_{-0.04}$	60/7	1.00E−10	185.0	5	3A	1235	1.1	...	...	2E	SNR	...	...
1ES0510−119	05 10 00	−11 56 02	$0.31^{+0.11}_{-0.09}$	13/8	2.57E−08	36.5	6	3A	...	...	...	...	SAO	S:B8V	SAO 150223	0.5
1ES0510−162	05 10 42	−16 16 16	$0.07^{+0.03}_{-0.02}$	24/3	8.62E−05	207.0	6	3A	1236	0.6	x	...	SAO	S:A0P	μ LEP	0.4
1ES0511−483	05 11 03	−48 20 29	$0.52^{+0.29}_{-0.21}$	5/4	3.54E−05	9.0	7	3A	...	...	...	...	...	...	...	...
1ES0512−401	05 12 31	−40 06 10	$0.89^{+0.55}_{-0.39}$	4/2	1.26E−05	4.3	5	3A	...	...	x1H0512−401	0.5	A3	XRB	Y COL	0.6

TABLE 6—*Continued*

Slew Desig.	RA 1950	DEC 1950	IPC Rate (cts s^{-1})	NP/NS	P_{rand}	Exp. (s)	PI	QI	EOS # EMSS	Δ2E (′)	A3 EXO	Δ1H (′)	Cat.	Class.: Type/s	Name	ΔC (′)
1ES0513−002	05 13 38	−00 12 51	$0.58^{+0.16}_{-0.14}$	18/1	1.00E−10	28.5	7	3A	1240	0.6	x	...	VV	AGN:0.033	AKN 120	0.6
1ES0518−458	05 18 24	−45 49 42	$0.47^{+0.08}_{-0.07}$	44/5	1.00E−10	85.6	6	3A	1252	0.2	x1H0507−459	1.0	VV	AGN:0.034	PIC A	1.0
1ES0519−690	05 19 55	−69 05 09	$0.68^{+0.07}_{-0.07}$	111/18	1.00E−10	151.7	6	3A	1257	0.1	...	...	2E	SNR	LMC	0.2
1ES0521−720	05 21 17	−72 00 27	$7.27^{+0.24}_{-0.24}$	919/18	1.00E−10	125.1	7	3A	1264	0.1	x1H0521−720	0.1	A3	XRB	LMC X-2	0.1
1ES0523−543	05 23 53	−54 19 13	$0.36^{+0.17}_{-0.13}$	8/4	1.04E−05	19.5	8	3A	...	...	...	...	...	...	...	...
1ES0524−711	05 24 50	−71 11 13	$0.12^{+0.04}_{-0.03}$	27/11	1.94E−06	144.8	6	3A	1276	1.2	...	...	SBD	S:Be	BI 156	2.2
1ES0525−660	05 25 22	−66 02 01	$0.34^{+0.08}_{-0.07}$	33/18	1.00E−10	79.1	5	3M	1277	0.4	x	...	2E	SNR	N49B (LMC)	0.3
1ES0525+713	05 25 51	+71 21 09	$0.36^{+0.21}_{-0.15}$	5/3	1.00E−04	12.5	5	3A	...	...	...	...	...	...	...	...
1ES0526−661	05 26 03	−66 07 35	$0.85^{+0.11}_{-0.10}$	78/30	1.00E−10	85.9	6	3A	1279	0.8	x	...	2E	SNR	N49 (LMC)	0.8
1ES0527+111	05 27 10	+11 11 38	$0.93^{+0.24}_{-0.21}$	29/2	1.69E−10	23.9	4	2A	...	...	...	...	...	...	...	...
1ES0527−328	05 27 37	−32 51 21	$0.14^{+0.05}_{-0.04}$	17/1	7.81E−06	86.5	9	3A	1286	0.4	x1H0527−328	0.6	A3	CV	TV COL	0.6
1ES0528−654	05 28 32	−65 29 15	$2.17^{+0.18}_{-0.18}$	150/30	1.00E−10	66.7	5	3A	1290	0.6	x	...	SAO	S:K1IIIp	SAO 249286	0.5
1ES0529−003	05 29 26	−00 19 55	$0.59^{+0.07}_{-0.07}$	84/4	1.00E−10	131.4	4	3A	1293	0.3	...	...	BSC	S:B0III+O9	δ ORI	0.3
1ES0529+097	05 29 30	+09 47 32	$0.28^{+0.08}_{-0.07}$	18/1	1.00E−10	55.1	5	3A	1294	0.3	...	...	GCV	S:M4VE	V 998ORI	0.2
1ES0531+100	05 31 48	+10 05 18	$0.18^{+0.05}_{-0.05}$	22/2	2.87E−08	95.4	5	3A	1315	0.1	...	...	SBD	S	HD 245059	0.3
1ES0532+215	05 32 12	+21 34 35	$3.96^{+1.38}_{-1.15}$	14/1	7.97E−08	3.0	7	2M	...	...	...	...	...	...	...	...
1ES0532−664	05 32 49	−66 24 19	$0.44^{+0.08}_{-0.07}$	41/16	1.00E−10	83.5	6	3A	1368	0.2	x1H0534−667	0.2	A3	XRB	LMC X-4	0.2
1ES0532−054	05 32 50	−05 25 07	$1.24^{+0.06}_{-0.06}$	455/7	1.00E−10	338.6	7	3A	1366	0.1	x	...	SAO	S:OE5	ORI STARS	0.2
1ES0532−059	05 32 57	−05 56 16	$0.44^{+0.05}_{-0.05}$	106/8	1.00E−10	212.1	4	3A	1377	0.7	x	...	BSC	S:O9III	HD 37043	0.5
1ES0533+215	05 33 04	+21 31 54	$1.90^{+0.46}_{-0.40}$	25/1	1.00E−10	11.6	7	2M	...	...	...	...	...	...	...	...
1ES0534−580	05 34 02	−58 03 53	$0.47^{+0.08}_{-0.07}$	44/5	1.00E−10	86.9	4	3A	1425	0.5	x1H0538−577	0.4	A3	CV	TW PIC	0.4
1ES0534−077	05 34 16	−07 42 00	$0.24^{+0.10}_{-0.08}$	9/6	3.92E−07	34.4	7	3A	...	...	...	...	SBD	...	KMS 66	1.9
1ES0534−699	05 34 27	−69 57 16	$0.06^{+0.02}_{-0.02}$	55/16	2.01E−05	437.0	5	3A	1436	0.9	...	...	2E	SNR	DEM 238	0.7
1ES0535−660	05 35 40	−66 03 59	$2.83^{+0.16}_{-0.16}$	321/30	1.00E−10	111.6	6	3A	1461	0.2	x	...	2E	SNR	N63A (LMC)	0.1
1ES0536−580	05 36 36	−58 02 39	$0.13^{+0.06}_{-0.04}$	11/4	6.25E−05	66.7	9	3A	...	...	...	...	...	...	...	...
1ES0538−691A	05 38 05	−69 11 48	$0.12^{+0.02}_{-0.02}$	128/27	1.00E−10	518.9	7	3A	1499	0.6	x	...	2E	SNR	N157B (LMC)	0.6
1ES0538−019	05 38 14	−01 58 54	$0.73^{+0.31}_{-0.24}$	8/2	6.83E−08	10.3	5	3A	1500	1.0	...	...	SBD	S:O9Iab:	HD 37742*	0.9
1ES0538−641	05 38 40	−64 06 42	$16.98^{+0.56}_{-0.56}$	945/26	1.00E−10	55.3	7	3A	...	...	1H0538−641	0.2	A3	XRB	LMC X-3	0.1
1ES0538+037	05 38 46	+03 45 20	$0.20^{+0.07}_{-0.06}$	14/1	2.28E−06	55.7	5	3A	1507	0.6	...	...	SAO	S:G5	SAO 113040	0.9
1ES0538−691B	05 38 52	−69 06 32	$0.08^{+0.02}_{-0.02}$	97/22	3.86E−06	467.4	6	1M	1513	1.4	x	...	2E	SNR	2E	1.4
1ES0540−697	05 40 06	−69 46 09	$10.71^{+0.10}_{-0.10}$	11654/44	1.00E−10	1077.1	7	3A	1522	0.2	x1H0540−697	0.1	A3	XRB	LMC X-1	0.1
1ES0540−693	05 40 37	−69 21 35	$0.48^{+0.03}_{-0.03}$	553/42	1.00E−10	947.5	7	3A	1525	0.2	x	...	2E	P	2E	0.4
1ES0543−555	05 43 02	−55 34 09	$0.40^{+0.19}_{-0.15}$	8/5	1.87E−05	17.2	5	3A	...	...	...	...	RNG	GAL:0.015	NGC 2087	3.0

TABLE 6—*Continued*

Slew Desig.	RA 1950	DEC 1950	IPC Rate (cts s^{-1})	NP/NS	P_{rand}	Exp. (s)	PI	QI	EOS # EMSS	Δ2E (′)	A3 EXO	Δ1H (′)	Cat.	Class.: Type/s	Name	ΔC (′)
1ES0543−683	05 43 39	−68 23 17	$0.22^{+0.06}_{-0.05}$	23/7	6.01E−10	82.4	5	3A	1550	1.0	x	...	2E	S	...	...
1ES0545−336	05 45 12	−33 38 50	$0.40^{+0.15}_{-0.12}$	10/4	1.76E−08	23.1	4	3A	...	...	...	...	...	...	...	...
1ES0546−642	05 46 30	−64 15 18	$0.17^{+0.07}_{-0.06}$	12/11	1.21E−05	56.5	5	3A	...	...	...	...	...	...	...	...
1ES0547−697	05 47 35	−69 42 44	$0.04^{+0.01}_{-0.01}$	114/18	3.81E−07	1018.2	6	3A	1570	0.8	...	...	2E	SNR	N138 (LMC)	0.8
1ES0548−322	05 48 50	−32 16 54	$2.22^{+0.16}_{-0.16}$	194/3	1.00E−10	85.7	5	3A	1574	0.2	x1H0548−322	0.3	HB	BL:0.069	PKS	0.1
1ES0549+891	05 49 10	+89 07 20	$0.73^{+0.54}_{-0.36}$	3/1	1.07E−04	4.0	13	1A	...	...	...	...	...	...	...	...
1ES0552−641	05 52 04	−64 06 06	$0.17^{+0.07}_{-0.06}$	13/9	5.06E−05	56.1	7	3A	...	...	...	...	...	...	...	...
1ES0556−532	05 56 57	−53 16 07	$0.34^{+0.15}_{-0.12}$	8/4	4.66E−06	20.8	6	2A	...	...	...	...	...	...	...	...
1ES0558−504	05 58 33	−50 27 29	$2.00^{+0.46}_{-0.40}$	22/6	1.00E−10	10.9	4	3A	...	...	x1H0557−503	0.6	HB	AGN:0.137	PKS	0.6
1ES0559−399	05 59 51	−39 56 35	$0.07^{+0.02}_{-0.02}$	32/4	8.98E−05	247.8	6	3A	...	...	...	...	EXC	GAL	GAL 0559-3959	2.7
1ES0602−482	06 02 48	−48 17 36	$0.60^{+0.28}_{-0.22}$	8/4	2.33E−05	11.4	5	3M	...	...	...	...	...	...	...	...
1ES0603−484	06 03 27	−48 27 25	$0.84^{+0.33}_{-0.26}$	10/4	5.37E−08	10.8	3	3M	...	...	...	...	SAO	S:G5	SAO 217708	0.5
1ES0606+349	06 06 54	+34 58 56	$0.92^{+0.66}_{-0.44}$	3/1	4.24E−06	3.3	13	3A	...	...	...	...	...	...	...	...
1ES0613+227	06 13 52	+22 46 40	$0.97^{+0.31}_{-0.26}$	15/3	1.08E−07	12.7	7	3E	...	...	...	...	...	...	...	...
1ES0614+227	06 14 20	+22 45 29	$1.11^{+0.44}_{-0.36}$	12/2	1.02E−05	8.6	7	3E	...	...	...	...	HD	S:K2	HD254475	1.4
1ES0614+091	06 14 24	+09 09 07	$2.57^{+1.43}_{-1.05}$	5/1	8.27E−06	1.8	8	3A	...	...	x1H0610+091	0.4	A3	XRB	V1055 ORI	0.4
1ES0614−584	06 14 57	−58 24 41	$0.41^{+0.10}_{-0.09}$	24/9	1.00E−10	51.9	4	3A	...	...	...	...	...	...	...	...
1ES0615−655	06 15 27	−65 32 01	$0.22^{+0.10}_{-0.08}$	9/7	9.47E−05	33.3	5	3A	...	...	...	...	...	...	...	...
1ES0617−100	06 17 33	−10 00 09	$0.53^{+0.39}_{-0.26}$	3/1	3.34E−05	5.5	8	3A	...	...	...	...	...	...	...	...
1ES0618−580	06 18 25	−58 02 05	$0.33^{+0.10}_{-0.08}$	19/9	1.49E−10	48.9	5	3A	...	...	...	...	SAO	S:K2V	SAO 234448	0.2
1ES0620−666	06 20 13	−66 40 21	$0.20^{+0.09}_{-0.07}$	9/8	4.87E−05	36.3	6	3A	...	...	...	...	...	...	...	...
1ES0622−526	06 22 50	−52 40 19	$0.13^{+0.04}_{-0.03}$	29/7	3.47E−07	150.4	6	3A	1642	0.3	x	...	BSC	S:F0II	HD 45348	0.2
1ES0623+187	06 23 15	+18 47 57	$0.23^{+0.06}_{-0.05}$	20/2	1.00E−10	76.5	5	3A	1646	0.7	...	...	SAO	S:K3V+	WLY 233AB	0.6
1ES0625−536	06 25 16	−53 40 34	$0.13^{+0.04}_{-0.04}$	29/9	4.06E−07	145.3	6	3E	1656	2.0	...	...	ABL	CG:0.053	A3391	1.7
1ES0625−600	06 25 27	−60 01 12	$0.19^{+0.08}_{-0.07}$	11/5	3.82E−05	45.9	6	3A	...	...	...	...	...	...	...	...
1ES0626−544	06 26 31	−54 24 00	$0.07^{+0.02}_{-0.02}$	46/6	6.78E−05	311.0	5	3E	...	...	1H0623−539	2.0	ABL	CG:0.050	A3395	2.0
1ES0626−027	06 26 52	−02 47 02	$0.45^{+0.24}_{-0.18}$	6/4	9.83E−05	11.9	4	3A	1663	0.7	...	...	GCV	S:M4.5VE	V577 MON	0.8
1ES0627−018	06 27 17	−01 48 36	$0.49^{+0.22}_{-0.17}$	7/5	1.32E−07	13.6	6	3A	...	...	...	...	...	...	...	...
1ES0629+068	06 29 07	+06 49 03	$0.16^{+0.06}_{-0.05}$	16/7	3.29E−05	71.2	4	3A	1678	0.6	...	...	SAO	S:G3IV	SAO 114005	0.5
1ES0629+049	06 29 31	+04 57 17	$0.09^{+0.03}_{-0.03}$	28/6	1.00E−05	199.6	6	3E	1684	1.7	...	...	2E	SNR	MON. NEBULA	1.5
1ES0630+178	06 30 59	+17 48 41	$0.14^{+0.03}_{-0.03}$	40/8	1.00E−10	215.7	3	3A	1697	0.4	x	...	SBD	S	2CG 195 +04	0.1
1ES0630−540	06 30 59	−54 03 30	$0.15^{+0.04}_{-0.04}$	25/10	1.02E−07	119.1	6	3A	1695	1.0	...	...	2E	...	...	...
1ES0633−725	06 33 45	−72 35 56	$0.26^{+0.14}_{-0.10}$	6/5	8.41E−05	20.7	4	3A	...	...	...	...	...	...	...	...

TABLE 6—*Continued*

Slew Desig.	RA 1950	DEC 1950	IPC Rate (cts s^{-1})	NP/NS	P_{read}	Exp. (s)	PI	QI	EOS # EMSS	Δ2E (′)	A3 EXO	Δ1H (′)	Cat.	Class.: Type/s	Name	ΔC (′)
1ES0635−747	06 35 08	−74 44 13	$0.23^{+0.09}_{-0.08}$	13/6	1.15E−05	43.0	5	3A	1718	2.1	...	...	2E	...	...	...
1ES0635−206	06 35 23	−20 39 27	$0.14^{+0.06}_{-0.05}$	10/2	6.54E−05	57.1	6	3A	...	...	...	...	...	...	...	...
1ES0635−698	06 35 30	−69 49 44	$0.21^{+0.07}_{-0.06}$	18/11	7.73E−09	69.8	6	3A	...	...	...	...	SBD	S:G3V	HD 47875	2.2
1ES0637−337	06 37 20	−33 45 40	$0.65^{+0.48}_{-0.32}$	3/2	4.76E−05	4.5	3	3A	...	...	...	...	...	...	...	...
1ES0637−752	06 37 23	−75 14 09	$0.16^{+0.05}_{-0.05}$	23/5	6.82E−06	95.0	5	3A	1720	0.6	x1H0633−752	0.5	VV	AGN:0.651	PKS	0.5
1ES0637−614	06 37 26	−61 29 16	$0.56^{+0.15}_{-0.13}$	19/9	1.00E−10	30.7	4	3A	...	...	...	...	BSC	S:G1-2V	HD48189	0.3
1ES0638+099	06 38 12	+09 57 27	$0.18^{+0.04}_{-0.04}$	29/4	1.00E−10	129.1	4	3A	1723	0.8	x	...	BSC	S:O7Ve	MON. STARS	0.9
1ES0638+094	06 38 22	+09 29 07	$0.11^{+0.03}_{-0.03}$	31/4	1.28E−07	191.5	5	3A	1724	1.3	x	...	SAO	S:B3	MON. STARS	2.0
1ES0639−756	06 39 36	−75 36 11	$0.14^{+0.06}_{-0.05}$	16/7	1.06E−04	75.3	7	2A	1725	0.4	...	...	2E	...	...	...
1ES0640+059	06 40 47	+05 54 03	$0.10^{+0.04}_{-0.03}$	18/4	1.05E−05	122.0	9	3A	1726	0.4	...	...	SAO	S:G5III	SAO 114321	0.1
1ES0642−166	06 42 56	−16 39 08	$0.83^{+0.13}_{-0.12}$	50/3	1.00E−10	56.1	2	3A	1730	0.5	x	...	MCS	WD:DA2	α CMA B	0.3
1ES0643−167	06 43 04	−16 47 50	$0.21^{+0.08}_{-0.07}$	19/3	4.89E−05	59.0	8	3M	1731	0.6	x	...	2E	CV	HL CMA	0.6
1ES0644−541	06 44 30	−54 10 18	$0.27^{+0.09}_{-0.08}$	13/10	2.52E−08	42.7	5	3A	...	...	...	...	ABL	CG	A3404	1.3
1ES0646−515	06 46 00	−51 32 09	$0.32^{+0.10}_{-0.09}$	16/7	2.52E−09	43.2	5	3A	...	...	...	...	...	...	...	...
1ES0647+250	06 47 40	+25 05 34	$0.95^{+0.39}_{-0.31}$	8/2	1.59E−10	8.1	6	3A	...	...	...	...	...	...	...	...
1ES0650−371	06 50 17	−37 11 12	$0.61^{+0.30}_{-0.23}$	7/5	3.62E−05	10.1	10	3A	...	...	...	...	...	...	...	...
1ES0651−020	06 51 52	−02 01 48	$0.37^{+0.23}_{-0.16}$	4/2	4.39E−05	10.4	9	3A	...	...	...	...	SBD	S:B	HD 292785	1.5
1ES0655+542	06 55 30	+54 15 20	$0.23^{+0.10}_{-0.08}$	9/1	2.25E−06	35.0	5	3A	1750	1.1	x	...	VV	AGN:0.044	MKN 374	0.9
1ES0656−427	06 56 20	−42 42 05	$0.47^{+0.27}_{-0.20}$	5/3	3.31E−05	9.8	5	3A	...	...	...	...	...	...	...	...
1ES0657−558	06 57 28	−55 52 28	$0.22^{+0.06}_{-0.05}$	26/7	1.00E−10	96.6	6	3A	1759	0.2	...	...	2E	...	...	...
1ES0658−467	06 58 14	−46 45 44	$0.46^{+0.34}_{-0.23}$	3/3	2.23E−05	6.4	13	3A	...	...	...	...	...	...	...	...
1ES0702+646	07 02 27	+64 40 45	$0.17^{+0.08}_{-0.06}$	10/7	5.28E−05	46.6	4	3A	...	...	...	...	VV	AGN:0.079	VII ZW 118*	0.3
1ES0702−241	07 02 56	−24 07 24	$0.60^{+0.30}_{-0.23}$	6/2	3.00E−06	9.4	10	3A	...	...	...	...	...	...	...	...
1ES0710+521	07 10 27	+52 10 56	$0.95^{+0.70}_{-0.47}$	3/2	7.64E−05	3.1	14	3A	...	...	...	...	...	...	...	...
1ES0712−363	07 12 23	−36 21 17	$0.45^{+0.21}_{-0.16}$	8/5	1.86E−05	15.5	7	3A	...	...	...	...	SAO	S:F6-7V	SAO 197732	1.3
1ES0715−810	07 15 44	−81 03 11	$0.33^{+0.16}_{-0.12}$	7/5	8.03E−06	19.1	11	3A	...	...	...	...	...	...	...	...
1ES0715−703	07 15 45	−70 19 10	$0.21^{+0.09}_{-0.07}$	10/8	3.36E−05	38.6	4	3A	...	...	...	...	...	...	...	...
1ES0715−259	07 15 56	−25 59 24	$0.13^{+0.06}_{-0.05}$	12/7	1.04E−04	66.9	7	2A	...	...	...	...	...	...	...	...
1ES0716−248	07 16 38	−24 51 32	$0.06^{+0.02}_{-0.01}$	37/11	1.51E−06	373.3	6	3A	1804	0.1	...	...	SBD	S:O9Ib	HD 57061*	0.2
1ES0717+558	07 17 24	+55 52 47	$0.31^{+0.05}_{-0.05}$	53/2	1.00E−10	147.6	6	3A	1805	1.0	1H0712+558	2.8	ABL	CG:0.038	A576	2.9
1ES0717−572	07 17 29	−57 14 55	$0.48^{+0.18}_{-0.14}$	14/9	9.27E−09	25.5	5	3A	...	...	...	...	SAO	S:G0IV-V	SAO 235087	0.9
1ES0717−500	07 17 35	−50 00 56	$0.68^{+0.42}_{-0.30}$	4/3	2.18E−06	5.8	8	3A	...	...	...	...	...	...	...	...
1ES0718−313	07 18 29	−31 20 02	$0.40^{+0.17}_{-0.14}$	9/5	4.95E−06	19.8	2	3A	...	...	x	...	...	...	...	...

TABLE 6—*Continued*

Slew Desig.	RA 1950	DEC 1950	IPC Rate (cts s^{-1})	NP/NS	P_{rand}	Exp. (s)	PI	QI	EOS # EMSS	Δ2E (′)	A3 EXO	Δ1H (′)	Cat.	Class.: Type/s	Name	ΔC (′)
1ES0729+355	07 29 15	+35 35 55	$0.75^{+0.55}_{-0.37}$	3/1	2.22E−05	3.9	9	3A	...	...	...	...	...	...	...	...
1ES0730+074	07 30 06	+07 29 48	$0.38^{+0.17}_{-0.13}$	8/3	5.90E−06	18.8	9	3A	...	...	...	...	...	...	...	...
1ES0731+319	07 31 27	+31 58 41	$0.90^{+0.11}_{-0.10}$	79/5	1.00E−10	82.3	5	3A	1827	0.4	x1H0729+316	0.2	A3	AC	YY GEM	0.2
1ES0735+178	07 35 12	+17 48 54	$0.04^{+0.01}_{-0.01}$	44/14	6.70E−05	463.2	6	3A	1843	0.6	x	...	HB	BL:0.424	PKS	0.6
1ES0736+053	07 36 35	+05 21 25	$1.44^{+0.59}_{-0.47}$	8/1	1.25E−10	5.4	2	3A	1849	1.4	x	...	WLY	S:F5IV	α CMI A	1.5
1ES0737+395	07 37 08	+39 30 04	$0.35^{+0.17}_{-0.13}$	7/4	9.29E−06	17.8	9	3A	...	...	...	...	...	...	...	...
1ES0737+746	07 37 46	+74 40 58	$0.30^{+0.14}_{-0.11}$	7/3	2.95E−06	21.2	7	3A	m1855	0.6	...	...	MS	BL:0.315	MS	0.6
1ES0738+612	07 38 30	+61 15 37	$0.86^{+0.33}_{-0.26}$	9/2	1.00E−10	10.2	5	3A	...	...	...	...	SAO	S:K0	SAO 014296	1.1
1ES0738+499	07 38 48	+49 56 02	$1.16^{+0.74}_{-0.53}$	4/1	7.18E−05	3.3	6	3A	...	...	x1H0744+499	0.3	VV	AGN:0.022	MKN 79	0.4
1ES0740+290	07 40 11	+29 00 15	$2.09^{+0.15}_{-0.15}$	197/5	1.00E−10	92.0	5	3A	1861	0.2	x1H0741+289	0.1	A3	AC	σ Gem	0.2
1ES0740+228	07 40 38	+22 50 08	$0.42^{+0.19}_{-0.15}$	8/4	9.35E−06	16.7	6	3A	...	...	...	...	SAO	S:K0	SAO 079647	0.2
1ES0742+036	07 42 03	+03 40 27	$0.39^{+0.04}_{-0.04}$	115/5	1.00E−10	261.5	4	3A	1871	0.1	x1H0743+037	0.1	A3	AC	YZ CMI	0.1
1ES0744−594	07 44 41	−59 27 16	$0.32^{+0.18}_{-0.14}$	5/5	1.00E−04	14.2	6	2A	...	...	...	...	...	...	...	...
1ES0745+412	07 45 14	+41 12 58	$0.24^{+0.13}_{-0.10}$	6/4	9.06E−05	22.3	9	3A	...	...	...	...	...	...	...	...
1ES0745−150	07 45 46	−15 03 13	$0.40^{+0.25}_{-0.18}$	4/2	6.80E−06	9.6	9	3A	...	...	...	...	...	...	...	...
1ES0746−007	07 46 38	−00 43 45	$0.58^{+0.36}_{-0.26}$	4/1	2.92E−05	6.6	9	3A	...	...	...	...	...	...	...	...
1ES0749+369	07 49 51	+36 54 32	$0.56^{+0.35}_{-0.25}$	4/3	2.32E−05	6.9	9	3A	...	...	...	...	...	...	...	...
1ES0752+393	07 52 06	+39 19 30	$0.26^{+0.07}_{-0.06}$	22/1	1.00E−10	71.0	5	3A	1888	0.4	x	...	VV	AGN:0.034	MKN 382	0.6
1ES0758+467	07 58 06	+46 46 40	$0.33^{+0.21}_{-0.15}$	4/2	4.65E−05	11.4	12	3A	...	...	...	...	...	...	...	...
1ES0758+574	07 58 29	+57 24 49	$0.25^{+0.06}_{-0.06}$	26/3	1.00E−10	85.8	5	3A	1900	0.3	...	...	BSC	AC:F8V	HD65626	0.5
1ES0801−398	08 01 50	−39 52 06	$0.34^{+0.09}_{-0.08}$	21/4	1.31E−10	52.3	5	3A	1910	0.4	x	...	BSC	S:O5Iaf	HD66811	0.4
1ES0801+242	08 01 51	+24 16 07	$0.91^{+0.49}_{-0.37}$	5/1	1.57E−06	5.3	9	3A	...	...	...	...	...	...	...	...
1ES0804+761	08 04 50	+76 11 34	$0.59^{+0.22}_{-0.18}$	11/3	6.73E−09	16.9	5	3A	1919	0.7	x1H0758+762	0.9	A3	AGN:0.099	PG	0.9
1ES0806+524	08 06 05	+52 27 53	$0.80^{+0.46}_{-0.34}$	5/3	8.36E−05	5.7	5	3A	...	...	...	...	...	...	...	...
1ES0807−471	08 07 59	−47 11 03	$0.18^{+0.05}_{-0.04}$	26/5	1.00E−10	114.7	6	3A	1936	0.3	...	...	BSC	S:WC8+O7.5e	γ VEL	0.2
1ES0808+627	08 08 06	+62 45 39	$0.57^{+0.07}_{-0.06}$	92/6	1.00E−10	151.6	5	3A	1938	0.4	x1H0811+625	0.3	A3	CV	SU UMA	0.3
1ES0808+195	08 08 18	+19 32 22	$0.85^{+0.62}_{-0.42}$	3/2	3.76E−05	3.4	10	3A	...	...	...	...	...	...	...	...
1ES0809+330	08 09 06	+33 02 43	$0.79^{+0.45}_{-0.33}$	5/2	4.13E−05	5.9	9	3A	...	...	...	...	...	...	...	...
1ES0811+530	08 11 12	+53 01 44	$0.36^{+0.18}_{-0.14}$	7/2	4.60E−05	16.8	3	3A	...	...	...	...	...	...	...	...
1ES0811−570	08 11 30	−57 04 44	$0.39^{+0.13}_{-0.11}$	15/5	5.44E−08	32.0	8	3A	1955	0.5	...	...	2E	...	...	...
1ES0812+126	08 12 23	+12 39 29	$0.42^{+0.26}_{-0.19}$	4/3	1.75E−05	9.2	3	3A	...	...	...	...	...	...	...	...
1ES0812−188	08 12 49	−18 53 36	$2.77^{+0.40}_{-0.36}$	56/4	1.00E−10	19.7	3	3A	1959	1.1	x	...	SHA	CV	VV PUP	0.9
1ES0814−073	08 14 58	−07 21 47	$0.64^{+0.05}_{-0.05}$	215/12	1.00E−10	307.8	7	3E	1961	0.5	...	...	2E	CG:0.071	A644	0.5

TABLE 6—*Continued*

Slew Desig.	RA 1950	DEC 1950	IPC Rate (cts s^{-1})	NP/NS	P_{rand}	Exp. (s)	PI	QI	EOS # EMSS	Δ2E (′)	A3 EXO	Δ1H (′)	Cat.	Class.: Type/z	Name	ΔC (′)
1ES0815−480	08 15 49	−48 03 22	$0.23^{+0.10}_{-0.08}$	9/4	1.07E−05	33.5	10	3A	...	...	...	...	...	...	...	...
1ES0817−325	08 17 47	−32 30 40	$0.56^{+0.32}_{-0.23}$	5/3	3.04E−05	8.3	10	3A	...	...	...	...	...	...	...	...
1ES0818+544	08 18 51	+54 28 16	$0.16^{+0.07}_{-0.06}$	10/3	6.33E−05	48.9	4	3A	m1971	0.3	...	...	MS	AGN:0.086	MS	0.5
1ES0821−426	08 21 26	−42 41 34	$4.34^{+0.14}_{-0.00}$	1120/11	1.00E−10	135.0	5	2A	...	...	...	...	...	...	...	...
1ES0824+662	08 24 10	+66 12 23	$0.20^{+0.08}_{-0.07}$	12/2	2.31E−05	46.2	5	3A	1987	0.3	...	...	2E	...	...	...
1ES0825+045	08 25 20	+04 33 27	$0.32^{+0.17}_{-0.13}$	6/5	1.11E−04	16.7	8	3A	...	...	...	...	...	...	...	...
1ES0825−080	08 25 40	−08 02 39	$0.70^{+0.51}_{-0.34}$	3/3	2.57E−05	4.2	6	3A	...	...	...	...	...	...	...	...
1ES0826−703	08 26 20	−70 21 37	$0.23^{+0.10}_{-0.08}$	11/8	6.10E−05	37.5	5	3A	...	...	...	...	...	...	...	...
1ES0826−200	08 26 28	−20 04 05	$0.45^{+0.26}_{-0.19}$	5/2	8.86E−05	10.2	3	3A	...	...	...	...	...	...	...	...
1ES0826+660	08 26 34	+66 01 51	$0.15^{+0.06}_{-0.05}$	12/1	9.17E−05	61.1	6	3A	1995	1.1	...	...	2E	CG:0.181	A665	1.2
1ES0827−687	08 27 35	−68 43 09	$0.15^{+0.07}_{-0.06}$	9/7	1.02E−04	48.5	8	3A	...	...	...	...	...	...	...	...
1ES0829+237	08 29 11	+23 47 10	$0.32^{+0.15}_{-0.12}$	8/1	9.54E−06	21.7	11	3A	...	...	...	...	...	...	...	...
1ES0829+159	08 29 41	+15 59 17	$0.56^{+0.25}_{-0.20}$	8/3	7.11E−06	12.7	6	3A	...	...	...	...	SAO	S	SAO 097895	2.4
1ES0832−421	08 32 16	−42 10 50	$0.36^{+0.12}_{-0.10}$	24/2	9.11E−06	43.5	3	3E	...	...	...	...	...	...	...	...
1ES0833−450	08 33 38	−45 00 33	$1.36^{+0.19}_{-0.18}$	91/7	1.00E−10	51.0	6	3A	2014	0.4	x	...	2E	P	HU VEL	0.5
1ES0834+366	08 34 10	+36 36 22	$0.41^{+0.23}_{-0.17}$	5/3	4.11E−05	11.2	4	3A	...	...	...	...	...	...	...	...
1ES0834+651	08 34 52	+65 11 10	$0.35^{+0.16}_{-0.13}$	8/2	5.60E−06	20.1	3	3A	2018	0.8	x1H0833+654	0.8	A3	AC	π^1 UMA	0.8
1ES0836+319	08 36 01	+31 57 35	$0.14^{+0.06}_{-0.05}$	9/2	3.22E−05	52.3	7	3A	2022	0.8	...	...	SAO	AC:K2III+K4I	RZ CNC	1.1
1ES0836+710	08 36 20	+71 03 33	$0.33^{+0.13}_{-0.10}$	9/6	1.80E−08	25.6	8	3A	...	...	...	...	VV	AGN:2.160	4C 71.07	0.8
1ES0837−425	08 37 05	−42 31 35	$0.48^{+0.16}_{-0.14}$	31/4	6.44E−05	35.4	3	3M	...	...	...	...	...	...	...	...
1ES0837−430	08 37 12	−43 01 00	$1.39^{+0.35}_{-0.32}$	36/4	8.64E−08	16.6	4	3M	2027	2.5	...	...	2E	...	...	...
1ES0837−120	08 37 22	−12 05 23	$0.81^{+0.45}_{-0.33}$	5/2	7.67E−06	5.8	6	3A	2028	2.0	...	...	HB	AGN:0.198	3C 206	2.1
1ES0838+160	08 38 49	+16 00 26	$0.29^{+0.17}_{-0.12}$	5/3	2.79E−05	15.8	3	3A	...	...	...	...	...	...	...	...
1ES0839−333	08 39 03	−33 20 07	$0.37^{+0.23}_{-0.16}$	4/2	5.91E−06	10.4	9	3E	...	...	...	...	...	...	...	...
1ES0839−446	08 39 04	−44 39 13	$0.46^{+0.12}_{-0.11}$	38/3	4.66E−08	53.5	4	3E	...	...	...	...	...	...	...	...
1ES0839−445	08 39 19	−44 31 20	$0.71^{+0.14}_{-0.13}$	50/4	1.00E−10	52.2	4	3A	...	...	...	...	HD	S:A0	HD74209	2.5
1ES0840−420	08 40 03	−42 05 45	$0.31^{+0.11}_{-0.10}$	19/2	1.20E−05	42.4	4	3A	...	...	...	...	...	...	...	...
1ES0841−733	08 41 05	−73 23 48	$0.56^{+0.30}_{-0.23}$	6/4	6.00E−05	9.5	4	3A	...	...	...	...	...	...	...	...
1ES0841−436	08 41 50	−43 39 23	$0.21^{+0.07}_{-0.06}$	56/3	3.76E−05	119.5	3	1A	...	...	...	...	...	...	...	...
1ES0842−425	08 42 21	−42 35 06	$0.49^{+0.15}_{-0.14}$	32/2	1.40E−05	37.8	3	1A	...	...	...	...	...	...	...	...
1ES0844+349	08 44 35	+34 56 17	$0.13^{+0.06}_{-0.04}$	12/4	3.48E−05	69.9	5	3A	2048	0.3	x	...	VV	AGN:0.064	PG	0.3
1ES0847+267	08 47 42	+26 44 00	$0.19^{+0.09}_{-0.07}$	8/5	4.74E−05	36.0	6	3A	...	...	...	...	...	...	...	...
1ES0849+080	08 49 34	+08 04 57	$0.48^{+0.07}_{-0.07}$	58/3	1.00E−10	107.4	5	3A	m2060	0.3	x	...	VV	AGN:0.063	1E	0.7

TABLE 6—*Continued*

Slew Desig.	RA 1950	DEC 1950	IPC Rate (cts s^{-1})	NP/NS	P_{rand}	Exp. (s)	PI	QI	EOS # EMSS	Δ2E (′)	A3 EXO	Δ1H (′)	Cat.	Class.: Type/z	Name	ΔC (′)
1ES0851+392	08 51 05	+39 17 20	$0.53^{+0.19}_{-0.15}$	12/1	5.39E−09	20.6	3	3A	...	...	...	...	...	...	...	...
1ES0851+203	08 51 57	+20 18 07	$0.45^{+0.03}_{-0.03}$	243/17	1.00E−10	489.7	5	3A	2076	0.1	x	...	HB	BL:0.306	OJ 287	0.2
1ES0853−445	08 53 20	−44 32 51	$0.58^{+0.17}_{-0.15}$	28/1	1.07E−07	33.7	2	3E	...	...	...	...	...	...	...	...
1ES0853−448	08 53 58	−44 52 30	$0.69^{+0.21}_{-0.18}$	27/2	6.15E−07	26.4	3	3E	...	...	...	...	...	...	...	...
1ES0856+369	08 56 56	+36 58 04	$0.11^{+0.04}_{-0.04}$	15/5	2.78E−05	97.2	4	3A	2084	0.7	...	...	SBD	S:F8	SAO 61189	2.8
1ES0858+181	08 58 13	+18 06 09	$0.27^{+0.13}_{-0.10}$	7/3	3.56E−05	22.8	6	3A	...	...	x	...	SHA	CV	SY CNC	0.5
1ES0906−094A	09 06 20	−09 26 19	$0.25^{+0.07}_{-0.06}$	27/3	9.38E−08	75.5	6	3M	2100	2.6	1H0906−095	1.4	ABL	CG:0.053	A754	1.0
1ES0906−094B	09 06 45	−09 28 30	$0.49^{+0.09}_{-0.08}$	43/3	1.00E−10	73.9	7	3M	2103	1.2	x	...	2E	CG:0.053	A754	1.2
1ES0914+519	09 14 28	+51 55 48	$0.22^{+0.10}_{-0.08}$	8/6	3.54E−05	31.4	6	3A	...	...	...	...	ABL	CG:0.197	A773	0.9
1ES0915+165	09 15 40	+16 30 26	$0.47^{+0.08}_{-0.07}$	43/3	1.00E−10	85.3	7	3A	2116	0.6	...	...	VV	AGN:0.029	MKN 704	0.6
1ES0915−118	09 15 41	−11 53 15	$0.81^{+0.21}_{-0.18}$	20/3	1.00E−10	23.3	6	3A	2117	0.4	x1H0917−121	0.2	A3	AGN:0.055	3C218	0.2
1ES0919−549	09 19 03	−54 59 23	$4.21^{+1.84}_{-1.43}$	7/1	1.00E−10	1.6	6	3A	...	...	x1H0918−548	1.1	A3	XRB	...	...
1ES0919+404	09 19 15	+40 24 41	$0.86^{+0.39}_{-0.30}$	7/2	2.43E−08	7.8	6	3A	...	...	...	...	SAO	S:K2V	SAO 042826	1.0
1ES0920−136	09 20 30	−13 36 51	$0.63^{+0.31}_{-0.24}$	6/1	7.71E−07	9.0	7	3A	...	...	...	...	SAO	S:K0IV	SAO 155136	0.6
1ES0921+143	09 21 25	+14 22 29	$0.13^{+0.05}_{-0.04}$	16/2	1.19E−05	93.0	7	1A	2131	1.5	...	...	ABL	CG:0.136	A795	1.8
1ES0921−630	09 21 28	−63 04 39	$0.50^{+0.13}_{-0.11}$	21/9	1.00E−10	38.7	6	3A	...	...	x1H0920−629	0.4	A3	XRB	2S	0.4
1ES0921+525	09 21 44	+52 30 41	$1.41^{+0.25}_{-0.22}$	39/11	1.00E−10	26.5	5	3A	...	...	...	...	VV	AGN:0.036	MKN 110	0.6
1ES0923+129	09 23 18	+12 56 32	$0.34^{+0.15}_{-0.12}$	8/1	1.85E−06	20.9	5	3A	2139	0.7	x1H0929+122	0.7	VV	AGN:0.028	MKN 705	0.7
1ES0923+392	09 23 56	+39 15 09	$0.12^{+0.04}_{-0.04}$	22/3	1.05E−05	126.0	5	3A	2141	0.2	x	.	VV	AGN:0.698	4C 39.25	0.3
1ES0923−530	09 23 57	−53 03 13	$0.99^{+0.62}_{-0.44}$	4/1	3.68E−05	3.9	5	3A	...	...	...	...	SAO	S:F7V	SAO 236956	1.1
1ES0924+232	09 24 23	+23 13 00	$0.46^{+0.26}_{-0.19}$	5/2	1.05E−04	10.0	7	3A	...	...	...	...	UGC	GAL:0.026	UO5037*	1.0
1ES0927+500	09 27 11	+50 04 49	$0.65^{+0.24}_{-0.19}$	11/6	1.84E−09	15.6	5	3A	...	...	...	...	SBD	...	H 0927+50.1	2.6
1ES0927+586	09 27 15	+58 41 35	$0.41^{+0.21}_{-0.16}$	6/4	1.01E−05	13.6	5	3A	...	...	...	...	...	...	...	...
1ES0929+216	09 29 14	+21 41 48	$0.10^{+0.03}_{-0.03}$	19/4	1.66E−06	140.7	5	3A	2151	2.4	...	...	RNG	GAL:0.002	NGC 2903	1.1
1ES0930+700	09 30 04	+70 03 18	$0.82^{+0.10}_{-0.09}$	88/5	1.00E−10	102.6	5	3A	2153	0.2	...	...	BSC	S:G4III-IV	DK UMA	0.3
1ES0938−040	09 38 36	−04 02 26	$0.50^{+0.28}_{-0.21}$	5/2	5.76E−05	9.3	14	2A	...	...	...	...	...	...	...	...
1ES0939+759	09 39 18	+75 57 37	$0.37^{+0.19}_{-0.14}$	6/4	4.13E−06	15.1	9	3A	...	...	...	...	...	...	...	...
1ES0942+098	09 42 49	+09 50 03	$0.24^{+0.06}_{-0.06}$	21/4	1.00E−10	77.6	5	3A	m2182	0.4	1H0932+107	0.0	VV	AGN:0.013	VV	0.8
1ES0943−140	09 43 17	−14 05 55	$0.40^{+0.10}_{-0.09}$	25/6	1.00E−10	54.4	8	3A	2183	0.3	x1H0946−144	0.3	VV	AGN:0.008	NGC 2992	0.2
1ES0944+135	09 44 10	+13 33 49	$0.49^{+0.31}_{-0.22}$	4/2	7.89E−05	7.7	6	3A	m2185	0.4	...	...	MS	AGN:0.131	MS	0.8
1ES0950+495	09 50 52	+49 30 09	$0.23^{+0.08}_{-0.07}$	15/7	5.10E−07	53.4	5	3A	m2193	0.6	...	...	MS	BL	MS	1.2
1ES0951+693	09 51 24	+69 18 32	$0.19^{+0.03}_{-0.03}$	61/8	1.00E−10	260.6	6	3A	2195	0.4	x1H0950+696.B	0.5	VV	AGN:0.000	M81	0.5
1ES0951+699	09 51 39	+69 54 29	$0.41^{+0.06}_{-0.05}$	74/10	1.00E−10	160.4	6	3A	2197	0.6	x1H0950+696.A	0.5	A3	GAL:0.001	M82	0.5

TABLE 6—*Continued*

Slew Desig.	RA 1950	DEC 1950	IPC Rate (cts s^{-1})	NP/NS	P_{rand}	Exp. (s)	PI	QI	EOS # EMSS	Δ2E (′)	A3 EXO	Δ1H (′)	Cat.	Class.: Type/z	Name	ΔC (′)
1ES0952+749	09 52 31	+74 55 17	$0.34^{+0.19}_{-0.14}$	5/3	1.12E−04	13.5	7	3A	...	...	...	...	...	...	...	...
1ES0953+693	09 53 53	+69 18 37	$0.08^{+0.03}_{-0.02}$	28/4	3.08E−05	203.4	6	3A	2199	0.4	x	...	SBD	GAL:0.178	UGC 5336*	2.6
1ES0955+097	09 55 29	+09 43 24	$0.66^{+0.48}_{-0.32}$	3/1	6.28E−05	4.5	7	2A	...	...	...	...	...	...	...	...
1ES0957+247	09 57 09	+24 47 35	$0.97^{+0.30}_{-0.25}$	14/3	1.00E−10	13.7	4	3A	...	...	...	...	SAO	AC:K0VE+B:	DH LEO	1.3
1ES0959+594	09 59 03	+59 27 54	$0.69^{+0.39}_{-0.29}$	5/3	1.91E−05	6.8	10	3A	...	...	...	...	...	...	...	...
1ES1002−559	10 02 09	−55 56 13	$0.43^{+0.18}_{-0.14}$	9/5	1.13E−07	19.2	6	3A	...	...	...	...	SAO	S:K1-2III	SAO 237656	0.7
1ES1003+677	10 03 06	+67 46 59	$0.12^{+0.05}_{-0.04}$	15/4	1.95E−05	92.4	7	3A	2225	1.7	...	...	SHA	CV	CH UMA	0.5
1ES1007+491	10 07 09	+49 08 44	$0.21^{+0.10}_{-0.08}$	10/2	3.91E−05	37.4	5	3A	...	...	...	...	...	...	...	...
1ES1011+496	10 11 52	+49 41 07	$0.63^{+0.22}_{-0.16}$	12/2	1.00E−10	17.7	5	3A	2250	0.7	1H1013+498	0.6	HB	BL	GB 1011+498	0.6
1ES1016+201	10 16 49	+20 07 40	$1.58^{+0.20}_{-0.18}$	74/3	1.00E−10	45.3	4	3A	2259	1.0	x	...	WLY	S:M4EV	AD LEO	1.2
1ES1020+493	10 20 31	+49 20 17	$0.25^{+0.10}_{-0.08}$	11/4	3.36E−06	36.3	7	3A	...	...	...	...	SBD	S:F5	HD 89944	2.9
1ES1020+201	10 20 45	+20 07 31	$0.42^{+0.05}_{-0.05}$	82/7	1.00E−10	175.2	7	3A	2275	0.3	x1H1017+202	0.5	VV	AGN:0.004	NGC 3227	0.6
1ES1022+519	10 22 23	+51 57 09	$0.42^{+0.17}_{-0.14}$	10/4	1.27E−06	20.6	4	3A	2283	2.8	...	...	VV	AGN:0.045	MKN 142	1.3
1ES1023+207	10 23 00	+20 46 25	$0.15^{+0.07}_{-0.05}$	10/5	3.62E−05	54.7	7	3A	...	...	...	...	...	...	...	...
1ES1024−406	10 24 09	−40 37 19	$3.06^{+2.19}_{-1.47}$	3/1	2.06E−05	1.0	7	3A	...	...	...	...	...	...	...	...
1ES1026+620	10 26 34	+62 04 35	$0.27^{+0.14}_{-0.11}$	6/4	1.99E−05	20.1	4	3A	...	...	...	...	GCV	S:F8	ZZ UMA	1.0
1ES1028+511	10 28 14	+51 08 56	$1.92^{+0.53}_{-0.45}$	16/5	1.00E−10	8.3	4	3A	...	...	...	...	...	...	...	...
1ES1034−272	10 34 18	−27 17 32	$0.28^{+0.08}_{-0.07}$	23/3	2.21E−08	62.8	7	3A	...	...	1H1033−273	2.4	A3	CG:0.012	A1060	2.4
1ES1035−268	10 35 30	−26 51 48	$0.14^{+0.06}_{-0.05}$	14/3	2.10E−05	75.1	7	3A	2300	0.3	...	...	ZCT	GAL:0.010	12597*	2.7
1ES1039+238	10 39 14	+23 48 04	$0.62^{+0.34}_{-0.26}$	5/3	6.69E−06	7.6	10	3A	...	...	...	...	...	...	...	...
1ES1039−630	10 39 23	−63 00 21	$0.23^{+0.10}_{-0.08}$	9/8	7.45E−06	33.4	7	3A	...	...	...	...	...	...	...	...
1ES1039−471	10 39 26	−47 09 18	$0.41^{+0.23}_{-0.17}$	5/3	8.04E−05	11.3	7	3A	...	...	...	...	...	...	...	...
1ES1040−513	10 40 17	−51 23 15	$0.35^{+0.20}_{-0.15}$	5/4	1.04E−04	12.8	6	3A	...	...	...	...	...	...	...	...
1ES1042−594	10 42 28	−59 27 41	$0.20^{+0.07}_{-0.06}$	27/10	1.03E−04	77.1	6	3M	2313	1.6	...	...	SAO	S:B	SAO 238418	1.7
1ES1043−594	10 43 16	−59 25 16	$0.32^{+0.09}_{-0.08}$	33/9	4.36E−08	69.8	7	3M	2318	1.1	x1H1045−597	1.1	A3	S:PEC	η CAR	1.2
1ES1044−491	10 44 33	−49 07 58	$0.65^{+0.32}_{-0.24}$	6/5	9.65E−09	9.0	5	3A	2326	1.7	...	...	BSC	S:G5III+G2V	ν VEL	1.4
1ES1044+549	10 44 37	+54 54 35	$0.65^{+0.35}_{-0.26}$	5/2	1.46E−06	7.5	5	3A	...	...	...	...	...	...	...	...
1ES1047+070	10 47 46	+07 00 38	$0.17^{+0.08}_{-0.06}$	9/1	6.42E−05	42.3	8	3A	...	...	...	...	...	...	...	...
1ES1048−596	10 48 04	−59 37 21	$0.16^{+0.06}_{-0.05}$	15/6	8.42E−06	69.6	9	3A	2336	0.5	x	...	2E	P	2E	0.5
1ES1048+350	10 48 07	+35 00 36	$0.20^{+0.10}_{-0.08}$	7/2	6.14E−05	29.4	11	3A	2337	1.0	...	...	2E	...	...	...
1ES1052+607	10 52 33	+60 44 09	$0.57^{+0.10}_{-0.09}$	43/4	1.00E−10	69.2	5	3A	...	...	x1H1051+607	0.4	A3	AC	DM UMA	0.4
1ES1053+072	10 53 58	+07 17 16	$0.17^{+0.07}_{-0.06}$	10/2	8.64E−05	46.8	6	3A	2358	0.8	...	...	GCV	S:M6.5VE	CN LEO	2.8
1ES1054+380	10 54 41	+38 02 31	$0.72^{+0.53}_{-0.35}$	3/2	4.28E−05	4.1	7	3A	...	...	...	...	...	...	...	...

TABLE 6—*Continued*

Slew Desig.	RA 1950	DEC 1950	IPC Rate (cts s^{-1})	NP/NS	P_{rand}	Exp. (s)	PI	QI	EOS # EMSS	Δ2E (′)	A3 EXO	Δ1H (′)	Cat.	Class.: Type/z	Name	ΔC (′)
1ES1055+605	10 55 29	+60 31 47	$0.20^{+0.09}_{-0.07}$	9/4	1.86E−05	37.8	3	3A	...	...	x	...	HB	AGN:0.149	E1055+605	1.8
1ES1055−521	10 55 51	−52 11 24	$0.10^{+0.02}_{-0.02}$	67/10	1.00E−10	477.5	3	3A	2368	0.8	x	...	2E	P	2E	0.7
1ES1100+772	11 00 17	+77 15 01	$0.18^{+0.04}_{-0.04}$	36/5	1.00E−10	161.2	5	3A	2389	0.7	...	...	HB	AGN:0.311	3C249.1	0.6
1ES1101−606	11 01 03	−60 39 02	$0.21^{+0.04}_{-0.03}$	57/10	1.00E−10	218.3	7	3E	...	...	...	...	SAO	S:M0	SAO 251235	0.4
1ES1101−232	11 01 10	−23 12 08	$1.89^{+0.57}_{-0.47}$	14/3	1.00E−10	7.2	6	3A	...	...	1H1100−230	1.2	VV	BL	4U 1057-21	2.3
1ES1101+384	11 01 42	+38 28 26	$3.36^{+0.22}_{-0.22}$	236/4	1.00E−10	69.2	4	3A	2393	0.4	x1H1104+382	0.4	VV	BL:0.031	MKN 421*	0.4
1ES1102−465	11 02 52	−46 35 57	$0.71^{+0.41}_{-0.30}$	5/3	1.04E−04	6.4	6	1A	...	...	...	...	...	...	...	...
1ES1103+728	11 03 28	+72 50 03	$0.17^{+0.03}_{-0.03}$	45/5	1.00E−10	208.7	7	3A	2395	0.3	x	...	VV	AGN:0.009	NGC 3516	0.5
1ES1105−731	11 05 07	−73 11 46	$0.36^{+0.19}_{-0.15}$	6/5	1.08E−04	14.7	8	3A	...	...	...	...	...	...	...	...
1ES1105+833	11 05 20	+83 21 54	$0.47^{+0.22}_{-0.17}$	7/3	1.69E−06	13.6	3	3A	...	...	...	...	SAO	S:K0	SAO 001824	1.0
1ES1106+244	11 06 37	+24 27 14	$0.59^{+0.34}_{-0.25}$	5/2	5.00E−05	7.8	6	3A	...	...	...	...	...	...	...	...
1ES1111−374	11 11 38	−37 24 30	$0.26^{+0.05}_{-0.05}$	39/4	1.00E−10	126.5	5	3A	2424	0.2	...	...	2E	CV	V 436 CEN	0.1
1ES1113+432	11 13 01	+43 15 12	$10.20^{+1.33}_{-1.23}$	64/2	1.00E−10	6.3	3	3A	...	...	...	...	...	...	...	...
1ES1113−369	11 13 06	−36 58 13	$0.11^{+0.05}_{-0.04}$	12/3	9.79E−05	79.7	6	3A	...	...	...	...	...	...	...	...
1ES1113−119	11 13 13	−11 57 31	$0.64^{+0.36}_{-0.27}$	5/2	2.51E−05	7.3	8	3A	...	...	...	...	...	...	...	...
1ES1113−342	11 13 56	−34 13 13	$0.63^{+0.40}_{-0.29}$	4/2	6.91E−05	6.0	13	3A	...	...	...	...	...	...	...	...
1ES1115+318	11 15 28	+31 48 49	$2.57^{+0.56}_{-0.49}$	26/4	1.00E−10	9.8	6	3A	2440	0.6	1H1121+309.B	0.7	A3	AC	ξ UMA	0.7
1ES1116+686	11 16 21	+68 41 31	$0.38^{+0.17}_{-0.13}$	8/6	6.34E−07	19.0	5	3A	...	...	...	...	...	...	...	...
1ES1118+424	11 18 01	+42 28 51	$1.16^{+0.31}_{-0.26}$	18/5	1.00E−10	15.0	4	3A	...	...	x	...	A3	BL	EXO	1.2
1ES1119−603	11 19 02	−60 21 12	$8.32^{+0.45}_{-0.45}$	352/8	1.00E−10	41.8	7	3A	2450	0.4	x1H1118−602	0.2	A3	XRB	CEN X-3	0.2
1ES1119−031	11 19 30	−03 06 38	$0.41^{+0.30}_{-0.20}$	3/2	4.71E−05	7.1	5	3A	...	...	...	...	...	...	...	...
1ES1121−012	11 21 02	−01 14 51	$0.52^{+0.28}_{-0.20}$	5/3	3.43E−09	9.5	6	3A	...	...	...	...	SBD	GAL	Z 1121.0-0117	2.2
1ES1122−589	11 22 15	−58 59 09	$5.82^{+0.31}_{-0.31}$	371/20	1.00E−10	62.9	6	3A	2460	1.3	x1H1121−591	1.1	A3	SNR	MSH 11-54	1.1
1ES1126−610	11 26 48	−61 00 17	$0.38^{+0.17}_{-0.14}$	8/5	1.75E−05	18.5	7	2A	...	...	...	...	SBD	S:A	HD 306536	0.4
1ES1133+704	11 33 24	+70 26 14	$1.71^{+0.21}_{-0.20}$	79/9	1.00E−10	44.0	4	3A	2487	0.9	x1H1137+699	0.8	VV	BL:0.046	MKN 180	0.7
1ES1135−175	11 35 32	−17 35 41	$0.34^{+0.19}_{-0.14}$	5/4	4.33E−05	13.6	6	3A	...	...	...	...	...	...	...	...
1ES1136−374	11 36 34	−37 27 54	$0.84^{+0.07}_{-0.07}$	151/6	1.00E−10	171.1	6	3A	2501	0.2	x1H1135−372	0.3	VV	AGN:0.009	NGC 3783	0.3
1ES1136+342	11 36 34	+34 12 42	$0.35^{+0.15}_{-0.12}$	9/2	4.28E−07	22.9	5	3A	m2499	0.6	...	...	VV	AGN:0.033	VV	0.5
1ES1137+660	11 37 06	+66 03 55	$0.14^{+0.03}_{-0.03}$	41/6	1.00E−10	217.8	5	3A	2503	0.7	x	...	HB	AGN:0.646	3C 263	0.6
1ES1137−651	11 37 06	−65 07 18	$1.29^{+0.39}_{-0.33}$	14/4	1.00E−10	10.5	6	3A	...	...	1H1137−649	0.4	A3	AC	HD101379	0.4
1ES1138+522	11 38 05	+52 16 38	$0.17^{+0.07}_{-0.06}$	15/5	1.73E−05	63.0	6	3A	2507	0.2	...	...	GCV	AC:F9+K1IV	RW UMA	0.1
1ES1140+719	11 40 48	+71 58 10	$0.40^{+0.08}_{-0.07}$	38/9	1.00E−10	82.4	6	3A	m2515	0.3	1H1140+719	0.2	A3	CV	YY DRA	0.2
1ES1141+799	11 41 56	+79 57 50	$0.47^{+0.22}_{-0.17}$	7/5	3.87E−06	13.6	6	3A	...	...	...	...	UGC	GAL	UO6728	1.5

TABLE 6—*Continued*

Slew Desig.	RA 1950	DEC 1950	IPC Rate (cts s^{-1})	NP/NS	P_{rand}	Exp. (s)	PI	QI	EOS # EMSS	Δ2E (′)	A3 EXO	Δ1H (′)	Cat.	Class.: Type/z	Name	ΔC (′)
1ES1142+198	11 42 28	+19 52 42	$0.18^{+0.03}_{-0.03}$	65/3	1.13E−10	266.5	6	3E	2521	0.7	x	...	VV	AGN:0.021	NGC 3862	0.5
1ES1143−550	11 43 20	−55 04 04	$0.20^{+0.10}_{-0.08}$	8/5	4.24E−05	33.2	4	3A	...	...	...	...	...	...	...	...
1ES1145+204	11 45 27	+20 29 37	$0.41^{+0.10}_{-0.09}$	23/3	1.00E−10	50.6	5	3A	2534	0.6	...	...	SAO	AC:A7V+G5III	SAO 081998	0.3
1ES1145−619	11 45 35	−61 54 25	$0.38^{+0.14}_{-0.11}$	13/7	1.05E−07	29.1	6	3A	2535	1.2	x1H1144−617.B	1.3	2E	P	V801 CEN	1.3
1ES1147+032	11 47 02	+03 16 08	$0.37^{+0.21}_{-0.16}$	5/1	1.08E−04	12.3	3	3A	...	...	...	...	...	...	...	...
1ES1147−625	11 47 36	−62 30 24	$0.31^{+0.08}_{-0.07}$	30/6	1.09E−10	74.4	5	3E	2541	0.4	x	...	SBD	S:B9V	HD 102867	1.9
1ES1148−624	11 48 56	−62 24 34	$0.20^{+0.07}_{-0.06}$	21/3	2.57E−05	68.2	5	3E	...	...	...	...	SBD	S:B8	HD 309207	2.7
1ES1148−620	11 48 57	−62 01 35	$0.29^{+0.10}_{-0.09}$	17/7	1.36E−06	44.6	5	3A	2550	1.1	x	...	2E	...	...	...
1ES1149−110	11 49 33	−11 05 21	$0.63^{+0.25}_{-0.20}$	9/6	5.08E−09	13.5	4	3A	...	...	...	...	VV	AGN:0.049	PG	0.6
1ES1153−583	11 53 38	−58 23 05	$0.40^{+0.26}_{-0.18}$	4/2	7.30E−05	9.4	4	2A	...	...	...	...	...	...	...	...
1ES1154+568	11 54 02	+56 51 56	$0.32^{+0.16}_{-0.12}$	6/4	1.61E−05	17.4	12	3A	...	...	...	...	...	...	...	...
1ES1155+557	11 55 25	+55 43 51	$0.44^{+0.11}_{-0.09}$	26/2	1.00E−10	51.7	5	3A	2561	0.3	x	...	VV	AGN:0.003	NGC 3998	0.6
1ES1159+583	11 59 37	+58 19 14	$0.09^{+0.03}_{-0.03}$	19/4	9.26E−05	140.0	5	3E	2574	0.4	...	...	2E	CG:0.103	A1446	1.0
1ES1200+448	12 00 35	+44 48 36	$0.94^{+0.08}_{-0.08}$	164/8	1.00E−10	166.2	4	3A	2578	0.3	x1H1205+440	0.2	VV	AGN:0.002	NGC 4051	0.2
1ES1201−415	12 01 25	−41 35 34	$0.48^{+0.30}_{-0.21}$	4/1	5.85E−05	8.0	8	2A	...	...	...	...	...	...	...	...
1ES1201+021	12 01 54	+02 09 44	$0.47^{+0.21}_{-0.17}$	8/4	1.20E−05	15.0	5	3A	2583	0.7	...	...	2E	CG:0.020	MKW 4	0.8
1ES1202+281	12 02 09	+28 10 35	$0.23^{+0.07}_{-0.06}$	17/2	3.71E−08	60.0	6	3A	2584	0.5	...	...	HB	AGN:0.165	GQ COM	0.3
1ES1204−526	12 04 29	−52 36 04	$0.08^{+0.03}_{-0.02}$	28/14	2.83E−05	198.6	6	3A	...	...	...	...	...	...	...	...
1ES1207−521	12 07 24	−52 09 45	$0.07^{+0.02}_{-0.02}$	44/13	8.12E−05	311.6	6	3A	2599	0.2	...	...	2E	SNR	PKS	0.2
1ES1208+396	12 08 02	+39 41 04	$0.31^{+0.03}_{-0.03}$	158/15	1.00E−10	438.9	6	3A	2603	0.2	x1H1210+393	0.1	VV	AGN:0.003	NGC 4151	0.2
1ES1209−524	12 09 00	−52 26 43	$0.08^{+0.02}_{-0.02}$	67/11	3.63E−05	344.1	4	3E	...	...	...	...	...	...	...	...
1ES1209−606	12 09 15	−60 40 19	$0.21^{+0.12}_{-0.09}$	5/4	9.69E−05	21.2	7	3A	...	...	...	...	...	...	...	...
1ES1210−646	12 10 36	−64 36 06	$0.55^{+0.10}_{-0.09}$	42/12	1.00E−10	69.5	7	3A	...	...	...	...	...	...	...	...
1ES1211+143	12 11 45	+14 20 02	$1.38^{+0.17}_{-0.16}$	75/2	1.00E−10	52.7	5	3A	2620	0.4	x	...	VV	AGN:0.085	PG	0.2
1ES1212−652	12 12 04	−65 15 40	$0.25^{+0.10}_{-0.09}$	11/8	8.67E−05	33.1	7	3E	...	...	...	...	SBD	S:G0/G1V:	HD 106392	1.7
1ES1212−651	12 12 30	−65 09 31	$0.42^{+0.13}_{-0.11}$	16/9	7.51E−10	33.1	5	3E	...	...	...	...	...	...	...	...
1ES1212+334	12 12 33	+33 28 08	$0.17^{+0.05}_{-0.05}$	19/4	1.23E−07	88.4	7	3A	2626	0.6	...	...	UGC	GAL:0.004	NGC 4203	0.6
1ES1212+078	12 12 36	+07 48 53	$0.25^{+0.11}_{-0.09}$	10/7	3.38E−05	32.4	7	3A	...	...	...	...	SAO	S:K0	SAO 119284	0.9
1ES1213+728	12 13 26	+72 49 32	$0.58^{+0.08}_{-0.08}$	62/9	1.00E−10	99.1	5	3A	2631	0.3	1H1213+718.A	0.4	A3	AC	DK DRA	0.4
1ES1214+328	12 14 32	+32 48 14	$0.15^{+0.06}_{-0.05}$	11/3	2.36E−05	59.6	9	3A	...	...	...	...	...	...	...	...
1ES1214−037	12 14 36	−03 44 23	$0.43^{+0.24}_{-0.18}$	5/2	3.13E−05	10.9	11	3A	...	...	...	...	...	...	...	...
1ES1215+039	12 15 03	+03 54 51	$0.34^{+0.13}_{-0.11}$	11/4	1.64E−06	27.7	7	3A	...	...	...	...	SBD	GAL:0.075	4C +04.41*	1.6
1ES1215+303	12 15 20	+30 22 34	$0.22^{+0.06}_{-0.06}$	21/4	2.92E−10	78.3	4	3A	2644	1.2	x	...	HB	BL	ON 325	1.1

TABLE 6—*Continued*

Slew Desig.	RA 1950	DEC 1950	IPC Rate (cts s^{-1})	NP/NS	P_{rand}	Exp. (s)	PI	QI	EOS # EMSS	Δ2E (′)	A3 EXO	Δ1H (′)	Cat.	Class.: Type/s	Name	ΔC (′)
1ES1215+300	12 15 55	+30 05 24	$0.95^{+0.14}_{-0.12}$	59/5	1.00E−10	58.8	4	3A	m2648	0.4	x1H1219+301.B	0.2	VV	AGN:0.012	MKN 766	0.2
1ES1216+426	12 16 21	+42 39 16	$0.23^{+0.11}_{-0.08}$	8/4	2.01E−05	30.3	8	3A	...	...	...	...	...	...	...	...
1ES1217−168	12 17 40	−16 49 44	$0.54^{+0.34}_{-0.24}$	4/2	2.70E−05	7.1	9	3A	...	...	...	...	SBD	GAL	MCG-3.32.4	0.6
1ES1217+023	12 17 40	+02 19 30	$0.26^{+0.05}_{-0.04}$	47/10	1.00E−10	147.3	6	3A	2661	1.1	x	...	HB	AGN:0.240	ON 029	0.9
1ES1218+637	12 18 05	+63 43 44	$0.39^{+0.19}_{-0.15}$	7/2	2.21E−05	16.0	9	3A	...	...	...	...	...	...	...	...
1ES1218−637	12 18 45	−63 47 07	$0.13^{+0.04}_{-0.04}$	18/9	1.67E−06	106.3	5	3A	2671	0.4	...	...	2E	...	...	...
1ES1218+304	12 18 50	+30 27 12	$2.27^{+0.77}_{-0.63}$	11/2	1.00E−10	4.8	5	3A	...	...	x1H1219+301.A	0.4	VV	BL	3A 1218+303	0.3
1ES1218+285	12 18 57	+28 30 39	$0.23^{+0.07}_{-0.06}$	19/2	6.13E−09	66.3	7	3A	2673	1.1	...	...	VV	BL:0.102	ON 231	0.9
1ES1219+755	12 19 31	+75 35 29	$0.47^{+0.04}_{-0.04}$	147/13	1.00E−10	281.9	5	3A	m2677	0.2	x1H1211+762	0.3	HB	AGN:0.070	MKN 205	0.3
1ES1219+044	12 19 48	+04 29 32	$0.13^{+0.03}_{-0.03}$	43/6	5.72E−10	220.7	6	3A	2679	0.6	...	...	HB	AGN:0.965	PKS	0.5
1ES1223+132	12 23 37	+13 14 48	$0.30^{+0.08}_{-0.07}$	26/3	2.43E−10	68.1	5	3A	2707	2.2	...	...	UGC	GAL:-0.001	N4406	1.5
1ES1223−628	12 23 57	−62 48 58	$1.16^{+0.28}_{-0.24}$	21/9	1.00E−10	17.7	4	3A	...	...	x	...	SAO	S:B1V+B0.5V	α^2 CRU	1.0
1ES1225+447	12 25 20	+44 47 35	$0.27^{+0.14}_{-0.11}$	7/3	7.90E−05	22.1	8	3A	...	...	...	...	...	...	...	...
1ES1225−551	12 25 33	−55 06 44	$0.31^{+0.15}_{-0.12}$	7/3	6.80E−05	19.2	5	3A	...	...	...	...	SAO	S:A2	SAO 239967	2.9
1ES1226+023	12 26 34	+02 19 44	$3.20^{+0.12}_{-0.12}$	712/8	1.00E−10	218.5	5	3A	2729	0.2	x1H1226+022	0.1	VV	AGN:0.158	3C 273.0	0.2
1ES1227+082	12 27 15	+08 16 18	$0.25^{+0.04}_{-0.04}$	70/9	1.00E−10	225.3	6	3A	2735	0.2	1H1228+081	0.2	A3	GAL:0.003	N4472	0.3
1ES1228−465	12 28 08	−46 30 24	$0.45^{+0.21}_{-0.16}$	7/4	4.68E−07	14.7	7	3A	...	...	...	...	SAO	S:F5V	SAO 223481	0.8
1ES1228+126	12 28 17	+12 39 01	$2.50^{+0.51}_{-0.46}$	37/4	1.00E−10	12.6	6	3E	2744	1.0	x1H1226+128	1.0	A3	CG:0.004	VIRGO CL.	1.0
1ES1229+734	12 29 18	+73 28 40	$0.25^{+0.13}_{-0.10}$	7/4	7.05E−05	23.7	6	2A	...	...	...	...	...	...	...	...
1ES1229+710	12 29 30	+71 00 35	$0.20^{+0.07}_{-0.06}$	18/10	6.35E−08	70.5	5	3A	...	...	...	...	...	...	...	...
1ES1230+176	12 30 13	+17 39 55	$0.21^{+0.10}_{-0.08}$	9/5	4.94E−05	35.4	9	3A	...	...	...	...	...	...	...	...
1ES1231+100	12 31 49	+10 05 13	$0.17^{+0.07}_{-0.06}$	15/8	9.38E−06	64.9	6	3A	...	...	...	...	...	...	...	...
1ES1233−634	12 33 45	−63 27 54	$0.45^{+0.14}_{-0.12}$	15/3	2.36E−09	29.2	6	3A	...	...	...	...	...	...	...	...
1ES1234+223	12 34 01	+22 18 56	$0.16^{+0.06}_{-0.05}$	14/4	4.28E−06	67.7	6	3A	...	...	...	...	...	...	...	...
1ES1234+459	12 34 26	+45 55 22	$0.32^{+0.13}_{-0.11}$	10/4	2.78E−06	26.6	6	3A	...	...	...	...	SBD	GAL	Z 1234.5+4556	0.9
1ES1235+120	12 35 10	+12 05 16	$0.23^{+0.04}_{-0.04}$	47/9	1.00E−10	161.7	6	3A	2801	0.6	...	...	VV	AGN:0.005	NGC 4579	0.6
1ES1235−399	12 35 42	−39 55 37	$0.10^{+0.04}_{-0.03}$	24/5	6.33E−05	150.5	6	3A	...	...	...	...	...	...	...	...
1ES1236+654	12 36 51	+65 25 14	$0.36^{+0.20}_{-0.15}$	5/3	7.70E−05	12.9	11	3A	...	...	...	...	...	...	...	...
1ES1238−332	12 38 07	−33 17 59	$0.38^{+0.18}_{-0.14}$	7/4	1.56E−05	16.6	7	3A	...	...	...	...	SBD	GAL	ESO 381- 7	0.4
1ES1239−011	12 39 04	−01 10 45	$0.86^{+0.42}_{-0.32}$	6/1	2.07E−07	6.7	4	3A	...	...	...	...	WLY	S:F0V	WLY 482A	0.8
1ES1239+069	12 39 23	+06 54 56	$0.25^{+0.11}_{-0.09}$	10/6	2.43E−05	32.4	7	3A	...	...	...	...	...	...	...	...
1ES1239−627	12 39 50	−62 46 38	$0.26^{+0.08}_{-0.07}$	17/3	3.89E−09	55.9	7	3A	2828	0.3	1H1249−637	0.6	BSC	S:B2pe	HD 110432	0.6
1ES1240+029	12 40 17	+02 57 38	$0.36^{+0.07}_{-0.06}$	46/7	1.00E−10	107.2	5	3A	2829	0.2	...	...	UGC	GAL:0.003	N4636	0.4

TABLE 6—*Continued*

Slew Desig.	RA 1950	DEC 1950	IPC Rate (cts s^{-1})	NP/NS	P_{rand}	Exp. (s)	PI	QI	EOS # EMSS	Δ2E (′)	A3 EXO	Δ1H (′)	Cat.	Class.: Type/z	Name	ΔC (′)
1ES1241+275	12 41 06	+27 33 10	$0.32^{+0.15}_{-0.12}$	7/4	6.85E−06	19.7	4	3A	...	...	...	...	ABL	CG:0.241	A1602	1.6
1ES1241+723	12 41 24	+72 16 16	$0.24^{+0.11}_{-0.09}$	8/5	6.08E−05	28.3	7	3A	...	...	...	...	...	...	...	...
1ES1241−586	12 41 28	−58 38 28	$0.30^{+0.16}_{-0.12}$	6/4	1.03E−04	17.5	4	3A	...	...	...	...	...	...	...	...
1ES1243+506	12 43 31	+50 37 26	$0.47^{+0.26}_{-0.19}$	5/3	1.08E−05	10.0	10	3A	...	...	...	...	...	...	...	...
1ES1244+026	12 44 02	+02 38 32	$0.39^{+0.07}_{-0.06}$	52/7	1.00E−10	116.3	5	3A	2854	0.4	...	...	VV	AGN:0.048	PG	0.0
1ES1245−259	12 45 18	−25 58 56	$0.22^{+0.12}_{-0.09}$	5/2	6.84E−05	20.7	12	2A	...	...	...	...	...	...	...	...
1ES1245−243	12 45 35	−24 22 17	$0.45^{+0.25}_{-0.19}$	5/3	1.90E−05	10.5	10	3A	...	...	...	...	...	...	...	...
1ES1246−410	12 46 00	−41 01 34	$1.04^{+0.09}_{-0.09}$	161/7	1.00E−10	135.7	6	3A	2862	1.0	x1H1244−409	0.7	ABL	CG:0.011	A3526	1.2
1ES1246+085	12 46 03	+08 35 43	$0.08^{+0.03}_{-0.03}$	25/4	1.64E−05	186.8	6	3A	2861	0.7	...	...	2E	...	...	...
1ES1246+605	12 46 30	+60 35 50	$0.19^{+0.05}_{-0.04}$	26/2	1.00E−10	111.6	6	3A	2865	0.3	1H1241+626.B	0.3	A3	AC	HD111456	0.3
1ES1246−588	12 46 39	−58 48 40	$1.90^{+0.40}_{-0.36}$	27/7	1.00E−10	13.7	7	3A	...	...	x1H1244−588	0.5	A3	XRB	X1246-588	0.5
1ES1248−296	12 48 55	−29 39 45	$0.41^{+0.18}_{-0.14}$	8/4	8.54E−07	17.8	8	3E	...	...	...	...	...	...	...	...
1ES1249−296	12 49 06	−29 37 03	$0.35^{+0.17}_{-0.13}$	7/6	1.43E−05	17.6	6	3A	...	...	...	...	...	...	...	...
1ES1249+174	12 49 13	+17 28 11	$0.20^{+0.10}_{-0.08}$	8/4	9.53E−05	32.6	9	3A	...	...	...	...	...	...	...	...
1ES1249+278	12 49 17	+27 48 03	$0.48^{+0.17}_{-0.14}$	12/3	4.00E−10	22.8	4	3A	2874	0.9	x	...	BSC	S:G0IIIp	HD111812	0.8
1ES1249−131	12 49 36	−13 07 52	$0.45^{+0.20}_{-0.16}$	8/2	2.76E−06	15.9	6	3A	...	...	x	...	VV	AGN:0.014	IRAS 1249-13	0.8
1ES1249−289	12 49 43	−28 58 41	$4.08^{+0.22}_{-0.22}$	354/5	1.00E−10	85.6	6	3A	2876	0.2	x1H1251−291	0.0	A3	CV	EX HYA	0.1
1ES1251−281	12 51 46	−28 10 03	$0.43^{+0.23}_{-0.17}$	6/3	2.44E−05	12.6	2	3A	...	...	...	...	SBD	AGN:0.069	ESO 443- 5	0.7
1ES1252−060	12 52 20	−06 03 36	$0.12^{+0.05}_{-0.04}$	16/3	6.42E−05	88.6	7	3A	...	...	...	...	WLY	S:K8V	WLY 9424	0.6
1ES1253+275	12 53 14	+27 31 15	$0.23^{+0.09}_{-0.07}$	15/4	7.19E−06	49.3	5	3A	2896	0.6	...	...	SBD	GAL:0.024	Z 1253.3+2731	1.4
1ES1253−055	12 53 38	−05 31 13	$0.19^{+0.04}_{-0.04}$	31/4	1.00E−10	132.6	6	3A	2900	0.5	x	...	HB	AGN:0.538	3C 279	0.5
1ES1254−690	12 54 27	−69 00 21	$6.92^{+2.04}_{-1.70}$	14/2	1.00E−10	2.0	8	3A	2908	0.8	x1H1254−690	0.9	A3	XRB	X1254-690	1.0
1ES1254−171	12 54 31	−17 08 59	$0.24^{+0.06}_{-0.05}$	32/2	1.00E−10	105.9	6	3A	2909	0.6	...	...	SBD	CG:0.048	A1644	0.8
1ES1254−635	12 54 35	−63 33 37	$0.75^{+0.47}_{-0.33}$	4/2	6.94E−06	5.1	8	3A	...	...	...	...	...	...	...	...
1ES1254+223	12 54 36	+22 18 06	$0.63^{+0.06}_{-0.06}$	136/12	1.00E−10	200.9	2	3A	2912	0.6	x	...	MCS	WD:DA	EG 187	0.3
1ES1254−172	12 54 51	−17 12 21	$0.12^{+0.04}_{-0.02}$	21/2	6.21E−05	110.2	7	2A	...	...	...	...	EXC	GAL:0.046	GAL 1254-1710*	1.7
1ES1254−684	12 54 55	−68 25 03	$0.44^{+0.26}_{-0.19}$	5/3	8.41E−05	10.3	4	3A	...	...	...	...	...	...	...	...
1ES1255+244	12 55 06	+24 28 54	$0.36^{+0.12}_{-0.10}$	14/8	1.18E−09	34.2	7	3A	...	...	...	...	...	...	...	...
1ES1255+354	12 55 20	+35 29 16	$0.17^{+0.03}_{-0.03}$	53/6	1.00E−10	243.9	4	3A	m2920	0.7	...	...	WLY	S:M0EV	BF CVN	0.6
1ES1256−014	12 56 08	−01 28 58	$0.58^{+0.09}_{-0.08}$	53/3	1.00E−10	82.6	6	3A	2925	0.5	...	...	ABL	CG:0.084	A1650	1.0
1ES1256−039	12 56 45	−03 54 22	$0.51^{+0.20}_{-0.17}$	10/2	3.89E−07	17.3	6	3A	...	...	...	...	ABL	CG:0.083	A1651	1.0
1ES1257+282	12 57 10	+28 13 02	$0.71^{+0.07}_{-0.07}$	244/4	1.00E−10	235.6	6	3A	2931	0.6	x	...	RNG	CG:0.023	COMA CL.	1.1
1ES1257+286	12 57 59	+28 40 41	$0.14^{+0.03}_{-0.03}$	62/4	1.00E−10	268.7	5	3A	2935	0.7	x	...	HB	AGN:0.092	X COM	0.5

TABLE 6—*Continued*

Slew Desig.	RA 1950	DEC 1950	IPC Rate (cts s^{-1})	NP/NS	P_{rand}	Exp. (s)	PI	QI	EOS # EMSS	Δ2E (′)	A3 EXO	Δ1H (′)	Cat.	Class.: Type/s	Name	ΔC (′)
1ES1258+126	12 58 19	+12 37 54	$0.33^{+0.10}_{-0.08}$	18/2	1.46E−10	47.8	3	3A	2940	0.7	x	...	WLY	S:M2EV	DT VIR	0.8
1ES1259+289	12 59 07	+28 54 05	$0.12^{+0.04}_{-0.03}$	28/5	8.16E−07	149.8	5	3A	2946	0.7	...	...	GCV	S:G2III	UX COM*	0.3
1ES1259+337	12 59 20	+33 46 07	$0.12^{+0.04}_{-0.03}$	19/5	9.39E−07	122.0	5	3A	...	...	...	...	...	...	...	...
1ES1300+300	13 00 39	+30 01 44	$0.36^{+0.18}_{-0.14}$	7/4	9.99E−05	16.4	7	3A	...	...	...	...	...	...	...	...
1ES1301−239	13 01 01	−23 57 41	$0.20^{+0.07}_{-0.06}$	15/5	5.83E−07	61.3	7	3A	...	...	...	...	ABL	CG	A1664*	0.7
1ES1301−411	13 01 45	−41 08 10	$0.29^{+0.13}_{-0.10}$	8/5	3.31E−06	24.3	6	3A	...	...	...	...	SBD	S:K0	CD-40 7655	2.7
1ES1303+182	13 03 16	+18 17 28	$0.39^{+0.10}_{-0.09}$	20/6	1.00E−10	46.5	6	3A	2967	0.2	x	...	2E	CV	GP COM	0.5
1ES1304−650	13 04 48	−65 02 09	$0.14^{+0.04}_{-0.04}$	30/7	5.71E−08	146.3	7	3A	2972	0.5	...	...	BSC	S:B0Ia+WC5:	θ MUS	0.5
1ES1306−013	13 06 51	−01 23 19	$0.09^{+0.03}_{-0.03}$	19/5	1.96E−05	140.5	8	2A	m2975	2.2	...	...	2E	...	...	...
1ES1307+086	13 07 19	+08 36 14	$0.35^{+0.09}_{-0.08}$	22/1	1.00E−10	55.7	6	3A	2978	0.8	...	...	HB	AGN:0.155	PG	0.8
1ES1308+326	13 08 07	+32 36 46	$0.16^{+0.04}_{-0.03}$	40/8	1.00E−10	181.7	5	3A	2979	0.5	x	...	HB	BL:0.049	OP 313	0.2
1ES1308+361	13 08 17	+36 11 58	$0.38^{+0.07}_{-0.07}$	39/7	1.00E−10	90.5	4	3A	2980	0.2	x	...	WLY	AC:F4V	RS CVN	0.2
1ES1308−010	13 08 55	−01 04 51	$0.42^{+0.07}_{-0.06}$	47/3	1.00E−10	101.7	6	3A	2986	0.3	...	...	ABL	CG:0.181	A1689	1.7
1ES1309+281	13 09 32	+28 08 12	$0.16^{+0.05}_{-0.04}$	20/2	2.86E−08	97.0	4	3A	2990	0.4	...	...	WLY	S:G0V	WLY 502	0.3
1ES1309+355	13 09 58	+35 31 53	$0.09^{+0.03}_{-0.03}$	20/5	1.38E−05	146.8	6	3A	...	...	...	...	HB	AGN:0.184	TON 1565	0.6
1ES1310−327	13 10 29	−32 42 39	$1.78^{+0.42}_{-0.36}$	23/2	1.00E−10	12.3	3	3A	...	...	...	...	ABL	CG	S724	1.7
1ES1312+347	13 12 02	+34 46 08	$0.31^{+0.09}_{-0.08}$	17/6	2.19E−10	48.0	4	3A	...	...	...	...	...	...	...	...
1ES1312−423	13 12 08	−42 20 33	$0.50^{+0.14}_{-0.12}$	19/8	1.00E−10	33.7	6	3A	m3002	0.4	...	...	MS	BL:0.108	MS	0.6
1ES1314+293	13 14 04	+29 22 09	$5.49^{+0.77}_{-0.70}$	57/7	1.00E−10	10.2	3	3A	3009	0.8	x	...	MCS	WD:DA1	HZ 43A	0.9
1ES1314+096	13 14 19	+09 41 16	$0.31^{+0.09}_{-0.08}$	17/3	1.11E−10	48.1	5	3A	3010	0.2	x	...	SAO	S:G0V	SAO 119847	0.2
1ES1314+172	13 14 26	+17 16 34	$0.31^{+0.12}_{-0.10}$	11/6	9.96E−07	30.0	6	3A	...	...	...	...	WLY	S:K2V+M2V	WLY 505AB	1.0
1ES1316−424	13 16 40	−42 29 50	$0.19^{+0.07}_{-0.06}$	14/3	5.99E−07	59.8	4	3A	m3018	0.2	...	...	MS	S:M1.5E	MS	0.8
1ES1318+274	13 18 07	+27 27 53	$0.30^{+0.15}_{-0.11}$	6/4	3.73E−06	18.9	4	3A	...	...	...	...	SBD	GAL	G 149 -80	1.3
1ES1318−632	13 18 14	−63 17 50	$0.49^{+0.19}_{-0.16}$	10/6	3.64E−07	18.2	6	3A	...	...	...	...	SBD	S:B	LS 3039	2.1
1ES1319−438	13 19 58	−43 51 50	$0.52^{+0.29}_{-0.21}$	5/2	8.25E−06	9.1	8	3A	...	...	...	...	...	...	...	...
1ES1319+429	13 19 59	+42 55 32	$0.13^{+0.05}_{-0.04}$	17/4	6.42E−05	89.5	8	3A	...	...	...	...	...	...	...	...
1ES1320+701	13 20 20	+70 09 09	$0.12^{+0.04}_{-0.04}$	32/7	9.34E−05	147.6	6	3A	...	...	...	...	...	...	...	...
1ES1320+084	13 20 23	+08 25 34	$1.44^{+0.69}_{-0.52}$	6/2	9.69E−10	4.1	6	3A	...	...	...	...	VV	AGN:0.050	MKN 1347	0.5
1ES1322−108	13 22 32	−10 53 38	$0.25^{+0.05}_{-0.05}$	33/6	1.00E−10	112.8	3	3A	3039	0.3	...	...	BSC	S:B1III-IV+B	α VIR	0.5
1ES1322−427	13 22 33	−42 45 41	$1.01^{+0.09}_{-0.09}$	130/5	1.00E−10	120.9	10	3A	3038	0.1	1H1323−428	0.3	A3	AGN:0.002	CEN A	0.3
1ES1322−297	13 22 48	−29 46 20	$0.16^{+0.07}_{-0.06}$	11/2	7.64E−05	52.7	8	3A	...	...	...	...	...	...	...	...
1ES1323+717	13 23 32	+71 47 26	$0.27^{+0.11}_{-0.09}$	13/2	2.50E−05	36.6	5	3A	...	...	...	...	EXC	GAL:0.072	GAL 1323+7145	2.8
1ES1324−269	13 24 04	−26 54 37	$0.15^{+0.04}_{-0.04}$	29/4	8.91E−07	129.5	7	3P	...	...	...	...	SBD	GAL:0.046	ESO 509- 9	1.7

TABLE 6—*Continued*

Slew Desig.	RA 1950	DEC 1950	IPC Rate (cts s^{-1})	NP/NS	P_{rand}	Exp. (s)	PI	QI	EOS # EMSS	Δ2E (′)	A3 EXO	Δ1H (′)	Cat.	Class.: Type/z	Name	ΔC (′)
1ES1324−268	13 24 48	−26 53 10	$0.15^{+0.04}_{-0.04}$	29/4	8.81E−07	127.2	8	3P	...	...	...	...	SBD	GAL	ESO 509- 14	1.8
1ES1325−261	13 25 07	−26 06 35	$0.17^{+0.08}_{-0.06}$	9/2	6.23E−05	43.5	7	3A	...	...	...	...	SBD	S:K5III	HD 117033	2.7
1ES1325−312	13 25 14	−31 17 14	$0.69^{+0.30}_{-0.24}$	8/4	1.11E−06	10.5	6	3A	...	...	...	...	SAO	S:F5V	SAO 204500	2.7
1ES1325−119	13 25 39	−11 54 15	$0.42^{+0.24}_{-0.18}$	5/2	7.87E−05	10.9	4	3A	...	...	...	...	...	...	...	...
1ES1326+789	13 26 34	+78 54 04	$0.38^{+0.16}_{-0.13}$	9/7	6.43E−07	21.1	6	3A	...	...	...	...	BSC	S:G2.5IIIb	HD 117566	0.1
1ES1327−313	13 27 12	−31 19 54	$0.17^{+0.07}_{-0.06}$	13/3	7.27E−05	57.8	6	3A	...	...	...	...	SAO	S:K1III	SAO 204527	2.6
1ES1327−369	13 27 50	−36 55 55	$0.42^{+0.27}_{-0.19}$	4/3	7.21E−05	9.0	8	3A	...	...	...	...	...	...	...	...
1ES1328−547	13 28 08	−54 43 35	$0.20^{+0.06}_{-0.05}$	18/2	3.45E−09	73.5	6	3A	3071	0.8	...	...	SHA	CV	BV CEN	0.6
1ES1328+244	13 28 25	+24 29 31	$0.21^{+0.05}_{-0.05}$	27/4	1.00E−10	104.7	5	3A	3074	0.1	...	...	SAO	S:G5	FK COM	0.4
1ES1330+022	13 30 22	+02 15 15	$0.19^{+0.05}_{-0.04}$	23/4	1.00E−10	98.8	5	3A	3081	0.9	...	...	VV	AGN:0.215	3C287.1	1.0
1ES1330−313	13 30 45	−31 23 58	$0.27^{+0.06}_{-0.06}$	31/7	1.00E−10	96.0	6	3A	3083	0.7	x	...	ABL	CG:0.050	A3562	1.2
1ES1331−108	13 31 40	−10 53 17	$0.66^{+0.48}_{-0.32}$	3/2	2.20E−05	4.5	6	2A	...	...	...	...	...	...	...	...
1ES1332−080	13 32 05	−08 05 16	$0.16^{+0.05}_{-0.04}$	20/3	2.70E−09	99.6	4	3A	3091	0.6	x	...	WLY	S:K5EV	EQ VIR	0.5
1ES1332+374	13 32 34	+37 25 35	$1.21^{+0.32}_{-0.28}$	19/4	1.00E−10	14.7	4	3A	3098	0.8	1H1332+372	0.7	A3	AC	SAO 063623	0.7
1ES1332−295	13 32 40	−29 35 22	$0.16^{+0.04}_{-0.03}$	35/7	1.00E−10	168.7	7	3A	m3100	0.3	x	...	2E	...	...	...
1ES1333−340	13 33 03	−34 02 33	$1.76^{+0.17}_{-0.17}$	113/10	1.00E−10	62.3	6	3A	3102	0.4	x1H1334−340	0.3	VV	AGN:0.008	MCG-6.30.15	0.3
1ES1333+412	13 33 05	+41 14 57	$0.21^{+0.06}_{-0.05}$	22/5	5.21E−09	84.1	7	3A	3103	1.0	...	...	ABL	CG:0.228	A1763	2.0
1ES1334−296	13 34 19	−29 36 30	$0.10^{+0.02}_{-0.02}$	41/5	5.33E−10	287.9	6	3A	3112	1.2	x	...	RNG	GAL:0.002	NGC 5236	0.4
1ES1336+280	13 36 13	+28 00 36	$0.20^{+0.08}_{-0.07}$	11/5	5.01E−05	44.0	12	3A	...	...	...	...	SBD	GAL:0.036	Z 1336.4+2800	2.3
1ES1339−688	13 39 20	−68 52 06	$0.79^{+0.43}_{-0.32}$	5/2	6.51E−07	6.1	3	3A	...	...	...	...	SAO	S:G2IV-V	SAO 252423	0.7
1ES1339+266	13 39 31	+26 40 06	$0.48^{+0.25}_{-0.19}$	6/3	1.49E−05	11.4	5	3A	3123	2.8	...	...	UGC	CG:0.072	A1775	2.1
1ES1340−611	13 40 35	−61 07 02	$0.68^{+0.11}_{-0.10}$	50/3	1.00E−10	69.4	5	3A	3127	0.2	1H1338−604.B	0.1	A3	AC	SAO 0252429	0.1
1ES1344+510	13 44 36	+51 01 09	$0.23^{+0.13}_{-0.10}$	5/4	9.92E−05	20.3	4	3A	...	...	...	...	...	...	...	...
1ES1344−326	13 44 43	−32 37 09	$1.17^{+0.52}_{-0.41}$	8/3	1.34E−06	6.2	6	3A	...	...	1H1344−326	1.7	ABL	CG:0.040	A3571	1.5
1ES1346−300	13 46 26	−30 03 45	$1.68^{+0.23}_{-0.21}$	64/2	1.00E−10	36.5	7	3A	3141	0.8	x1H1345−300	0.4	VV	AGN:0.014	IC 4329A	0.4
1ES1346+268	13 46 34	+26 50 07	$1.24^{+0.12}_{-0.12}$	118/3	1.00E−10	90.2	5	3A	3142	0.5	x1H1348+267	0.3	ABL	CG:0.062	A1795	1.8
1ES1348−588	13 48 05	−58 49 45	$0.46^{+0.26}_{-0.19}$	5/4	6.84E−05	10.1	7	3A	...	...	...	...	SAO	S:B9IV	SAO 241229	1.3
1ES1351+400	13 51 38	+40 05 24	$0.07^{+0.03}_{-0.02}$	30/5	6.15E−05	232.5	5	3A	m3146	0.5	...	...	MS	AGN:0.062	MS	0.8
1ES1351+695	13 51 57	+69 33 24	$1.36^{+0.17}_{-0.16}$	80/7	1.00E−10	55.4	5	3A	3147	0.2	x1H1350+696	0.5	VV	AGN:0.031	MKN 279*	0.2
1ES1354−314	13 54 42	−31 24 22	$0.66^{+0.31}_{-0.24}$	7/2	5.80E−06	9.7	6	3A	...	...	...	...	SAO	S:K0V	SAO 205032	0.3
1ES1355−086	13 55 05	−08 38 40	$0.36^{+0.23}_{-0.16}$	4/2	6.14E−05	10.5	9	2A	...	...	...	...	...	...	...	...
1ES1358−673	13 58 20	−67 18 08	$0.77^{+0.48}_{-0.34}$	4/2	3.92E−05	5.0	8	2A	...	...	...	...	SAO	S:K1II-III	SAO 252570	1.1
1ES1402+042	14 02 16	+04 16 26	$0.08^{+0.03}_{-0.02}$	24/7	6.90E−06	200.3	5	3A	m3177	0.9	x	...	HB	BL	2E	0.9

TABLE 6—*Continued*

Slew Desig.	RA 1950	DEC 1950	IPC Rate (cts s^{-1})	NP/NS	P_{rand}	Exp. (s)	PI	QI	EOS # EMSS	Δ2E (′)	A3 EXO	Δ1H (′)	Cat.	Class.: Type/z	Name	ΔC (′)
1ES1404−267	14 04 36	−26 46 33	$0.55^{+0.19}_{-0.16}$	13/4	4.83E−09	21.1	5	3A	...	...	1H1409−267	0.5	ABL	CG:0.021	A3561	0.4
1ES1405−183	14 05 38	−18 20 12	$0.33^{+0.21}_{-0.15}$	4/3	7.35E−05	11.6	6	1A	...	...	...	...	...	...	...	...
1ES1405−450	14 05 51	−45 03 01	$0.43^{+0.16}_{-0.13}$	11/3	7.59E−08	22.7	5	3A	3194	1.4	x1H1404−450	1.3	A3	CV	1E1405-451	1.3
1ES1407−461	14 07 08	−46 06 42	$0.24^{+0.13}_{-0.10}$	6/3	1.03E−05	22.6	6	3A	...	...	...	...	...	...	...	...
1ES1410−029	14 10 38	−02 58 28	$0.31^{+0.03}_{-0.03}$	112/8	1.00E−10	309.1	8	3A	3205	0.1	x1H1408−031	0.2	VV	AGN:0.006	NGC 5506	0.3
1ES1410+683	14 10 58	+68 19 20	$0.33^{+0.16}_{-0.13}$	8/5	7.68E−05	20.0	4	3A	...	...	...	...	...	...	...	...
1ES1414+203	14 14 13	+20 21 27	$0.28^{+0.13}_{-0.10}$	8/3	3.50E−05	24.4	3	3A	...	...	...	...	BSC	S:F8V	HD 125040	0.2
1ES1414−197	14 14 42	−19 43 34	$0.26^{+0.10}_{-0.09}$	11/3	4.11E−06	35.6	5	3A	...	...	...	...	SAO	S:A5IV	SAO 158468	0.5
1ES1415+451	14 15 03	+45 10 34	$0.27^{+0.13}_{-0.10}$	8/6	1.04E−04	24.5	3	3A	...	...	...	...	HB	AGN:0.114	PG	0.7
1ES1415−230	14 15 11	−23 05 23	$0.46^{+0.29}_{-0.21}$	4/2	4.85E−05	8.2	5	3A	...	...	...	...	...	...	...	...
1ES1415−209	14 15 29	−20 57 23	$0.21^{+0.09}_{-0.07}$	9/5	2.40E−05	36.2	8	3A	...	...	...	...	...	...	...	...
1ES1416−129	14 16 23	−12 57 03	$0.21^{+0.04}_{-0.04}$	37/7	1.00E−10	145.4	6	3A	m3238	0.4	x	...	HB	AGN:0.129	PG	0.4
1ES1417−192	14 17 00	−19 14 09	$0.15^{+0.05}_{-0.04}$	17/2	4.72E−07	88.1	5	3A	3244	0.5	...	...	VV	AGN:0.119	PKS	0.8
1ES1419+434	14 19 40	+43 27 09	$0.52^{+0.33}_{-0.23}$	4/4	4.63E−05	7.3	3	3A	...	...	...	...	...	...	...	...
1ES1421+582	14 21 09	+58 15 09	$0.46^{+0.18}_{-0.14}$	10/6	5.87E−08	19.9	5	3A	...	...	...	...	...	...	...	...
1ES1421+404	14 21 40	+40 28 29	$0.88^{+0.55}_{-0.39}$	4/2	4.06E−05	4.4	8	3A	...	...	...	...	...	...	...	...
1ES1421−051	14 21 59	−05 06 17	$0.36^{+0.26}_{-0.18}$	3/2	6.38E−05	8.1	5	3A	...	...	...	...	...	...	...	...
1ES1423+520	14 23 29	+52 04 34	$0.38^{+0.08}_{-0.07}$	33/3	1.00E−10	76.2	5	3A	3265	0.2	...	...	WLY	S:F6V	WLY 549A	0.4
1ES1426−624	14 26 04	−62 27 53	$0.33^{+0.04}_{-0.04}$	78/4	1.00E−10	210.4	4	3A	3278	0.4	x	...	SBD	S:MVE	PM14263-6228	1.7
1ES1426+015	14 26 33	+01 30 31	$0.34^{+0.08}_{-0.07}$	28/6	1.00E−10	69.7	5	3A	m3280	0.5	x1H1427+013	0.3	VV	AGN:0.086	MKN 1383	0.2
1ES1426+428	14 26 38	+42 53 41	$2.56^{+0.68}_{-0.58}$	17/3	1.00E−10	6.6	4	3A	...	...	x1H1430+423	0.3	A3	BL	H1426+427	0.4
1ES1435−067	14 35 37	−06 45 18	$0.22^{+0.08}_{-0.07}$	14/2	3.30E−06	50.6	5	3A	3305	0.2	...	...	HB	AGN:0.129	PG	0.1
1ES1435−606	14 35 48	−60 37 09	$0.76^{+0.16}_{-0.14}$	29/2	1.00E−10	36.5	2	3A	3308	1.3	...	...	SBD	S:G2V	α CEN AB	2.9
1ES1436−624	14 36 38	−62 26 07	$1.49^{+0.34}_{-0.30}$	28/1	1.00E−10	16.7	5	2A	...	...	x	...	SAO	S:A0	SAO 252841	1.6
1ES1437−252	14 37 52	−25 17 43	$0.82^{+0.45}_{-0.33}$	5/3	1.14E−06	5.9	10	3A	...	...	...	...	SBD	S:F0/F2V	HD 129009	2.9
1ES1439+111	14 39 35	+11 11 56	$0.35^{+0.17}_{-0.14}$	7/5	5.64E−05	17.3	3	3A	...	...	...	...	...	...	...	...
1ES1440+122	14 40 22	+12 13 16	$0.52^{+0.19}_{-0.16}$	11/6	1.23E−08	19.1	5	3A	...	...	...	...	...	...	...	...
1ES1442+058	14 42 42	+05 48 15	$0.34^{+0.19}_{-0.14}$	5/4	4.62E−05	13.6	6	3A	...	...	...	...	...	...	...	...
1ES1444+058	14 44 19	+05 50 51	$0.33^{+0.21}_{-0.15}$	4/3	7.33E−05	11.4	2	3A	...	...	...	...	...	...	...	...
1ES1444+361	14 44 43	+36 06 23	$0.38^{+0.22}_{-0.16}$	5/4	7.29E−05	12.2	8	3A	...	...	...	...	...	...	...	...
1ES1445+439	14 45 31	+43 56 35	$0.51^{+0.33}_{-0.23}$	4/1	1.07E−04	7.4	12	2A	...	...	...	...	...	...	...	...
1ES1449+193	14 49 07	+19 18 17	$0.79^{+0.12}_{-0.11}$	54/5	1.00E−10	63.9	4	3A	3337	0.3	1H1450+190.B	0.5	SAO	S:G8V+K4V	HD131156AB	0.2
1ES1450+679	14 50 07	+67 56 10	$0.10^{+0.04}_{-0.03}$	16/4	3.02E−05	114.6	8	3A	3340	3.0	...	...	2E	...	...	...

TABLE 6—*Continued*

Slew Desig.	RA 1950	DEC 1950	IPC Rate (cts s^{-1})	NP/NS	P_{rand}	Exp. (s)	PI	QI	EOS # EMSS	Δ2E (′)	A3 EXO	Δ1H (′)	Cat.	Class.: Type/z	Name	ΔC (′)
1ES1452+188	14 52 14	+18 50 24	$0.29^{+0.05}_{-0.05}$	45/7	1.00E−10	130.2	5	3A	3350	0.3	1H1450+190.A	0.9	ABL	CG:0.059	A1991	0.6
1ES1454+225	14 54 58	+22 32 09	$0.32^{+0.12}_{-0.10}$	11/4	1.75E−07	30.5	6	3A	m3356	0.6	...	...	MS	CG:0.259	MS	0.6
1ES1456+648	14 56 02	+64 51 52	$0.24^{+0.12}_{-0.09}$	7/4	2.73E−05	25.4	8	3A	...	...	...	...	...	...	...	...
1ES1456−400	14 56 32	−40 01 14	$0.75^{+0.38}_{-0.29}$	6/1	4.56E−06	7.5	9	3A	...	...	...	...	SBD	S:F7/F8V	HD 132349	2.3
1ES1457+033	14 57 17	+03 18 23	$0.41^{+0.20}_{-0.15}$	6/3	3.61E−06	13.9	6	3A	...	...	...	...	...	...	...	...
1ES1458+215	14 58 02	+21 33 12	$0.24^{+0.07}_{-0.06}$	19/2	9.75E−09	63.0	8	3E	3363	0.7	1H1457+214.	1.3	ABL	CG:0.153	A2009	0.9
1ES1458+018	14 58 21	+01 50 41	$0.63^{+0.39}_{-0.28}$	4/3	1.44E−05	6.1	10	3A	...	...	...	...	...	...	...	...
1ES1459+032	14 59 08	+03 15 16	$0.42^{+0.24}_{-0.18}$	5/3	4.57E−05	11.1	10	3A	...	...	...	...	...	...	...	...
1ES1500−415	15 00 17	−41 35 59	$0.49^{+0.06}_{-0.06}$	136/1	1.00E−10	204.3	5	3E	...	...	...	...	...	...	...	...
1ES1501+663	15 01 25	+66 23 56	$2.05^{+0.27}_{-0.25}$	65/13	1.00E−10	30.8	3	3A	...	...	x	...	MCS	WD	WD1501+664	0.3
1ES1501−370	15 01 30	−37 04 03	$1.67^{+1.03}_{-0.74}$	4/1	7.88E−06	2.3	6	3A	...	...	...	...	...	...	...	...
1ES1501+106	15 01 35	+10 38 06	$0.57^{+0.10}_{-0.09}$	39/2	1.00E−10	63.1	5	3A	3372	0.5	x	...	VV	AGN:0.036	MKN 841	0.4
1ES1502+478	15 02 07	+47 50 55	$2.24^{+0.52}_{-0.45}$	23/7	1.00E−10	10.0	4	3A	3373	0.2	x1H1504+473	0.2	A3	AC	ZZ BOO	0.2
1ES1503−320	15 03 43	−32 01 27	$0.42^{+0.30}_{-0.20}$	3/2	8.68E−05	6.9	8	3A	...	...	...	...	...	...	...	...
1ES1503+017	15 03 57	+01 47 59	$0.14^{+0.04}_{-0.04}$	21/3	1.81E−06	109.8	5	3A	3380	0.2	...	...	RNG	GAL:0.006	NGC 5846*	0.4
1ES1507−076	15 07 02	−07 38 24	$0.48^{+0.27}_{-0.20}$	5/3	1.57E−05	9.9	11	3A	...	...	...	...	SAO	S:K0	SAO 140351*	2.7
1ES1508+337	15 08 06	+33 42 30	$0.40^{+0.17}_{-0.13}$	9/5	1.32E−07	20.4	6	3A	...	...	1H1510+335	1.9	ABL	CG:0.151	A2034	1.3
1ES1508+059	15 08 26	+05 55 55	$1.54^{+0.27}_{-0.24}$	39/3	1.00E−10	24.3	6	3A	3385	0.4	1H1508+060	1.6	ABL	CG:0.077	A2029	1.5
1ES1509+763	15 09 01	+76 22 44	$0.44^{+0.20}_{-0.15}$	8/3	1.91E−06	16.4	5	3A	...	...	...	...	SAO	S:G5	SAO 008175	1.1
1ES1509−589	15 09 48	−58 56 14	$0.89^{+0.20}_{-0.17}$	31/1	1.00E−10	30.4	8	3A	3389	1.6	x	...	2E	P	...	...
1ES1509−588	15 09 49	−58 49 42	$0.43^{+0.15}_{-0.13}$	17/1	2.76E−06	29.7	6	3M	3388	0.6	x	...	2E	SNR	MSH 15-52	2.0
1ES1513+002	15 13 47	+00 16 17	$0.15^{+0.05}_{-0.04}$	24/4	8.18E−07	112.6	8	3A	3404	0.8	...	...	ABL	CG:0.118	A2050	0.8
1ES1514+072	15 14 18	+07 12 15	$0.94^{+0.15}_{-0.14}$	46/2	1.00E−10	46.1	6	3A	3407	0.2	x1H1514+072	0.7	ABL	CG:0.035	A2052	1.3
1ES1517+656	15 17 07	+65 36 26	$0.91^{+0.29}_{-0.24}$	13/7	1.00E−10	13.7	5	3A	...	...	1H1515+660	0.2	A3	BL	H1517+656	0.2
1ES1518−071	15 18 13	−07 10 36	$0.23^{+0.11}_{-0.09}$	8/1	2.03E−05	29.3	9	2A	...	...	...	...	...	...	...	...
1ES1518+593	15 18 13	+59 18 51	$0.36^{+0.14}_{-0.12}$	11/7	1.72E−06	26.0	3	2A	...	...	...	...	VV	AGN:0.079	SBS1518+593	0.4
1ES1519+078	15 19 22	+07 52 48	$0.41^{+0.13}_{-0.11}$	15/7	1.59E−09	31.7	6	3A	3419	1.1	...	...	UGC	CG:0.045	MKW 3S	0.5
1ES1519+211	15 19 41	+21 08 10	$0.33^{+0.17}_{-0.13}$	6/2	4.26E−05	16.4	3	3A	...	...	...	...	WLY	S:M0EV	WLY 9520	1.3
1ES1520−168	15 20 19	−16 48 56	$0.35^{+0.20}_{-0.15}$	5/2	4.44E−05	13.2	11	3A	...	...	...	...	...	...	...	...
1ES1520+278	15 20 20	+27 53 12	$0.33^{+0.07}_{-0.07}$	29/3	1.00E−10	76.1	7	3E	3426	0.7	...	...	2E	CG:0.072	A2065	0.8
1ES1520+087	15 20 36	+08 47 08	$0.61^{+0.10}_{-0.09}$	51/6	1.00E−10	74.2	8	3A	3427	0.7	1H1521+083	2.3	ABL	CG:0.034	A2063	1.9
1ES1522+300	15 22 13	+30 00 54	$0.18^{+0.06}_{-0.05}$	17/3	5.43E−07	71.7	5	3A	m3432	3.0	...	...	2E	CG:0.115	A2069	2.8
1ES1524+482	15 24 42	+48 14 24	$0.54^{+0.33}_{-0.24}$	4/2	1.49E−06	7.2	4	3A	...	...	...	...	...	...	...	...

TABLE 6—*Continued*

Slew Desig.	RA 1950	DEC 1950	IPC Rate (cts s^{-1})	NP/NS	P_{rand}	Exp. (s)	PI	QI	EOS # EMSS	Δ2E (′)	A3 EXO	Δ1H (′)	Cat.	Class.: Type/z	Name	ΔC (′)
1ES1527+714	15 27 21	+71 24 15	$0.13^{+0.05}_{-0.04}$	14/5	8.60E−05	79.2	5	2A	...	...	...	...	...	...	...	...
1ES1531+091	15 31 16	+09 10 38	$0.20^{+0.12}_{-0.09}$	5/1	8.25E−05	22.6	7	3A	...	...	...	...	...	...	...	...
1ES1533+535	15 33 36	+53 30 00	$0.49^{+0.18}_{-0.14}$	11/6	1.18E−09	20.7	6	3A	...	...	...	...	...	...	...	...
1ES1536+515	15 36 48	+51 34 02	$0.32^{+0.16}_{-0.12}$	7/3	1.74E−05	19.4	5	3A	...	...	...	...	...	...	...	...
1ES1538+257	15 38 24	+25 43 07	$0.34^{+0.21}_{-0.15}$	4/3	6.54E−05	11.3	7	3A	...	...	...	...	...	...	...	...
1ES1539+187	15 39 57	+18 44 48	$0.24^{+0.11}_{-0.09}$	9/6	1.84E−05	31.7	8	3A	...	...	...	...	...	...	...	...
1ES1541+457	15 41 43	+45 43 05	$0.36^{+0.20}_{-0.15}$	5/4	4.71E−06	13.2	7	3A	...	...	...	...	...	...	...	...
1ES1543+362	15 43 12	+36 13 11	$0.12^{+0.04}_{-0.04}$	16/5	2.53E−05	94.9	6	3E	...	...	1H1544+360	1.6	ABL	CG:0.065	A2124	1.2
1ES1544+820	15 44 08	+82 04 32	$0.53^{+0.14}_{-0.12}$	19/12	1.00E−10	33.1	5	3A	...	...	...	...	...	...	...	...
1ES1545+210	15 45 32	+21 01 17	$0.19^{+0.02}_{-0.02}$	112/11	1.00E−10	474.4	6	3A	3500	0.3	...	...	VV	AGN:0.264	3C 323.1	0.2
1ES1546+104	15 46 40	+10 25 38	$0.25^{+0.11}_{-0.09}$	8/5	4.58E−06	28.8	9	3A	...	...	...	...	...	...	...	...
1ES1547+262	15 47 31	+26 13 14	$0.20^{+0.07}_{-0.06}$	14/7	2.56E−07	58.3	4	3A	3507	0.1	...	...	BSC	S:G3.5III-IV	HD 141714	0.2
1ES1548+114	15 48 21	+11 29 11	$0.09^{+0.03}_{-0.03}$	21/6	6.88E−06	152.1	7	3A	3508	0.6	...	...	HB	AGN:0.436	MC	0.6
1ES1549+203	15 49 50	+20 22 27	$0.10^{+0.03}_{-0.03}$	25/5	1.67E−07	179.4	5	3A	m3513	0.4	...	...	VV	AGN:0.250	LB 906*	0.5
1ES1550+191	15 50 31	+19 06 01	$1.21^{+0.31}_{-0.26}$	20/2	1.00E−10	15.8	3	3A	...	...	x	...	SHA	CV	MR SER	0.9
1ES1552+203	15 52 14	+20 20 22	$0.21^{+0.06}_{-0.05}$	24/4	1.47E−10	93.1	7	3A	m3523	0.6	...	...	2E	...	...	...
1ES1553+113	15 53 19	+11 20 20	$1.61^{+0.18}_{-0.17}$	94/3	1.00E−10	56.1	4	3A	3529	0.3	...	...	HB	BL:0.360	PG	0.5
1ES1555+086	15 55 14	+08 40 36	$0.74^{+0.54}_{-0.37}$	3/2	1.05E−04	3.9	9	1A	...	...	...	...	...	...	...	...
1ES1556+273	15 56 15	+27 22 33	$1.01^{+0.12}_{-0.11}$	87/8	1.00E−10	81.8	6	3A	3541	0.3	x1H1556+273	0.3	ABL	CG:0.090	A2142	0.9
1ES1556+257	15 56 38	+25 42 23	$0.30^{+0.15}_{-0.12}$	7/3	2.75E−05	20.4	6	3A	3543	0.3	...	...	SAO	S:K2V	SAO 084114	0.7
1ES1557+496	15 57 21	+49 37 59	$0.25^{+0.13}_{-0.10}$	6/4	8.67E−05	21.0	6	3A	...	...	...	...	...	...	...	...
1ES1559+161	15 59 58	+16 08 16	$0.11^{+0.03}_{-0.02}$	53/6	2.54E−06	249.6	6	3E	3565	2.0	...	...	UGC	CG:0.035	A2147	2.3
1ES1601+160	16 01 24	+16 02 11	$0.16^{+0.06}_{-0.05}$	22/7	2.88E−05	90.3	6	3A	3572	0.6	...	...	ZCT	GAL:0.100	1601+1602	1.5
1ES1601+669	16 01 36	+66 57 09	$0.17^{+0.04}_{-0.03}$	42/10	1.00E−10	179.2	3	3A	3573	1.5	x	...	SBD	S:K0	AG DRA	1.5
1ES1602+178	16 02 23	+17 51 57	$0.18^{+0.03}_{-0.03}$	78/17	1.00E−10	322.2	5	3A	3577	0.5	...	...	UGC	GAL:0.042	U10170*	1.5
1ES1602+240	16 02 42	+24 03 52	$0.14^{+0.05}_{-0.04}$	19/7	4.99E−07	101.1	7	3A	3581	1.6	...	...	UGC	CG:0.042	AWM 4	1.4
1ES1606+218	16 06 54	+21 53 30	$0.16^{+0.07}_{-0.06}$	10/6	7.16E−05	50.4	8	3A	...	...	...	...	SBD	S:K2	AG+21 1576	2.7
1ES1607+621	16 07 31	+62 06 10	$0.18^{+0.08}_{-0.07}$	10/6	1.12E−04	42.3	10	2A	...	...	...	...	...	...	...	...
1ES1609−522	16 09 01	−52 17 31	$7.48^{+1.79}_{-1.55}$	21/1	1.00E−10	2.8	8	3A	...	...	x1H1608−522	1.4	A3	XRB	QX NOR	1.4
1ES1610+669	16 10 08	+66 59 45	$0.15^{+0.05}_{-0.05}$	23/5	2.82E−05	96.7	5	3A	...	...	...	...	...	...	...	...
1ES1612+261	16 12 09	+26 11 52	$0.27^{+0.07}_{-0.06}$	22/9	1.00E−10	69.9	6	3A	3617	0.1	x	...	HB	AGN:0.131	TON 256	0.1
1ES1612+339	16 12 47	+33 59 14	$2.27^{+0.21}_{-0.21}$	129/12	1.00E−10	55.2	5	3A	3618	0.2	x	...	WLY	AC:F6V+G1V	WLY 9550AB	0.3
1ES1613+658	16 13 34	+65 50 53	$0.20^{+0.04}_{-0.04}$	35/10	1.00E−10	140.9	4	3A	3624	0.5	x1H1615+655	0.4	VV	AGN:0.129	MKN 876	0.3

TABLE 6—*Continued*

Slew Desig.	RA 1950	DEC 1950	IPC Rate (cts s^{-1})	NP/NS	P_{rand}	Exp. (s)	PI	QI	EOS # EMSS	Δ2E (′)	A3 EXO	Δ1H (′)	Cat.	Class.: Type/z	Name	ΔC (′)
1ES1613−509	16 13 58	−50 57 19	$4.42^{+0.31}_{-0.31}$	209/2	1.00E−10	46.1	6	3A	3626	0.6	x	...	2E	SNR	RCW 103	0.8
1ES1614+446	16 14 08	+44 40 38	$0.36^{+0.10}_{-0.09}$	18/12	1.00E−10	44.8	6	3A	...	...	...	...	SAO	S:G0	SAO 045997	0.4
1ES1614+171	16 14 10	+17 11 43	$0.66^{+0.50}_{-0.34}$	3/2	2.11E−05	4.3	6	3A	...	...	...	...	...	...	...	...
1ES1615+061	16 15 19	+06 11 11	$0.27^{+0.07}_{-0.06}$	27/5	2.10E−10	77.6	7	3A	3634	0.2	x	...	VV	AGN:0.038	H 1613+06	0.2
1ES1615+553	16 15 57	+55 22 47	$0.24^{+0.05}_{-0.04}$	37/8	1.00E−10	127.9	4	3A	3641	0.9	...	...	WLY	S:M1EV	WLY 9552	1.1
1ES1616+436	16 16 53	+43 36 54	$0.28^{+0.14}_{-0.11}$	8/6	1.08E−04	23.4	8	2A	...	...	...	...	...	...	...	...
1ES1618+411	16 18 11	+41 06 09	$0.14^{+0.04}_{-0.04}$	25/2	3.33E−08	131.1	5	3A	3650	0.1	...	...	2E	...	...	...
1ES1621+274	16 21 35	+27 26 56	$0.14^{+0.06}_{-0.05}$	12/5	2.31E−05	66.2	8	2A	3658	2.6	...	...	2E	...	...	...
1ES1622+261	16 22 06	+26 11 41	$0.09^{+0.03}_{-0.03}$	19/6	6.61E−05	144.0	7	3A	...	...	x	...	2E	AGN:0.040	EXO	0.8
1ES1625+261	16 25 01	+26 08 59	$0.10^{+0.04}_{-0.03}$	22/7	3.39E−05	137.0	8	2A	...	...	...	...	...	...	...	...
1ES1626+279	16 26 33	+27 58 54	$0.35^{+0.16}_{-0.13}$	8/6	2.09E−05	19.5	9	3A	...	...	...	...	...	...	...	...
1ES1626+396	16 26 54	+39 39 54	$1.63^{+0.09}_{-0.09}$	346/8	1.00E−10	199.5	6	3A	3705	0.4	x1H1631+394	1.7	ABL	CG:0.030	A2199	1.9
1ES1626+554	16 26 54	+55 29 53	$0.33^{+0.12}_{-0.10}$	12/6	1.02E−07	31.4	4	3A	...	...	...	...	VV	AGN:0.132	PG	0.9
1ES1627+402	16 27 22	+40 13 05	$0.19^{+0.06}_{-0.05}$	23/7	3.80E−09	93.1	4	3A	...	...	x	...	VV	AGN:0.270	EXO	1.0
1ES1630−272	16 30 44	−27 12 11	$0.51^{+0.37}_{-0.25}$	3/1	6.21E−05	5.7	7	1A	...	...	...	...	...	...	...	...
1ES1631+781	16 31 31	+78 11 18	$0.60^{+0.17}_{-0.15}$	17/10	1.00E−10	26.0	2	3A	...	...	...	...	WFC	WD:DA	WFC 1629+781	0.0
1ES1634−104	16 34 22	−10 27 43	$0.10^{+0.04}_{-0.04}$	14/3	1.00E−04	95.1	5	3A	3732	1.0	...	...	BSC	S:O9.5Vn	ζ OPH	0.6
1ES1635+663	16 35 39	+66 18 55	$0.16^{+0.04}_{-0.04}$	28/11	2.84E−09	130.6	8	3A	3739	0.1	...	...	ABL	CG:0.171	A2218	0.3
1ES1638+608	16 38 23	+60 48 15	$0.35^{+0.09}_{-0.08}$	24/16	1.00E−10	57.7	6	3A	3742	0.5	...	...	SAO	S:G0V	WW DRA	0.3
1ES1638+634	16 38 45	+63 29 33	$0.14^{+0.06}_{-0.05}$	13/10	2.66E−05	72.4	9	3A	...	...	...	...	...	...	...	...
1ES1641+399	16 41 18	+39 54 01	$0.23^{+0.04}_{-0.04}$	59/8	1.00E−10	200.5	5	3A	3752	0.3	...	...	VV	AGN:0.594	3C345.0	0.2
1ES1646−031	16 46 26	−03 06 49	$0.96^{+0.61}_{-0.44}$	4/2	8.54E−05	3.9	4	3A	...	...	...	...	...	...	...	...
1ES1647−135	16 47 26	−13 33 04	$0.31^{+0.17}_{-0.13}$	6/2	8.51E−05	17.0	4	2A	...	...	...	...	...	...	...	...
1ES1649−403	16 49 07	−40 20 24	$0.18^{+0.08}_{-0.07}$	9/2	3.42E−05	40.6	7	3A	...	...	...	...	...	...	...	...
1ES1649+758	16 49 34	+75 49 13	$0.18^{+0.08}_{-0.07}$	10/9	4.90E−05	43.5	7	3A	...	...	...	...	...	...	...	...
1ES1650−417	16 50 22	−41 47 30	$0.12^{+0.04}_{-0.04}$	20/2	2.95E−05	114.9	8	3A	...	...	...	...	SAO	S:B	SAO 227370	1.1
1ES1652+398	16 52 12	+39 50 25	$3.24^{+0.13}_{-0.13}$	616/11	1.00E−10	186.8	5	3A	3780	0.1	x1H1651+398	0.3	VV	BL:0.034	MKN 501	0.1
1ES1652−082	16 52 49	−08 15 17	$0.57^{+0.10}_{-0.09}$	39/1	1.00E−10	63.2	4	3A	3783	0.5	x1H1653−083	0.6	A3	AC	V1054 OPH	0.6
1ES1653+795	16 53 08	+79 35 09	$0.18^{+0.07}_{-0.06}$	13/8	2.21E−06	58.2	6	3A	...	...	...	...	...	...	...	...
1ES1653+449	16 53 09	+44 55 31	$0.47^{+0.29}_{-0.21}$	4/3	6.22E−05	8.2	11	3A	...	...	...	...	...	...	...	...
1ES1656+354	16 56 02	+35 25 12	$0.48^{+0.07}_{-0.06}$	70/6	1.00E−10	131.2	5	3A	3791	0.1	x1H1656+354	0.2	A3	XRB	HER X-1	0.1
1ES1659+341	16 59 12	+34 07 20	$0.16^{+0.07}_{-0.06}$	12/4	3.56E−05	57.5	7	3A	3805	1.2	...	...	2E	...	...	...
1ES1659+572	16 59 50	+57 17 07	$0.20^{+0.10}_{-0.08}$	8/8	8.22E−05	32.6	8	2A	...	...	...	...	...	...	...	...

TABLE 6—*Continued*

Slew Desig.	RA 1950	DEC 1950	IPC Rate (cts s^{-1})	NP/NS	P_{rand}	Exp. (s)	PI	QI	EOS # EMSS	Δ2E (′)	A3 EXO	ΔIH (′)	Cat.	Class.: Type/s	Name	ΔC (′)
1ES1700+341	17 00 52	+34 08 27	$0.49^{+0.16}_{-0.13}$	15/5	7.29E−10	26.8	6	3A	3809	0.8	1H1702+336	0.8	ABL	CG:0.097	A2244	1.5
1ES1701−369	17 01 38	−36 59 40	$0.14^{+0.04}_{-0.04}$	25/2	1.30E−06	121.8	8	2M	...	...	...	...	...	...	...	...
1ES1702+457	17 02 02	+45 44 26	$0.31^{+0.14}_{-0.11}$	9/5	2.53E−05	24.6	5	3A	...	...	...	...	SAO	S:F8	SAO 046462*	1.3
1ES1702−369	17 02 23	−36 58 24	$0.22^{+0.07}_{-0.06}$	19/2	3.31E−06	62.8	7	2A	...	...	...	...	SBD	...	IRAS 17023-3659	1.4
1ES1702+482	17 02 58	+48 12 50	$0.22^{+0.10}_{-0.08}$	8/5	8.63E−05	30.7	5	2A	...	...	...	...	...	...	...	...
1ES1704+545	17 04 10	+54 32 33	$0.18^{+0.07}_{-0.06}$	13/6	1.49E−05	54.5	4	3A	m3830	1.1	...	...	WLY	S:F6V	WLY 9584*	1.1
1ES1704+607	17 04 13	+60 47 56	$0.04^{+0.01}_{-0.01}$	67/22	5.66E−05	704.3	6	3A	3828	1.2	1H1704+605	1.3	HB	AGN:0.371	3C351	1.3
1ES1704+736	17 04 16	+73 36 28	$0.17^{+0.07}_{-0.06}$	12/9	1.75E−05	54.2	10	3A	...	...	...	...	...	...	...	...
1ES1704+240	17 04 31	+24 02 14	$0.68^{+0.09}_{-0.08}$	73/3	1.00E−10	100.3	7	3A	3831	0.4	x1H1706+241	0.2	SAO	S:M0	SAO 084844	0.3
1ES1706+787	17 06 58	+78 43 49	$0.38^{+0.04}_{-0.04}$	126/20	1.00E−10	280.5	7	3A	3842	0.8	...	...	UGC	GAL	U10726*	1.8
1ES1711−547	17 11 29	−54 47 08	$0.40^{+0.16}_{-0.13}$	10/1	2.57E−07	22.2	8	3A	...	...	...	...	SAO	S:F0IV-V	SAO 244557	1.4
1ES1711+657	17 11 48	+65 45 50	$0.16^{+0.07}_{-0.06}$	13/9	4.10E−05	59.4	9	3A	...	...	...	...	...	...	...	...
1ES1712+641	17 12 25	+64 06 28	$0.25^{+0.04}_{-0.04}$	54/14	1.00E−10	172.2	7	3A	3866	1.3	...	...	2E	CG:0.081	A2255	1.2
1ES1714+574	17 14 27	+57 27 19	$0.27^{+0.08}_{-0.07}$	17/10	6.09E−10	54.7	7	3A	...	...	...	...	RNG	GAL:0.028	NGC 6338*	1.3
1ES1716+551	17 16 16	+55 08 14	$0.21^{+0.09}_{-0.08}$	10/7	7.11E−05	37.9	9	3A	...	...	...	...	SAO	S:K0	SAO 030326	2.8
1ES1717+265	17 17 57	+26 32 18	$0.19^{+0.07}_{-0.06}$	14/1	1.06E−05	56.1	4	3A	m3884	0.6	...	...	MS	S:M4V+M5V	WLY 669AB	0.9
1ES1718+650	17 18 12	+65 01 48	$0.13^{+0.05}_{-0.04}$	15/5	6.83E−05	83.8	6	3A	...	...	...	...	...	...	...	...
1ES1718+266	17 18 12	+26 40 44	$0.28^{+0.08}_{-0.07}$	21/2	1.00E−10	63.6	6	3A	3885	0.4	1H1720+269.B	0.6	2E	CG:0.164	2E	0.3
1ES1720+309	17 20 46	+30 55 30	$0.35^{+0.09}_{-0.07}$	25/2	1.00E−10	63.3	5	3A	3893	0.2	x1H1727+308	0.1	VV	AGN:0.043	MKN 506	0.2
1ES1721+343	17 21 32	+34 20 34	$0.57^{+0.07}_{-0.07}$	83/7	1.00E−10	134.9	5	3A	3896	0.3	...	...	HB	AGN:0.206	4C 34.47	0.1
1ES1721+106	17 21 59	+10 41 06	$0.46^{+0.27}_{-0.20}$	5/4	8.93E−05	9.9	8	2A	...	...	...	...	...	...	...	...
1ES1722+119	17 22 43	+11 54 30	$0.64^{+0.34}_{-0.26}$	6/3	4.70E−05	8.4	6	3A	...	...	x1H1720+117	0.4	A3	BL	H1722+119	0.5
1ES1727+502	17 27 05	+50 15 14	$0.77^{+0.03}_{-0.03}$	571/21	1.00E−10	701.9	5	3A	3909	0.5	x1H1730+500	0.3	VV	BL:0.055	I ZW 187	0.3
1ES1727−214	17 27 40	−21 27 52	$2.99^{+0.32}_{-0.30}$	100/2	1.00E−10	32.6	5	3A	3911	1.4	x1H1728−213	1.0	A3	SNR	KEPLER	1.0
1ES1727+590	17 27 52	+59 04 13	$0.44^{+0.19}_{-0.15}$	8/6	1.74E−07	16.7	5	3A	...	...	...	...	SAO	S:G0	SAO 030416	0.9
1ES1728−169	17 28 49	−16 55 25	$67.83^{+3.52}_{-3.52}$	376/1	1.00E−10	5.5	6	3A	...	...	x1H1728−169	0.4	A3	XRB	GX9+9	0.3
1ES1730+098	17 30 08	+09 50 56	$0.45^{+0.24}_{-0.18}$	6/1	7.04E−05	12.0	5	2A	...	...	...	...	...	...	...	...
1ES1731−325	17 31 26	−32 32 53	$0.18^{+0.06}_{-0.05}$	20/2	1.03E−08	86.5	6	3A	3920	0.1	x	...	2E	XRB	TERZ 1*	0.6
1ES1734+742	17 34 10	+74 15 50	$0.80^{+0.12}_{-0.11}$	57/24	1.00E−10	65.8	5	3A	...	...	1H1739+744	0.5	A3	AC	SAO 008842	0.5
1ES1734+686	17 34 25	+68 40 36	$0.24^{+0.10}_{-0.08}$	9/6	2.85E−06	32.8	8	3A	...	...	...	...	...	...	...	...
1ES1735−269	17 35 09	−26 57 40	$0.91^{+0.23}_{-0.20}$	22/1	1.00E−10	21.7	7	3A	...	...	...	...	SBD	S	IRAS 17345-2656	1.0
1ES1735−444	17 35 19	−44 25 09	$39.04^{+1.79}_{-1.79}$	483/5	1.00E−10	12.3	7	3A	...	...	x1H1735−444	0.2	A3	XRB	V926 SCO	0.2
1ES1736+013	17 36 21	+01 20 00	$0.81^{+0.58}_{-0.39}$	3/1	3.16E−05	3.7	6	3A	...	...	...	...	...	...	...	...

TABLE 6—*Continued*

Slew Desig.	RA 1950	DEC 1950	IPC Rate (cts s^{-1})	NP/NS	P_{rand}	Exp. (s)	PI	QI	EOS # EMSS	Δ2E ($'$)	A3 EXO	Δ1H ($'$)	Cat.	Class.: Type/z	Name	ΔC ($'$)
1ES1737+612	17 37 58	+61 16 44	$0.23^{+0.10}_{-0.08}$	9/6	4.48E−06	33.9	5	3A	...	...	...	...	SBD	S:M	HD 160934	2.0
1ES1739+518	17 39 19	+51 51 44	$0.15^{+0.06}_{-0.05}$	15/7	9.30E−05	67.1	5	3A	3934	0.7	...	...	VV	AGN:0.061	E 1739+518	0.6
1ES1741+196	17 41 46	+19 36 16	$0.54^{+0.23}_{-0.18}$	9/4	1.72E−06	14.8	7	3A	...	...	...	...	...	...	...	...
1ES1742−294	17 42 55	−29 29 56	$1.86^{+0.25}_{-0.23}$	65/2	1.00E−10	33.4	9	3A	3943	1.8	x1H1744−293	0.3	A3	XRB	X1742-294	0.3
1ES1743+480	17 43 48	+48 03 41	$0.31^{+0.14}_{-0.11}$	8/5	9.12E−06	22.5	7	3A	...	...	...	...	...	...	...	...
1ES1745+720	17 45 10	+72 04 24	$0.17^{+0.06}_{-0.05}$	17/13	7.99E−07	79.3	7	3A	...	...	...	...	...	...	...	...
1ES1745+504	17 45 13	+50 29 16	$0.24^{+0.11}_{-0.09}$	9/5	5.61E−05	30.1	6	3A	...	...	...	...	...	...	...	...
1ES1746+748	17 46 29	+74 53 38	$0.19^{+0.07}_{-0.06}$	12/9	5.88E−06	51.4	4	3A	...	...	...	...	SAO	S:K0	SAO 008910	0.2
1ES1746−370	17 46 47	−37 02 11	$8.46^{+2.44}_{-2.05}$	15/1	1.00E−10	1.7	8	3A	...	...	x1H1746−370	0.4	A3	XRB	NGC 6441	0.3
1ES1747−637	17 47 06	−63 47 57	$0.34^{+0.17}_{-0.13}$	7/3	3.58E−05	18.2	6	3A	...	...	...	...	...	...	...	...
1ES1750+707	17 50 59	+70 47 52	$0.17^{+0.07}_{-0.06}$	16/9	3.00E−05	66.7	7	3A	m3969	1.3	x	...	2E	S	2E	1.6
1ES1753−290	17 53 19	−29 03 17	$2.10^{+1.18}_{-0.87}$	5/1	2.52E−05	2.2	6	3A	...	...	...	...	SAO	S:A3	HD 163300*	2.2
1ES1753+362	17 53 39	+36 12 14	$0.74^{+0.42}_{-0.31}$	5/2	2.82E−05	6.3	7	3A	...	...	...	...	SAO	S:G5	SAO 066472	0.9
1ES1754+062	17 54 03	+06 17 38	$0.27^{+0.14}_{-0.11}$	6/2	1.03E−04	19.6	8	3A	...	...	...	...	...	...	...	...
1ES1755−338	17 55 07	−33 49 47	$5.11^{+2.11}_{-1.66}$	8/1	1.50E−10	1.5	10	3A	...	...	...	...	BMC	XRB	4U1755-338	3.0
1ES1757−233	17 57 29	−23 20 25	$0.31^{+0.10}_{-0.08}$	23/2	3.59E−07	53.4	7	2E	...	...	...	...	...	...	...	...
1ES1758−250	17 58 02	−25 04 40	$57.05^{+1.99}_{-1.99}$	837/2	1.00E−10	14.6	9	3A	...	...	x1H1758−250	0.2	A3	XRB	GX5-1	0.3
1ES1758−257	17 58 06	−25 44 04	$2.63^{+0.50}_{-0.44}$	34/3	1.00E−10	12.4	8	3A	...	...	x	...	...	...	...	...
1ES1802+025	18 02 52	+02 30 28	$0.35^{+0.09}_{-0.08}$	25/1	1.00E−10	62.0	4	3A	4004	1.2	...	...	WLY	S:K0V+K5V	WLY 702AB	1.0
1ES1805−118	18 05 09	−11 53 00	$0.80^{+0.34}_{-0.27}$	8/2	7.98E−09	9.6	8	3A	...	...	...	...	...	...	...	...
1ES1807+698	18 07 11	+69 48 47	$0.08^{+0.02}_{-0.02}$	51/14	1.96E−08	394.2	6	3A	4023	0.9	x1H1803+696	0.7	VV	BL:0.051	3C 371.0	0.7
1ES1808−579	18 08 18	−57 57 43	$0.80^{+0.39}_{-0.30}$	6/2	7.57E−08	7.2	6	3A	...	...	...	...	...	...	...	...
1ES1810+696	18 10 23	+69 40 53	$0.06^{+0.02}_{-0.01}$	52/14	1.37E−06	482.2	5	2A	m4039	0.6	x	...	SAO	S:K2	SAO 017600	0.8
1ES1811+006	18 11 13	+00 39 25	$0.66^{+0.42}_{-0.30}$	4/1	8.69E−05	5.8	8	3A	...	...	...	...	SAO	S:K0	SAO 123267	0.8
1ES1811−171	18 11 34	−17 10 26	$18.80^{+2.67}_{-2.44}$	56/1	1.00E−10	2.9	8	3A	...	...	x1H1811−171	0.7	A3	XRB	GX13+1	0.8
1ES1814+782	18 14 38	+78 12 34	$0.13^{+0.05}_{-0.04}$	15/7	7.11E−05	81.1	5	3A	...	...	...	...	...	...	...	...
1ES1814+498	18 14 58	+49 50 29	$0.63^{+0.08}_{-0.08}$	69/7	1.00E−10	102.5	3	3A	4051	0.5	x1H1814+498	0.5	A3	CV	AM HER	0.5
1ES1817+537	18 17 10	+53 42 59	$0.55^{+0.20}_{-0.16}$	11/5	1.87E−10	18.9	4	3A	...	...	...	...	...	...	...	...
1ES1820−303	18 20 29	−30 23 23	$99.46^{+5.68}_{-5.68}$	309/1	1.00E−10	3.1	7	3A	...	...	x1H1820−303	0.2	A3	XRB	NGC 6624	0.3
1ES1821+643	18 21 43	+64 19 13	$1.08^{+0.23}_{-0.20}$	28/10	1.00E−10	24.3	6	3A	4066	0.3	x1H1820+643	0.3	HB	AGN:0.297	KUV 1821+64*	0.3
1ES1822−577	18 22 56	−57 47 00	$1.12^{+0.82}_{-0.55}$	3/1	2.73E−05	2.6	2	3A	...	...	...	...	...	...	...	...
1ES1824−698	18 24 30	−69 48 09	$2.49^{+1.82}_{-1.23}$	3/1	4.42E−05	1.2	4	3A	...	...	...	...	...	...	...	...
1ES1824+151	18 24 38	+15 07 03	$1.18^{+0.48}_{-0.38}$	8/1	1.00E−10	6.7	7	3A	...	...	...	...	SAO	S:K0	SAO 103722	1.2

TABLE 6—*Continued*

Slew Desig.	RA 1950	DEC 1950	IPC Rate (cts s^{-1})	NP/NS	P_{rand}	Exp. (s)	PI	QI	EOS # EMSS	Δ2E (′)	A3 EXO	Δ1H (′)	Cat.	Class.: Type/z	Name	ΔC (′)
1ES1827+206	18 27 48	+20 41 56	$0.14^{+0.06}_{-0.05}$	10/1	7.03E−05	58.3	8	2A	...	...	...	...	...	...	...	...
1ES1831−040	18 31 43	−04 02 11	$0.32^{+0.17}_{-0.13}$	6/1	6.28E−05	16.7	4	3A	...	...	...	...	...	...	...	...
1ES1832+516	18 32 43	+51 40 04	$1.02^{+0.30}_{-0.26}$	15/5	1.00E−10	14.0	5	3A	4094	0.9	x	...	WLY	AC:M0EV	BY DRA	1.0
1ES1833+326	18 33 11	+32 38 41	$0.49^{+0.10}_{-0.09}$	35/3	1.00E−10	65.4	7	3A	4097	0.7	x1H1835+326	0.6	VV	AGN:0.059	3C382.0	0.7
1ES1833+169	18 33 40	+16 56 41	$0.17^{+0.06}_{-0.05}$	18/5	7.53E−07	78.6	5	3A	...	...	...	...	BSC	S:G2V+G2V	HD 171746	0.6
1ES1837+348	18 37 04	+34 50 37	$0.39^{+0.22}_{-0.16}$	5/4	4.56E−05	11.9	12	3A	...	...	...	...	...	...	...	...
1ES1841−044	18 41 55	−04 27 10	$0.41^{+0.20}_{-0.16}$	7/2	2.22E−05	14.9	3	3A	...	...	...	...	GCV	S	FT SCT	1.6
1ES1845+797	18 45 41	+79 43 04	$0.20^{+0.02}_{-0.02}$	156/24	1.00E−10	618.8	7	3A	4136	0.2	x1H1858+797	0.2	VV	AGN:0.057	3C 390.3	0.2
1ES1846+005	18 46 22	+00 31 37	$0.22^{+0.08}_{-0.07}$	12/2	7.32E−08	48.3	6	3A	4138	0.2	x	...	SHA	CV	V603 AQL	0.2
1ES1846−238	18 46 45	−23 53 05	$0.43^{+0.13}_{-0.11}$	17/2	1.00E−10	35.4	3	3A	4140	0.6	...	...	WLY	S:M4EV	WLY 729	0.4
1ES1846−009	18 46 56	−00 59 03	$0.24^{+0.11}_{-0.09}$	8/1	1.03E−05	29.6	8	3A	...	...	...	...	...	...	...	...
1ES1847−318	18 47 33	−31 51 35	$0.52^{+0.27}_{-0.20}$	6/1	2.06E−05	10.5	3	3A	...	...	...	...	...	...	...	...
1ES1850+005	18 50 04	+00 34 51	$0.23^{+0.06}_{-0.05}$	26/3	1.00E−10	93.7	6	3A	4150	1.5	...	...	SBD	SNR	4C .70	2.9
1ES1850−087	18 50 20	−08 45 58	$4.21^{+0.27}_{-0.27}$	260/3	1.00E−10	60.9	7	3A	4151	0.2	x1H1850−087	0.3	A3	XRB	NGC6712	0.3
1ES1851−312	18 51 51	−31 13 27	$0.94^{+0.27}_{-0.23}$	16/3	1.00E−10	16.1	7	3A	...	...	x1H1853−312	0.5	A3	CV	V1223 SGR	0.5
1ES1853−379	18 53 13	−37 58 25	$0.86^{+0.32}_{-0.26}$	10/5	1.00E−10	11.2	3	3A	...	...	...	...	...	...	...	...
1ES1853+012	18 53 23	+01 16 13	$0.78^{+0.30}_{-0.24}$	11/2	1.76E−07	12.4	7	3A	...	...	1H1852+015	2.5	A3	SNR	G34.7-0	2.5
1ES1853+234	18 53 47	+23 28 41	$0.56^{+0.32}_{-0.23}$	5/3	4.64E−05	8.3	5	3A	...	...	...	...	WLY	S:K2V	V775 HER	1.0
1ES1853+671	18 53 56	+67 09 44	$0.15^{+0.06}_{-0.05}$	12/8	5.48E−05	59.6	6	3A	...	...	...	...	...	...	...	...
1ES1857−430	18 57 14	−43 04 55	$0.38^{+0.22}_{-0.16}$	5/3	7.70E−05	12.0	5	3A	...	...	...	...	...	...	...	...
1ES1858+303	18 58 01	+30 20 41	$0.47^{+0.27}_{-0.20}$	5/4	1.10E−04	9.7	9	3A	...	...	...	...	...	...	...	...
1ES1859+181	18 59 59	+18 10 00	$0.26^{+0.17}_{-0.12}$	4/3	9.62E−05	14.3	6	3A	...	...	...	...	...	...	...	...
1ES1900−410	19 00 02	−41 03 56	$0.56^{+0.33}_{-0.24}$	5/2	4.74E−05	7.9	9	3A	...	...	...	...	SBD	S:G8III	HD 176705	2.0
1ES1900+699	19 00 52	+69 54 36	$0.15^{+0.05}_{-0.04}$	18/5	1.12E−06	92.1	7	3A	...	...	...	...	ABL	CG:0.094	A2315	2.3
1ES1902−452	19 02 18	−45 15 03	$0.38^{+0.24}_{-0.17}$	4/3	1.09E−04	10.0	10	3A	...	...	...	...	...	...	...	...
1ES1902−524	19 02 22	−52 25 05	$1.11^{+0.61}_{-0.45}$	5/2	8.97E−07	4.3	7	3A	...	...	...	...	BSC	S:F7V	ρ TEL	0.2
1ES1905+070	19 05 08	+07 04 27	$0.45^{+0.22}_{-0.17}$	7/3	1.63E−05	14.0	6	2A	...	...	...	...	SBD	...	HSNH 111	0.7
1ES1905+000	19 05 51	+00 05 23	$3.87^{+0.68}_{-0.60}$	38/4	1.00E−10	9.7	8	3A	...	...	x1H1905+000	0.7	A3	XRB	X1905+000	0.8
1ES1907+523	19 07 14	+52 20 45	$0.81^{+0.26}_{-0.22}$	13/5	1.00E−10	15.1	4	3A	4195	0.2	...	...	BSC	AC:K1IV	HD179094	0.3
1ES1907+097	19 07 15	+09 44 48	$0.53^{+0.10}_{-0.09}$	38/6	1.00E−10	67.0	9	3A	...	...	x1H1909+096	0.1	A3	XRB-Be	X1907+097	0.1
1ES1908+090	19 08 44	+09 02 12	$0.25^{+0.09}_{-0.07}$	15/5	2.38E−08	50.1	7	3A	4203	0.7	...	...	2E	SNR	W49B	0.8
1ES1908+005	19 08 45	+00 30 30	$3.42^{+0.61}_{-0.55}$	39/2	1.00E−10	10.8	8	3A	...	...	...	...	BMC	XRB	AQL X-1	0.6
1ES1909+048	19 09 21	+04 53 45	$0.87^{+0.04}_{-0.04}$	437/21	1.00E−10	476.6	7	3A	4204	0.2	x1H1908+047	0.2	A3	SNR	SS433	0.2

TABLE 6—*Continued*

Slew Desig.	RA 1950	DEC 1950	IPC Rate (cts s^{-1})	NP/NS	P_{read}	Exp. (s)	PI	QI	EOS # EMSS	Δ2E (′)	A3 EXO	Δ1H (′)	Cat.	Class.: Type/s	Name	ΔC (′)
1ES1914+092	19 14 38	+09 15 09	$0.14^{+0.05}_{-0.04}$	18/2	4.16E−06	93.6	6	2A	...	...	...	...	SAO	S:K2II	SAO 124465*	1.2
1ES1916−053	19 16 07	−05 19 54	$7.14^{+0.37}_{-0.37}$	382/6	1.00E−10	53.0	7	3A	4222	0.1	x1H1916−053	0.3	SHA	CV	V1336 AQL	1.5
1ES1916+195	19 16 39	+19 30 53	$0.28^{+0.13}_{-0.10}$	8/5	5.69E−06	25.3	8	3A	4225	0.6	...	...	SAO	S:B8III+K	U SGE	0.3
1ES1920+223	19 20 44	+22 23 02	$0.53^{+0.29}_{-0.21}$	5/4	1.99E−06	9.1	7	3A	...	...	...	...	SBD	S:A2	HD 344230	1.9
1ES1921−293	19 21 45	−29 20 31	$0.07^{+0.03}_{-0.02}$	29/4	3.57E−05	222.2	7	3A	4245	0.6	x	...	HB	AGN:0.352	OV 236	0.6
1ES1921−566	19 21 51	−56 38 24	$1.21^{+0.89}_{-0.60}$	3/2	6.22E−05	2.4	6	3A	...	...	...	...	...	...	...	...
1ES1925+524	19 25 32	+52 27 12	$0.39^{+0.22}_{-0.16}$	5/4	6.17E−05	11.9	4	3A	...	...	...	...	...	...	...	...
1ES1927+654	19 27 00	+65 28 02	$0.93^{+0.17}_{-0.15}$	37/17	1.00E−10	37.9	5	3A	...	...	...	...	...	...	...	...
1ES1928+738	19 28 56	+73 51 28	$0.34^{+0.13}_{-0.11}$	11/7	2.39E−07	28.3	7	2A	...	...	x1H1922+746	0.5	VV	AGN:0.302	4C 73.18	0.5
1ES1928+233	19 28 57	+23 23 48	$0.68^{+0.43}_{-0.30}$	4/2	4.51E−05	5.6	11	3A	...	...	...	...	SBD	S:M8	IRC +20412*	1.2
1ES1930+605	19 30 43	+60 35 30	$0.27^{+0.14}_{-0.11}$	6/6	6.99E−05	19.6	4	3A	...	...	...	...	...	...	...	...
1ES1932+695	19 32 28	+69 33 36	$0.11^{+0.04}_{-0.04}$	13/6	4.62E−05	88.8	5	3A	4267	0.4	...	...	WLY	S:K0V	WLY 764	1.0
1ES1934−063	19 34 53	−06 19 38	$1.49^{+0.46}_{-0.39}$	13/3	1.00E−10	8.6	7	3A	...	...	1H1934−063.A	0.3	A3	AGN:0.011	SS 442	0.3
1ES1934−463	19 34 59	−46 18 30	$0.51^{+0.29}_{-0.21}$	5/1	6.12E−05	9.1	2	3A	...	...	...	...	...	...	...	...
1ES1935+501	19 35 09	+50 07 07	$0.12^{+0.04}_{-0.03}$	24/7	3.86E−08	144.1	3	3A	4269	0.5	...	...	SAO	S:F4V	SAO 031815	0.7
1ES1940+435	19 40 26	+43 30 01	$0.74^{+0.46}_{-0.32}$	4/2	4.24E−06	5.3	4	3A	...	...	...	...	...	...	...	...
1ES1946−014	19 46 03	−01 24 55	$1.73^{+1.25}_{-0.84}$	3/1	7.54E−06	1.7	6	3A	...	...	...	...	...	...	...	...
1ES1948+087	19 48 23	+08 44 20	$0.07^{+0.02}_{-0.02}$	25/5	1.86E−05	228.1	5	3A	4294	0.4	x	...	SAO	S:A7V	SAO 125122	0.3
1ES1948+085	19 48 47	+08 34 35	$0.08^{+0.03}_{-0.03}$	25/6	2.14E−05	189.7	4	3A	4295	0.6	x	...	2E	S	AG+08 2640	0.3
1ES1955−557	19 55 29	−55 47 21	$0.58^{+0.37}_{-0.26}$	4/2	5.94E−05	6.6	6	2A	...	...	...	...	...	...	...	...
1ES1957+405	19 57 47	+40 35 54	$0.40^{+0.11}_{-0.10}$	23/1	8.66E−10	46.3	8	3E	4309	0.3	1H1958+406	0.5	A3	AGN:0.058	CYG A	0.6
1ES1959+650	19 59 35	+65 00 14	$1.58^{+0.28}_{-0.25}$	38/10	1.00E−10	23.1	6	3A	...	...	...	...	...	...	...	...
1ES2001+068	20 01 41	+06 51 03	$1.18^{+0.58}_{-0.45}$	7/1	2.02E−05	5.2	4	2A	...	...	...	...	SBD	S:K2	HD 190342	2.4
1ES2002−593	20 02 00	−59 19 38	$0.80^{+0.57}_{-0.39}$	3/2	3.61E−05	3.7	4	1A	...	...	...	...	...	...	...	...
1ES2005+175	20 05 20	+17 33 30	$0.20^{+0.05}_{-0.04}$	32/3	1.00E−10	132.0	5	3A	4322	0.2	x	...	SHA	CV	WZ SGE	0.1
1ES2005+160	20 05 44	+16 01 30	$0.55^{+0.31}_{-0.23}$	5/1	3.06E−05	8.4	5	3A	...	...	...	...	SAO	S:G5	SAO 105730	0.3
1ES2005−489	20 05 47	−48 58 45	$1.45^{+0.71}_{-0.54}$	6/4	1.50E−07	4.0	6	3A	...	...	x	...	VV	BL:0.071	PKS	0.1
1ES2008−570	20 08 23	−57 01 20	$0.46^{+0.21}_{-0.17}$	9/6	9.99E−05	15.9	6	2A	4331	2.6	...	...	SBD	GAL:0.055	ESO 186- 11	2.8
1ES2010+463	20 10 33	+46 20 06	$0.38^{+0.07}_{-0.06}$	43/12	1.00E−10	99.0	7	3A	4336	0.3	...	...	2E	S	31 CYG	0.4
1ES2013+448	20 13 12	+44 52 37	$0.17^{+0.07}_{-0.06}$	11/7	7.43E−06	52.9	6	3A	...	...	...	...	SAO	S:K0	SAO 049357	0.4
1ES2018+436	20 18 49	+43 41 30	$0.36^{+0.12}_{-0.10}$	14/7	1.37E−08	33.9	6	3A	...	...	x1H2018+439	0.4	SAO	S:WC7P+O5	SAO 049491	0.4
1ES2023−461	20 23 40	−46 09 27	$0.85^{+0.53}_{-0.37}$	4/2	9.43E−06	4.6	5	3A	...	...	...	.	...	...	...	...
1ES2024+063	20 24 31	+06 19 38	$0.49^{+0.26}_{-0.20}$	6/2	3.17E−05	11.0	4	3A	...	...	...	...	...	...	...	...

TABLE 6—*Continued*

Slew Desig.	RA 1950	DEC 1950	IPC Rate (cts s^{-1})	NP/NS	P_{rand}	Exp. (s)	PI	QI	EOS # EMSS	Δ2E (′)	A3 EXO	Δ1H (′)	Cat.	Class.: Type/z	Name	ΔC (′)
1ES2024−743	20 24 44	−74 23 28	$0.25^{+0.14}_{-0.10}$	5/2	6.81E−05	18.6	5	3A	...	...	...	...	...	...	...	...
1ES2025+573	20 25 19	+57 22 34	$0.24^{+0.12}_{-0.09}$	7/5	1.95E−05	26.1	8	3A	...	...	...	...	...	...	...	...
1ES2028+513	20 28 10	+51 19 47	$0.24^{+0.13}_{-0.10}$	5/5	5.10E−08	20.3	4	3A	...	...	...	...	...	...	...	...
1ES2028+042	20 28 20	+04 14 41	$1.22^{+0.88}_{-0.59}$	3/1	6.41E−06	2.4	7	3A	...	...	...	...	...	...	...	...
1ES2030+407	20 30 39	+40 47 13	$14.21^{+0.10}_{-0.10}$	19909/26	1.00E−10	1384.8	8	3A	4376	0.4	x1H2030+407	0.2	A3	XRB	CYG X-3	0.3
1ES2031+411	20 31 28	+41 08 43	$0.11^{+0.01}_{-0.01}$	250/18	1.00E−10	1059.0	7	3A	4382	0.2	...	...	SAO	S	SAO 049781	0.5
1ES2032−451	20 32 33	−45 07 29	$0.64^{+0.40}_{-0.28}$	4/1	2.55E−05	6.0	6	3A	...	...	...	...	...	...	...	...
1ES2033+110	20 33 05	+11 00 18	$0.13^{+0.06}_{-0.04}$	12/2	6.88E−05	69.8	8	3A	...	...	...	...	...	...	...	...
1ES2037−010	20 37 35	−01 03 02	$0.16^{+0.07}_{-0.06}$	12/2	4.12E−05	56.8	4	3A	4404	0.3	x	...	SHA	CV	AE AQR	0.2
1ES2037+521	20 37 57	+52 09 42	$0.10^{+0.04}_{-0.03}$	16/7	6.99E−05	111.1	6	3A	4405	0.6	...	...	2E	...	...	...
1ES2038−007	20 38 18	−00 46 43	$0.10^{+0.04}_{-0.03}$	18/4	7.81E−06	123.6	6	3A	m4408	0.6	...	...	SAO	S:F8	SAO 144692	1.2
1ES2039+758	20 39 42	+75 51 07	$0.24^{+0.12}_{-0.09}$	7/5	1.44E−05	25.9	9	2A	...	...	...	...	...	...	...	...
1ES2041−108	20 41 27	−10 53 42	$1.00^{+0.56}_{-0.41}$	5/1	1.70E−05	4.7	6	3A	...	...	x1H2041−108	0.6	VV	AGN:0.035	MKN 509	0.6
1ES2042+335	20 42 49	+33 31 51	$0.10^{+0.04}_{-0.03}$	19/11	3.12E−05	127.8	6	3A	...	...	...	...	SAO	S:G5	SAO 070451	2.2
1ES2047+643	20 47 45	+64 19 34	$0.29^{+0.17}_{-0.12}$	5/5	3.06E−05	15.9	4	3A	...	...	...	...	...	...	...	...
1ES2048+314	20 48 50	+31 25 17	$0.26^{+0.07}_{-0.07}$	185/11	1.00E−10	181.6	4	3A	...	...	...	...	SAO	S:K0	SAO 070569	0.9
1ES2052+441	20 52 08	+44 11 40	$1.00^{+0.21}_{-0.19}$	29/10	1.00E−10	27.3	5	3A	...	...	...	...	SAO	S:G2V	SAO 050198	0.5
1ES2052−172	20 52 58	−17 17 17	$0.63^{+0.34}_{-0.25}$	6/2	5.83E−05	8.5	5	1A	...	...	...	...	SAO	S:F8V	SAO 163989	1.4
1ES2055+298	20 55 55	+29 51 05	$0.25^{+0.12}_{-0.09}$	9/4	8.50E−05	29.2	7	3A	...	...	...	...	...	...	...	...
1ES2055+443	20 55 57	+44 20 43	$0.28^{+0.14}_{-0.11}$	8/4	9.27E−05	23.4	6	2A	...	...	...	...	...	...	...	...
1ES2056+461	20 56 10	+46 07 33	$0.22^{+0.13}_{-0.09}$	5/4	5.11E−05	20.7	13	3A	...	...	...	...	...	...	...	...
1ES2056+504	20 56 53	+50 29 55	$0.20^{+0.08}_{-0.07}$	11/3	3.05E−06	45.6	7	2A	...	...	...	...	...	...	...	...
1ES2058+398	20 58 08	+39 52 07	$0.41^{+0.13}_{-0.11}$	14/7	1.00E−10	30.7	4	3A	...	...	...	...	WLY	AC:M3EV+M3EV	WLY 815AB	0.6
1ES2100+276	21 00 18	+27 36 26	$0.57^{+0.08}_{-0.07}$	69/8	1.00E−10	111.8	5	3A	4438	0.1	x	...	SAO	S:G0V+G5V	ER VUL	0.4
1ES2127+119	21 27 34	+11 56 56	$4.29^{+0.67}_{-0.61}$	47/5	1.00E−10	10.8	7	3A	...	...	x1H2128+120	0.3	A3	XRB	M15	0.3
1ES2128−284	21 28 39	−28 24 02	$1.80^{+1.15}_{-0.82}$	4/1	7.80E−05	2.1	5	3A	...	...	...	...	...	...	...	...
1ES2128+231	21 28 47	+23 06 50	$0.46^{+0.16}_{-0.14}$	9/3	3.11E−10	18.8	5	3A	...	...	...	...	SBD	S:K8	BD+22 4409	0.7
1ES2129−026	21 29 31	−02 37 12	$0.22^{+0.10}_{-0.08}$	10/1	8.17E−05	35.4	5	3A	...	...	...	...	SBD	S	PHL 26	1.3
1ES2129+470	21 29 36	+47 04 11	$1.25^{+0.17}_{-0.15}$	70/2	1.00E−10	52.8	8	3A	4485	0.2	1H2131+473	0.1	A3	XRB	X2129+470	0.1
1ES2131+812	21 31 24	+81 17 38	$0.40^{+0.17}_{-0.13}$	8/5	7.63E−08	18.8	6	3A	...	...	...	...	...	...	...	...
1ES2132+509	21 32 01	+50 54 06	$0.29^{+0.15}_{-0.12}$	6/4	1.01E−04	18.5	7	3A	...	...	...	...	...	...	...	...
1ES2132+288	21 32 51	+28 50 22	$1.01^{+0.63}_{-0.45}$	4/2	3.69E−05	3.8	13	3A	...	...	...	...	SBD	S:A0	AG+28 2503	2.0
1ES2135−147	21 35 01	−14 46 16	$0.14^{+0.04}_{-0.04}$	24/4	4.51E−08	132.1	7	3A	4497	0.1	x	...	VV	AGN:0.200	PHL 1657	0.2

TABLE 6—*Continued*

Slew Desig.	RA 1950	DEC 1950	IPC Rate (cts s^{-1})	NP/NS	P_{rand}	Exp. (s)	PI	QI	EOS # EMSS	Δ2E (′)	A3 EXO	Δ1H (′)	Cat.	Class.: Type/z	Name	ΔC (′)
1ES2135+011	21 35 02	+01 10 38	$0.20^{+0.09}_{-0.07}$	11/8	7.33E−05	43.0	8	2A	...	...	...	...	SBD	S:K0	AG+01 2623	2.4
1ES2136+729	21 36 16	+72 58 19	$0.29^{+0.15}_{-0.11}$	7/4	9.13E−05	20.6	8	2A	...	...	...	...	...	...	...	...
1ES2137+204	21 37 00	+20 26 22	$0.21^{+0.10}_{-0.08}$	8/7	8.51E−05	32.2	7	2A	...	...	...	...	...	...	...	...
1ES2137+241	21 37 26	+24 10 25	$0.75^{+0.37}_{-0.28}$	6/3	4.71E−07	7.6	5	3A	...	...	...	...	...	...	...	...
1ES2143+751	21 43 03	+75 10 25	$0.29^{+0.11}_{-0.09}$	11/5	1.37E−08	34.0	5	3A	...	...	...	...	...	...	...	...
1ES2144−366	21 44 48	−36 41 11	$0.97^{+0.69}_{-0.47}$	3/1	2.32E−05	3.1	4	3A	...	...	...	...	...	...	...	...
1ES2145+095	21 45 56	+09 32 56	$0.56^{+0.41}_{-0.28}$	3/2	2.90E−05	5.2	6	3A	...	...	...	...	...	...	...	...
1ES2148+583	21 48 46	+58 19 45	$0.32^{+0.18}_{-0.14}$	5/4	4.21E−05	14.4	10	3A	...	...	...	...	...	...	...	...
1ES2149+054	21 49 40	+05 24 21	$0.18^{+0.06}_{-0.05}$	19/2	1.89E−08	82.2	5	3A	4536	0.5	...	...	2E	...	...	...
1ES2152−548	21 52 53	−54 52 47	$0.68^{+0.24}_{-0.20}$	12/3	8.52E−10	16.1	4	3A	...	...	...	...	...	...	...	...
1ES2153+441	21 53 14	+44 10 17	$0.59^{+0.13}_{-0.12}$	25/8	1.00E−10	40.1	6	3A	...	...	...	...	SAO	S:K0	SAO 051437	1.0
1ES2155−081	21 55 14	−08 08 32	$0.13^{+0.05}_{-0.04}$	14/3	9.44E−05	78.8	5	3A	...	...	...	...	SBD	S	BD-08 5773	0.7
1ES2155−304	21 55 58	−30 27 48	$5.08^{+0.16}_{-0.16}$	1043/5	1.00E−10	202.1	4	3A	4544	0.1	x1H2156−304	0.1	VV	BL:0.117	PKS	0.1
1ES2156+032	21 56 20	+03 15 35	$0.08^{+0.03}_{-0.03}$	19/1	8.10E−05	153.9	12	2A	...	...	...	...	...	...	...	...
1ES2157−521	21 57 36	−52 09 14	$0.54^{+0.30}_{-0.22}$	5/4	1.85E−05	8.8	6	3A	...	...	...	...	...	...	...	...
1ES2157+570	21 57 57	+57 04 09	$0.29^{+0.18}_{-0.13}$	4/4	7.55E−05	13.0	7	3A	...	...	...	...	SAO	S:A0	SAO 033950	2.3
1ES2158−580	21 58 27	−58 05 01	$0.47^{+0.27}_{-0.20}$	5/5	6.65E−05	9.9	2	3A	...	...	...	...	...	...	...	...
1ES2159+436	21 59 29	+43 38 56	$0.12^{+0.02}_{-0.02}$	59/8	1.00E−10	360.0	6	3A	4550	0.1	...	...	SAO	S:G5	SAO 051563	0.5
1ES2200+826	22 00 09	+82 37 38	$0.60^{+0.28}_{-0.21}$	7/5	4.78E−07	11.0	7	3A	...	...	x	...	BSC	S:F6IV-V	HD 209942	0.2
1ES2200+420	22 00 40	+42 01 47	$0.27^{+0.07}_{-0.06}$	22/4	1.00E−10	72.2	7	3A	4558	0.5	x	...	VV	BL:0.070	BL LAC	0.4
1ES2201+315	22 01 02	+31 31 13	$0.22^{+0.10}_{-0.08}$	8/1	1.69E−05	31.2	6	3A	4561	0.3	...	...	HB	AGN:0.297	4C 31.63	0.2
1ES2201+193	22 01 31	+19 21 26	$0.43^{+0.24}_{-0.18}$	5/3	2.15E−05	10.9	12	1A	...	...	...	...	...	...	...	...
1ES2202+469	22 02 56	+46 59 06	$0.30^{+0.11}_{-0.09}$	12/2	1.94E−07	33.9	4	3A	4567	0.4	1H2213+464	0.4	A3	AC	HK LAC	0.4
1ES2206+445	22 06 25	+44 30 34	$0.11^{+0.04}_{-0.03}$	17/2	6.45E−06	111.0	6	3A	...	...	...	...	...	...	...	...
1ES2206+455	22 06 40	+45 30 02	$1.86^{+0.08}_{-0.08}$	576/6	1.00E−10	302.0	5	3A	4573	0.2	x1H2207+455	0.3	A3	AC	AR LAC	0.3
1ES2207+643	22 07 06	+64 20 20	$0.14^{+0.06}_{-0.05}$	12/5	8.06E−05	62.8	7	3A	...	...	...	...	...	...	...	...
1ES2207−124	22 07 37	−12 25 27	$0.29^{+0.05}_{-0.04}$	55/5	1.00E−10	168.3	6	3A	4575	1.3	...	...	ABL	CG:0.084	A2420	1.3
1ES2216+845	22 16 16	+84 30 24	$0.28^{+0.13}_{-0.10}$	8/6	6.32E−06	25.0	5	3A	...	...	...	...	SAO	S:K2	SAO 003717	0.5
1ES2216+565	22 16 58	+56 35 39	$0.22^{+0.09}_{-0.08}$	11/6	4.15E−05	39.1	5	3A	...	...	...	...	...	...	...	...
1ES2217−354	22 17 39	−35 25 11	$0.40^{+0.21}_{-0.16}$	6/3	6.48E−05	13.4	6	3A	...	...	...	...	ABL	CG	A3866	0.6
1ES2221−018	22 21 22	−01 50 48	$0.18^{+0.06}_{-0.05}$	18/3	8.21E−08	81.1	8	3A	4597	1.6	1H2221−017.A	1.3	ABL	CG:0.090	A2440	1.0
1ES2223−051	22 23 09	−05 11 51	$0.17^{+0.03}_{-0.03}$	42/6	1.00E−10	200.4	7	3A	4603	0.5	x	...	VV	AGN:1.404	3C 446	0.7
1ES2235+434	22 35 04	+43 25 15	$0.48^{+0.35}_{-0.23}$	3/3	2.11E−05	6.1	6	3A	...	...	...	...	SAO	S:A3	SAO 052191	1.6

TABLE 6—*Continued*

Slew Desig.	RA 1950	DEC 1950	IPC Rate (cts s^{-1})	NP/NS	P_{rand}	Exp. (s)	PI	QI	EOS # EMSS	Δ2E (′)	A3 EXO	Δ1H (′)	Cat.	Class.: Type/z	Name	ΔC (′)
1ES2236−208	22 36 04	−20 52 31	$0.66^{+0.09}_{-0.08}$	70/4	1.00E−10	99.4	4	3A	4632	0.4	x	...	SAO	AC:M2V+M4V	WLY 867AB	0.4
1ES2239+475	22 39 38	+47 35 52	$0.66^{+0.41}_{-0.29}$	4/3	1.85E−05	5.8	13	2A	...	...	...	...	...	...	...	...
1ES2240+294	22 40 18	+29 28 17	$1.88^{+0.35}_{-0.32}$	33/7	1.00E−10	17.2	5	3A	...	...	1H2239+294	0.5	VV	AGN:0.025	AKN 564	0.5
1ES2244−019	22 44 48	−01 54 11	$0.15^{+0.05}_{-0.04}$	16/4	1.09E−06	82.4	13	2A	...	...	...	...	...	...	...	...
1ES2246−646	22 46 36	−64 41 41	$0.44^{+0.19}_{-0.15}$	9/6	7.94E−07	18.1	6	2E	...	...	1H2245−646	2.8	ABL	CG	A3921	2.8
1ES2247+106	22 47 53	+10 37 37	$0.76^{+0.33}_{-0.26}$	8/2	3.90E−07	9.7	6	3A	...	...	...	...	ABL	CG:0.077	A2495*	0.5
1ES2248−163	22 48 59	−16 19 33	$0.52^{+0.28}_{-0.21}$	5/1	3.26E−06	9.3	13	3A	...	...	...	...	...	...	...	...
1ES2249+442	22 49 35	+44 16 58	$0.68^{+0.39}_{-0.28}$	5/2	3.29E−05	6.8	7	3A	...	...	...	...	...	...	...	...
1ES2251+376	22 51 23	+37 40 29	$0.16^{+0.05}_{-0.04}$	20/2	9.67E−08	93.7	4	3A	4644	0.0	...	...	SAO	S:K0V	SW LAC	0.6
1ES2251−178	22 51 26	−17 50 20	$0.45^{+0.10}_{-0.09}$	31/2	1.00E−10	61.4	8	3A	4645	0.6	x1H2251−179	0.6	HB	AGN:0.068	MR 2251-178	0.6
1ES2254−029	22 54 43	−02 55 43	$0.92^{+0.68}_{-0.46}$	3/1	5.90E−05	3.2	14	3A	...	...	...	...	...	...	...	...
1ES2254−371	22 54 52	−37 11 34	$0.28^{+0.07}_{-0.06}$	25/4	1.00E−10	76.2	4	3A	m4664	0.7	...	...	MS	AGN:0.039	MS	0.6
1ES2256−246	22 56 15	−24 41 56	$0.62^{+0.39}_{-0.28}$	4/1	3.72E−05	6.1	13	3A	...	...	...	...	...	...	...	...
1ES2257−153	22 57 20	−15 18 44	$0.28^{+0.18}_{-0.13}$	4/4	1.05E−04	13.2	10	3A	...	...	...	...	...	...	...	...
1ES2257−340	22 57 38	−34 01 28	$0.45^{+0.21}_{-0.16}$	7/4	1.53E−06	14.3	4	3A	...	...	...	...	SAO	S:G5VP	SAO 214237	1.7
1ES2257+620	22 57 39	+62 04 26	$0.15^{+0.06}_{-0.05}$	13/8	1.31E−05	68.5	7	3A	...	...	...	...	...	...	...	...
1ES2259+586	22 59 06	+58 36 31	$0.93^{+0.10}_{-0.10}$	128/10	1.00E−10	116.9	7	3A	4673	0.3	x1H2258+585	0.4	A3	SNR	G109.1-1.0	0.4
1ES2300−698	23 00 34	−69 51 33	$1.40^{+0.72}_{-0.54}$	6/1	1.01E−05	4.0	5	3A	...	...	...	...	...	...	...	...
1ES2304−333	23 04 10	−33 21 10	$0.45^{+0.25}_{-0.18}$	5/3	8.06E−06	10.6	12	3A	...	...	...	...	...	...	...	...
1ES2304+042	23 04 29	+04 16 40	$1.10^{+0.44}_{-0.35}$	9/2	2.43E−09	7.7	7	3A	...	...	x1H2303+039	0.3	VV	AGN:0.042	PG	0.3
1ES2304+252	23 04 38	+25 12 19	$0.11^{+0.04}_{-0.04}$	13/4	1.28E−05	92.0	7	3A	4682	0.9	1H2315+257	0.7	A3	AC	56 PEG B	0.7
1ES2307+476	23 07 33	+47 41 36	$0.54^{+0.15}_{-0.13}$	19/7	1.00E−10	32.0	4	3A	4687	1.2	...	...	SAO	AC:G5	KZ AND	1.6
1ES2310−219	23 10 20	−21 54 55	$0.20^{+0.04}_{-0.04}$	41/4	1.00E−10	160.5	7	3A	4695	0.7	1H2307−222.A	0.9	ABL	CG:0.086	A2556	1.3
1ES2311−430	23 11 13	−43 00 13	$1.03^{+0.13}_{-0.12}$	78/7	1.00E−10	71.6	6	3A	m4699	0.4	x	...	2E	CG:0.056	S1101*	0.8
1ES2316−423	23 16 22	−42 22 24	$0.12^{+0.03}_{-0.03}$	42/10	1.00E−10	240.1	6	3A	m4709	0.6	...	...	MS	CG:0.045	S1111	0.4
1ES2317+787	23 17 59	+78 43 09	$0.35^{+0.19}_{-0.14}$	6/4	5.72E−05	15.1	4	3A	...	...	x1H2313+783	0.7	A3	AC	SAO 010697	0.7
1ES2319−421	23 19 00	−42 10 15	$0.15^{+0.04}_{-0.04}$	26/9	3.04E−08	122.7	7	3A	m4721	2.0	...	...	ABL	CG	A3998	1.1
1ES2320−101	23 20 14	−10 06 42	$1.33^{+0.97}_{-0.66}$	3/1	3.38E−05	2.2	12	3A	...	...	...	...	...	...	...	...
1ES2321+585	23 21 06	+58 33 08	$28.66^{+1.17}_{-1.17}$	612/12	1.00E−10	21.2	7	3A	4724	0.6	x1H2321+585	0.8	A3	SNR	CAS A	0.8
1ES2321+419	23 21 23	+41 54 59	$0.12^{+0.05}_{-0.04}$	12/4	3.04E−05	78.3	8	1A	4725	1.2	1H2318+417	1.1	A3	BL	H2321+419	1.0
1ES2321+143	23 21 47	+14 22 26	$0.14^{+0.04}_{-0.04}$	23/3	1.29E−07	123.0	8	2E	...	...	1H2320+146	2.6	A3	CG:0.041	A2593	2.7
1ES2321−274	23 21 55	−27 29 10	$0.39^{+0.21}_{-0.16}$	6/4	9.00E−05	13.6	13	3A	...	...	...	...	...	...	...	...
1ES2322−409	23 22 02	−40 56 46	$0.70^{+0.29}_{-0.23}$	8/4	1.23E−09	11.0	6	3A	...	...	...	...	...	...	...	...

TABLE 6—*Continued*

Slew Desig.	RA 1950	DEC 1950	IPC Rate (cts s^{-1})	NP/NS	P_{rand}	Exp. (s)	PI	QI	EOS # EMSS	Δ2E (′)	A3 EXO	Δ1H (′)	Cat.	Class.: Type/z	Name	ΔC (′)
1ES2322−124	23 22 46	−12 24 27	$0.55^{+0.16}_{-0.14}$	17/2	1.00E−10	28.0	8	3A	4728	0.8	...	...	ABL	CG:0.085	A2597	1.7
1ES2326+174	23 26 29	+17 28 13	$0.34^{+0.18}_{-0.14}$	6/5	1.72E−05	15.9	6	3A	...	...	...	...	...	...	...	...
1ES2326+411	23 26 59	+41 11 16	$0.38^{+0.17}_{-0.13}$	8/4	5.83E−07	19.4	2	3A	...	...	...	...	SBD	S:M2	G 190 -28	0.4
1ES2329+196	23 29 20	+19 39 44	$0.54^{+0.06}_{-0.06}$	88/6	1.00E−10	151.1	4	3A	4733	0.2	x	...	WLY	S:M4E+M6E	WLY 896AB	0.0
1ES2332−512	23 32 51	−51 12 24	$1.11^{+0.68}_{-0.48}$	4/3	3.76E−06	3.5	8	3A	...	...	...	...	...	...	...	...
1ES2334+063	23 34 07	+06 18 05	$0.32^{+0.14}_{-0.11}$	9/3	7.38E−06	24.5	8	3A	...	...	...	...	SAO	S:G0	SAO 128282	0.8
1ES2335+461	23 35 06	+46 11 20	$2.85^{+0.18}_{-0.18}$	251/8	1.00E−10	86.6	5	3A	4740	0.2	x1H2336+462	0.2	A3	AC	λ AND	0.1
1ES2340−152	23 40 53	−15 12 37	$0.17^{+0.07}_{-0.06}$	11/1	3.46E−05	50.8	3	3A	m4755	0.6	x	...	ZCT	GAL:0.137	MS	0.8
1ES2342+089	23 42 25	+08 55 11	$0.38^{+0.06}_{-0.05}$	65/8	1.00E−10	150.4	6	3A	4758	0.5	1H2343+090	2.9	A3	CG:0.040	A2657	2.9
1ES2343−151	23 43 02	−15 06 15	$0.23^{+0.10}_{-0.08}$	9/2	1.15E−05	34.1	5	3A	4760	0.4	...	...	SBD	...	068.16-70.38	0.6
1ES2344+047	23 44 18	+04 47 03	$0.62^{+0.40}_{-0.28}$	4/2	1.10E−04	6.0	5	3A	...	...	...	...	...	...	...	...
1ES2344+514	23 44 37	+51 25 50	$0.43^{+0.16}_{-0.13}$	10/7	1.22E−08	21.6	7	3A	...	...	...	...	...	...	...	...
1ES2347+361	23 47 12	+36 08 53	$0.36^{+0.20}_{-0.15}$	5/3	1.01E−04	12.6	5	3A	...	...	...	...	SAO	S:G1IIIE	SAO 073535	0.3
1ES2347+485	23 47 58	+48 31 57	$0.40^{+0.19}_{-0.15}$	7/3	9.62E−06	15.9	4	3A	...	...	...	...	...	...	...	...
1ES2349−561	23 49 31	−56 11 39	$0.88^{+0.43}_{-0.33}$	6/4	7.55E−08	6.6	6	3A	...	...	...	...	ABL	CG	S1158	1.4
1ES2352−208	23 52 03	−20 51 58	$1.06^{+0.65}_{-0.46}$	4/1	3.69E−07	3.7	3	3A	...	...	...	...	...	...	...	...
1ES2352+283	23 52 32	+28 21 49	$2.97^{+0.58}_{-0.51}$	31/6	1.00E−10	10.2	4	3A	4789	0.5	x1H2354+285	0.9	HD	S:K0V	HD 224085	0.8
1ES2352+600	23 52 54	+60 03 32	$0.32^{+0.16}_{-0.12}$	6/4	3.66E−07	18.0	7	3A	...	...	...	...	...	...	...	...
1ES2352+512	23 52 59	+51 15 33	$0.76^{+0.41}_{-0.30}$	5/3	4.34E−07	6.4	4	3A	...	...	...	...	...	...	...	...

Table 7: New Identified X-ray Sources

Name	Type/z	Counterpart Name	Other Counterpart Names
		AGN	
1ES0702+646	0.079	VII ZW 118*	...
1ES0836+710	2.160	4C 71.07	S5 0836+710
1ES0921+525	0.036	MKN 110	...
1ES1149−110	0.049	PG	...
1ES1251−281	0.069	ESO 443- 5	...
1ES1309+355	0.184	TON 1565	PG
1ES1320+084	0.050	MKN 1347	...
1ES1415+451	0.114	PG	...
1ES1518+593	0.079	SBS1518+593	...
1ES1626+554	0.132	PG	...
		Galaxies[a]	
1ES0005+145	...	Z 0005.5+1433	...
1ES0205+492	...	G 173 -39	...
1ES0257+442	...	U02468	...
1ES0403−373	0.055	ESO 359- 19	...
1ES0412−382	0.050	ESO(B) 303R	...
1ES0502+675	...	Z 0502.3+6735	...
1ES0543−555	0.015	NGC 2087	ESO 159-26
1ES0559−399	...	GAL 0559-3959	...
1ES0924+232	0.026	UO5037*	...
1ES1121−012	...	Z 1121.0-0117	...
1ES1141+799	...	UO6728	...
1ES1215+039	0.075	4C +04.41*	PKS 1214+038
1ES1217−168	...	MCG-3.32.4	...
1ES1234+459	...	Z 1234.5+4556	...
1ES1238−332	...	ESO 381- 7	...
1ES1254−172	0.046	GAL 1254-1710*	...
1ES1318+274	...	G 149 -80	...
1ES1323+717	0.072	GAL 1323+7145	...
1ES1324−269	0.046	ESO 509- 9	...
1ES1324−268	...	ESO 509- 14	...
1ES1336+280	0.036	Z 1336.4+2800	...
1ES1714+574	0.028	NGC 6338*	U10784
		Clusters of Galaxies	
1ES0058+345	...	ZW 314	...
1ES0122+084A	0.045	A193*	...
1ES0122+084B	0.045	A193*	...
1ES0644−541	...	A3404	...
1ES0914+519	0.197	A773	...
1ES1241+275	0.241	A1602	...
1ES1256−039	0.083	A1651	...
1ES1301−239	...	A1664*	...
1ES1310−327	...	S724	...

1ES1900+699	0.094	A2315	...
1ES2217−354	...	A3866	...
1ES2247+106	0.077	A2495*	...
1ES2349−561	...	S1158	...
		White Dwarfs	
1ES1631+781	DA	WFC 1629+781	...
		Stars: Known to be Active	
1ES0957+247	K0VE+B	DH LEO	SAO 081134
1ES2058+398	M3EV+M3EV	WLY 815AB	...
		Stars: Binaries	
1ES0154−518	G5IV+	WLY 81AB	SAO 23273, χ ERI, HD 11937
1ES0309−291	F8IV+	WLY 127AB	SAO 168373, α FOR, HD 20010
1ES1314+172	K2V+M2V	WLY 505AB	SAO 100491
1ES1833+169	G2V+G2V	HD 171746	SAO 103886
		Stars: Early Type	
1ES0157+706	A3IV	SAO 4554	48 CAS, HD 12111
1ES0324+095	B9Vn	HD 21364	214 TAU, SAO 168373
1ES0426−131	B1Vne	DU ERI	HD 28497, SAO 149674
1ES0510−119	B8V	SAO 150223	309 LEP, HD 33802
1ES0651−020	B	HD 292785	...
1ES0839−445	A0	HD74209	...
1ES1126−610	A	HD 306536	...
1ES1148−624	B8	HD 309207	...
1ES1225−551	A2	SAO 239967	...
1ES1318−632	B	LS 3039	...
1ES1348−588	B9IV	SAO 241229	...
1ES1414−197	A5IV	SAO 158468	...
1ES1650−417	B	SAO 227370	...
1ES1753−290	A3	HD 163300*	...
1ES1920+223	A2	HD 344230	...
1ES2132+288	A0	AG+28 2503	...
1ES2157+570	A0	SAO 033950	...
1ES2235+434	A3	SAO 052191	...
		Stars: Late Type[b]	
1ES0013+195	M4	G 32 -6*	...
1ES0032−622	K5V	HD 3221	...
1ES0048+236	F5	AG+23 78	...
1ES0054−702	F8	SAO 255722	...
1ES0120+004	G0	HD 8358*	...
1ES0133+484	gK1	HD 9746	SAO 037351
1ES0143−253	F1V	ϵ SCL	HD 10830, SAO 167275
1ES0226−615	F8	SAO 248569	...

1ES0238+057	M	BD+05 378	...
1ES0305−284	K7V	CD-28 1030*	...
1ES0308−055	K0	SAO 130323	...
1ES0315+681	F0	AG+68 165*	...
1ES0357−400	K0	HD 25300	...
1ES0415+231	K0	HD 284303	...
1ES0419+148	F8	HD 285758	...
1ES0423+146	G7III	SAO 093935	7316 TAU, HD 28100
1ES0424+326	G8	HD 282099	...
1ES0428+366	G5	SAO 057285	...
1ES0429+130	F8	HD 286840*	...
1ES0444−704	K7	HD270712	...
1ES0447+068	F6V	SAO 112106	WLY 178, 116^3 ORI, HD 30652
1ES0504−575	F8V	WLY 189	ZETA DOR, HD 33262, SAO 233822
1ES0603−484	G5	SAO 217708	HD 41824
1ES0614+227	K2	HD254475	...
1ES0618−580	K2V	SAO 234448	...
1ES0635−698	G3V	HD 47875	...
1ES0637−614	G1-2V	HD48189	SAO 249604
1ES0712−363	F6-7V	SAO 197732	...
1ES0717−572	G0IV-V	SAO 235087	...
1ES0738+612	K0	SAO 014296	...
1ES0740+228	K0	SAO 079647	...
1ES0919+404	K2V	SAO 042826	...
1ES0920−136	K0IV	SAO 155136	...
1ES0923−530	F7V	SAO 236956	...
1ES1002−559	K1-2III	SAO 237656	...
1ES1020+493	F5	HD 89944	...
1ES1026+620	F8	ZZ UMA	...
1ES1101−606	M0	SAO 251235	...
1ES1105+833	K0	SAO 001824	...
1ES1212−652	G0/G1V	HD 106392	...
1ES1212+078	K0	SAO 119284	...
1ES1228−465	F5V	SAO 223481	...
1ES1239−011	F0V	WLY 482A	SAO 138917, HD 110379, HD 110380
1ES1252−060	K8V	WLY 9424	...
1ES1301−411	K0	CD-40 7655	...
1ES1325−261	K5III	HD 117033	...
1ES1325−312	F5V	SAO 204500	...
1ES1326+789	G2.5IIIb	HD 117566	SAO 007821
1ES1327−313	K1III	SAO 204527	...
1ES1339−688	G2IV-V	SAO 252423	...
1ES1354−314	K0V	SAO 205032	...
1ES1358−673	K1II-III	SAO 252570	...
1ES1414+203	F8V	HD 125040	SAO 083259
1ES1437−252	F0/F2V	HD 129009	...
1ES1456−400	F7/F8V	HD 132349	...

1ES1507−076	K0	SAO 140351*	...
1ES1509+763	G5	SAO 008175	...
1ES1519+211	M0EV	WLY 9520	...
1ES1606+218	K2	AG+21 1576	...
1ES1614+446	G0	SAO 045997	...
1ES1702+457	F8	SAO 046462*	...
1ES1711−547	F0IV-V	SAO 244557	...
1ES1716+551	K0	SAO 030326	...
1ES1727+590	G0	SAO 030416	...
1ES1737+612	M	HD 160934	...
1ES1746+748	K0	SAO 008910	...
1ES1753+362	G5	SAO 066472	...
1ES1811+006	K0	SAO 123267	...
1ES1824+151	K0	SAO 103722	...
1ES1853+234	K2V	V775 HER	WLY 9638
1ES1900−410	G8III	HD 176705	...
1ES1902−524	F7V	ρ TEL	HD 177171
1ES1914+092	K2II	SAO 124465*	...
1ES1928+233	M8	IRC +20412*	...
1ES2001+068	K2	HD 190342	...
1ES2005+160	G5	SAO 105730	...
1ES2013+448	K0	SAO 049357	...
1ES2042+335	G5	SAO 070451	...
1ES2048+314	K0	SAO 070569	...
1ES2052+441	G2V	SAO 050198	...
1ES2052−172	F8V	SAO 163989	...
1ES2128+231	K8	BD+22 4409	...
1ES2135+011	K0	AG+01 2623	...
1ES2153+441	K0	SAO 051437	...
1ES2216+845	K2	SAO 003717	...
1ES2257−340	G5VP	SAO 214237	...
1ES2326+411	M2	G 190 -28	...
1ES2334+063	G0	SAO 128282	...
1ES2347+361	G1IIIE	SAO 073535	HD 223460
	Stars: Type Unknown		
1ES0406+099	...	HG 7-114	...
1ES0437−046	...	BF ERI	...
1ES0437+444	...	OU PER	...
1ES0829+159	...	SAO 097895	...
1ES1735−269	...	IRAS 17345-2656	...
1ES1841−044	...	FT SCT	...
1ES2129−026	...	PHL 26	...
1ES2155−081	...	BD-08 5773	...

NOTES—[a] These galaxies, although catalogued as normal, may possess active nuclei.

[b] Many of the late type stars may be previously unknown active stars.

REFERENCES

Abell G., 1958, ApJS, 3, 211.

Abell G., Corwin , and Olowin, 1989, ApJS, 70, 1.

Bradt, H. V. D., and McClintock, J. E. 1983, ARA&A, 21, 13.

Cannon A.J., and Pickering E.C., 1918–1924, *The Henry Draper Catalogue*, Ann. Astron. Obs. Harvard College, 91–99.

Cooke B.A., *et al.*, 1991, Nature, submitted.

Giacconi R. *et al.*, 1979a, ApJ, 230, 540.

Giacconi R. *et al.*, 1979b, ApJ, 234, L1.

Gioia I.M., Maccacaro T., Schild R.E., Stocke J.T., Liebert J.W., Danziger I.J., Kunth D., and Lub J.,1984, ApJ, 283, 495.

Gioia I.M., Maccacaro T., Schild R.E., Wolter A., Stocke J.T., Morris S.L., and Henry J.P., 1990, ApJS, 72, 567.

Giommi P., 1991, ApJ, in press.clr

Gorenstein P., Harnden R.F., and Fabricant D.G., 1981 *IEEE Trans. Nucl. Sci.*, NS-28, 869.

Harnden R.F.Jr., Fabricant D.G., Harris D.E., and Schwarz J., 1984, *SAO Special Report No. 393.*

Harris D.E. *et al.*, 1991, *Einstein IPC Source Catalog*, NASA Publication, in press.

Harris D.E., Stern C.P. and Biretta J.A., 1990, in *Imaging X-ray Astronomy*, ed. M. Elvis, [CUP, Cambridge], p. 299.

Hewitt A.,, and Burbidge G., 1986, ApJS, 65, 603.

Hoffleit, D. (with the collaboration of Jaschek, C.) 1982, The Bright Star Catalogue, 4th revised edition (New Haven: Yale University Observatory).

Huchra J.P., 1990, in preparation.

Huchra J.P., and Geller M.J., 1984, ApJ, 257, 423.

Kholopov, P. N., et al. 1985-1988, "General Catalogue of Variable Stars", 4th Edition (Moscow: Nauka Publishing House).

Koch D., Hall R., Tsao H., Wollman H., and Kilinski R., 1978, *IEEE Trans. Nucl. Sci.*, NS-25, 473.

Kowalski, M. P., Ulmer, M. P., Cruddace, R. G., & Wood, K. S. 1984, ApJS, 56, 403.

Kraft R., Nousek J., and Burrows , 1991, ApJ, June 10, in press.

Maccacaro T., *et al.*, 1988, ApJ, 326, 680.

McCook and Sion, 1987, ApJS, 65, 603.

Morris S., Stocke J.T., Gioia I.M., Schild R.E., Wolter A., Maccacaro T., Della Cecca R., 1991, ApJ, submitted.

Nilsson, P. 1973, Uppsala General Catalogue of Galaxies. Uppsala Astron. Obs Ann. 6.

Plummer D., Schachter J., Garcia M., and Elvis M.. 1991, CD-ROM issued by

Smithsonian Astrophysical Observatory, Cambridge, MA.

Primini F.A., Murray S.S., Huchra J., Schild R., Burg R., and Giacconi R., 1991, ApJ, 374, 440.

Remillard R., *et al.* 1991, in preparation.

SAO Staff, 1966, "Star Catalog. Positions and Proper Motions of 258,997 Stars for the Epoch and Equinox of 1950.0", Pub. of the Smithsonian Institution of Washington, D.C. No. 4652 (Washington:Smithsonian Institution).

Schachter J., McDowell J.C., Plummer D., and Elvis M., 1991, BAAS, 22, 1195.

Schachter J., *et al.*, 1991, in preparation.

Schmidt M., 1990, in ***Imaging X-ray Astronomy***, ed. M. Elvis, [CUP, Cambridge], p. 201.

Schmidt M., and Green R.F., 1986, ApJ, 305, 68.

Schmidt M., and Green R.F., 1983, ApJ, 269, 352.

Shara, M. 1990, private communication.

Stocke J.T., Morris S.L., Gioia I.M., Maccacaro T., Schild R.E., and Wolter A., 1989, in ***BL Lac Objects***, eds. L. Maraschi, T. Maccacaro and M.-H. Ulrich [Springer-Verlag], p.242.

Struble, M. V., and Rood, H.J. 1987, ApJS, 63, 543.

Strassmeier, K. G., et al. 1988, A&A, 72, 291.

Sulentic, J. W. and Tifft, W. G. 1973, The Revised New General Catalogue of Nonstellar Astronomical Objects (Tucson: The University of Arizona Press).

Trümper J. *et al.* 1991, Nature, 349, 579.

Véron-Cetty M.-P. and Véron P., 1989, ***ESO Scientific Report No. 7.***

Wolter A., Gioia I.M., Maccacaro T., Morris S.L., and Stocke J.T., 1991, ApJ, 369, 314.

Woolley, R., Epps, E. A., Penston, M. J. and Pocock, S. B. 1970, Catalogue Stars within twenty-five parsecs of the Sun, Roy. Obs. Ann., No. 5.

Wood K.S., *et al.*, 1984, ApJS, 56, 507.

Figure Captions

Figure 1: Distribution of source fluxes from the Slew Survey (solid line) compared with those of the extended Medium Survey (dashed line; Gioia *et al.* 1989) and the Deep Survey (dotted line; Primini *et al.* 1991)

Figure 2: Exposure map for the Slew Survey in Galactic coordinates. Slew paths are readily seen going in great circles between the Ecliptic poles.

Figure 3: GX 5-1 (1ES1758-250) seen before (*a*) and after (*b*) Slew aspect was applied. Applying the slew aspect correction, which takes into account the motion of the satellite, produces a well-defined image (*b*). The background over the whole 1×1 degree field shown is 65 counts for an exposure of 14 seconds.

Figure 4: Fraction of the sky to a given exposure in the Slew Survey.

Figure 5: Initial offsets in arcminutes between Slew derived and accurate X-ray source positions for 172 known X-ray sources (Remillard *et al.* 1991; 2E Catalog) detected in individual slews.

Figure 6: (*a*) Offset in arcminutes (perpendicular to slew direction) between the Slew calculated position at the end of the slew and the accurate position from the pointed, star tracker, solution *vs.* slew length in degrees. The plot is for the data before the application of the correction made by rotating the assumed plane of the gyro assembly, and is for gyro combination B. The solid curve shows the size of the correction. (*b*) Offsets as in (*a*) after gyro orientation corrections.

Figure 7: (*a*) Offsets of Slew source positions from Bright Star Catalog identifications, in R.A. and Dec., after all aspect corrections are applied. (*b*) Offsets as in (*a*) but for an artificial set of Slew Survey sources created by shifting the real Slew Survey source by one degree in R.A.. This shows the background rate of identifications due to accidental matches of position. (*c*) Radial version of (*a*) with a heavy line marking the false identification background rate from (*b*) (*d*). Integrated histogram of (*a*) with the background from (*b*) subtracted.

Figure 8: Percolation algorithm flowchart.

Figure 9: Four typical regions of the Slew Survey exposure map. Each region is 30′ on a side, the size of background region 2, and is centered on a Slew source. (The 1ES name is given for each.)

Figure 10: Number of candidate sources with 1 photon detected by the percolation algorithm *vs.* Poisson probability, P_{rand}. The solid line shows the number expected assuming there are no real sources in the data. This is a reasonable approximation for three decades of P_{rand}.

Figure 11: Integral histogram of number of candidate sources with greater than or equal to 3 photons detected by the percolation algorithm *vs.* Poisson probability, P_{rand}. The solid line is the number expected if there were no real sources in the data.

Figure 12: Percentage of Total Candidate sources that are false sources *vs.* Poisson probability, P_{rand}. The false source fraction reaches ~2% at our threshold of $log\, P_{rand} = -3.95$.

Figure 13: Offset in arcminutes between the Slew source positions and the accurate positions of known X-ray sources (for objects in Remillard *et al.* 1991 and nonextended objects in the 2E catalog) *vs.* probability of a source arising by chance.

Figure 14: Fraction of Slew sources lying within 2′ of the position of a known X-ray source (for objects in Remillard *et al.* 1991 and nonextended objects in the 2E catalog) *vs.* probability of a source arising by chance.

Figure 15: The M81/M82 region showing how the high density of background photons confuses the percolation algorithm with the standard percolation radius of 2 arcminutes.

Figure 16: (*a*) Slew Survey count rate *vs.* ratio of Slew/Pointed IPC count rate ('2E'). (*b*) Slew Survey count rate restricted to PI 2-10 *vs.* ratio of Slew/Pointed IPC count rate ('2E').

Figure 17: Distribution of Slew Survey sources in Galactic coordinates. The concentration of sources at the Ecliptic poles ('NEP' and 'LMC'), where the Slew Survey exposure time is greatest, is clear.

Figure 18: Slew Survey image of the Cygnus Loop. The mean exposure time in this image is ~150 seconds. 108,000 photons are included in the image. The field shown is 4×4 degrees.

Figure 19: The region of the Slew Survey within 10 degrees of the North Ecliptic Pole. The exposure time ranges from ~100sec (North) to ~30sec (South) which leads to the variations in photon density seen in the image. The image is not exposure corrected. The two darkest areas are short segments of data from the very beginning or end of slews when the spacecraft is virtually stationary. The 21 Slew Survey sources are circled. (One source is almost hidden in the heavily exposed region to the lower right.)

Figure 1

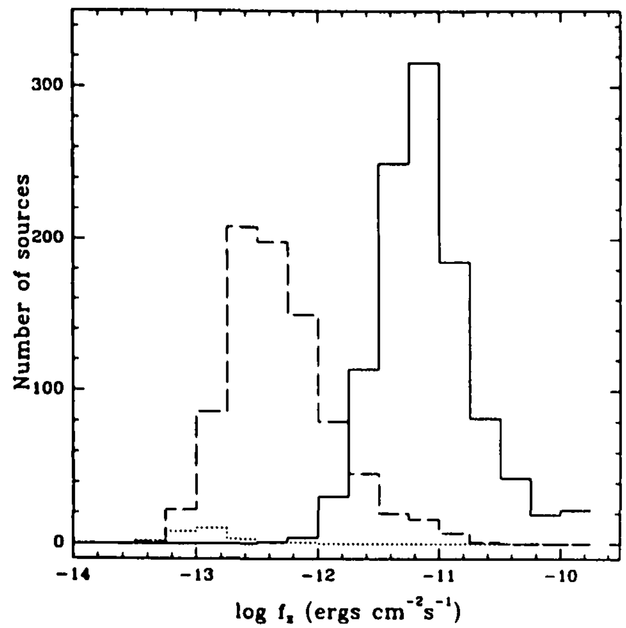

Figure 2

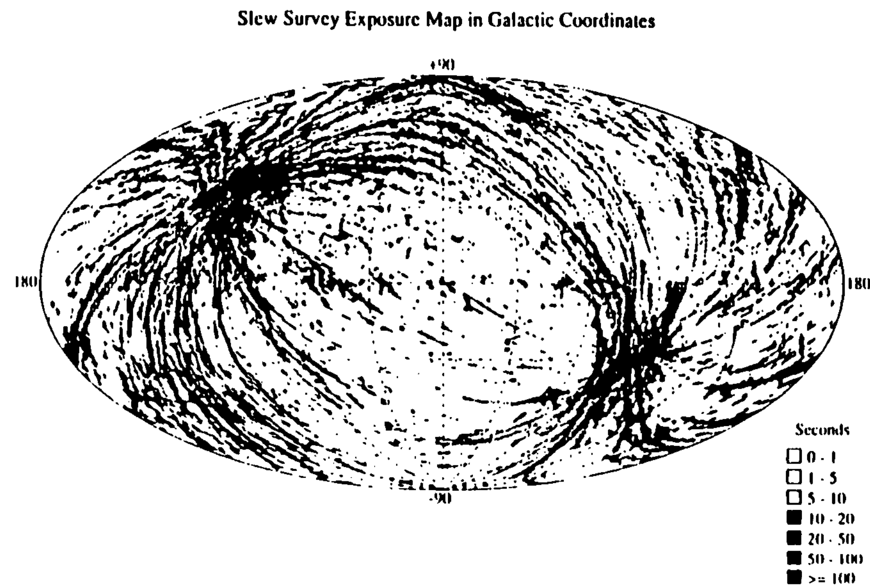

Figure 3a

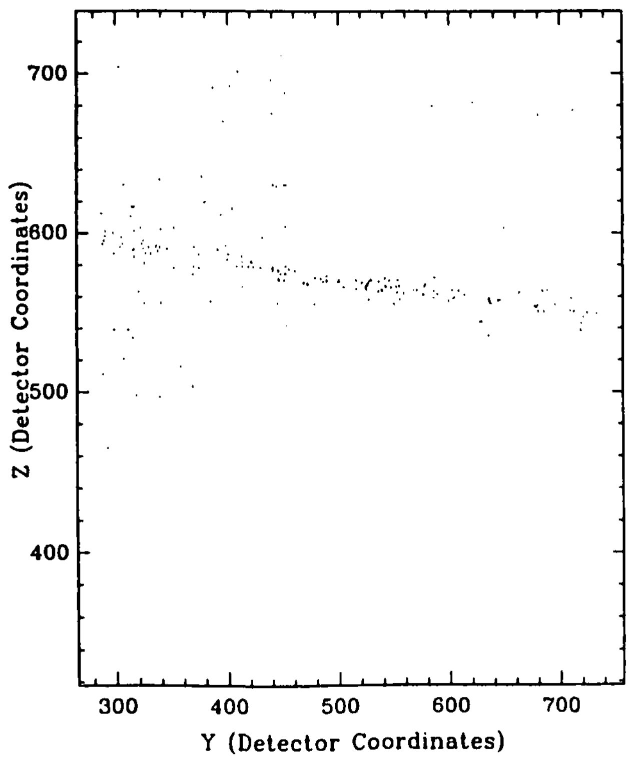

Figure 3b

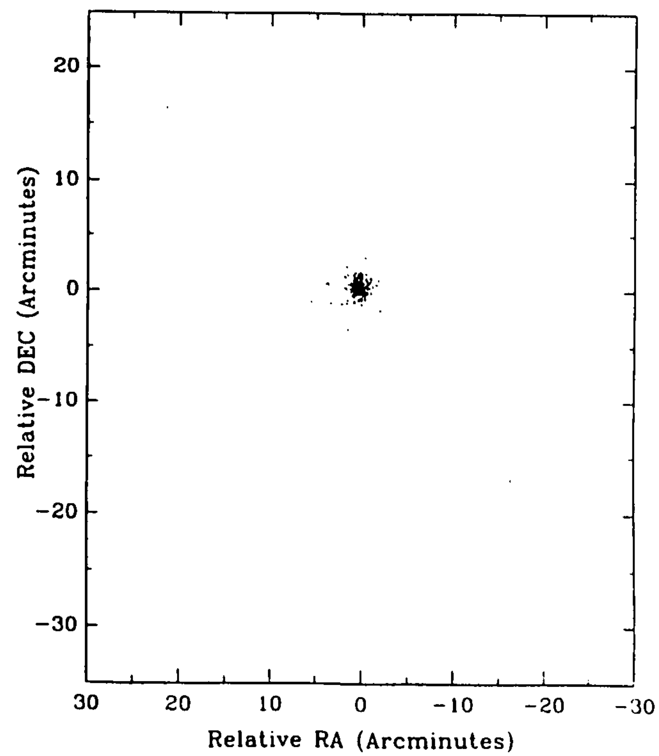

Figure 4

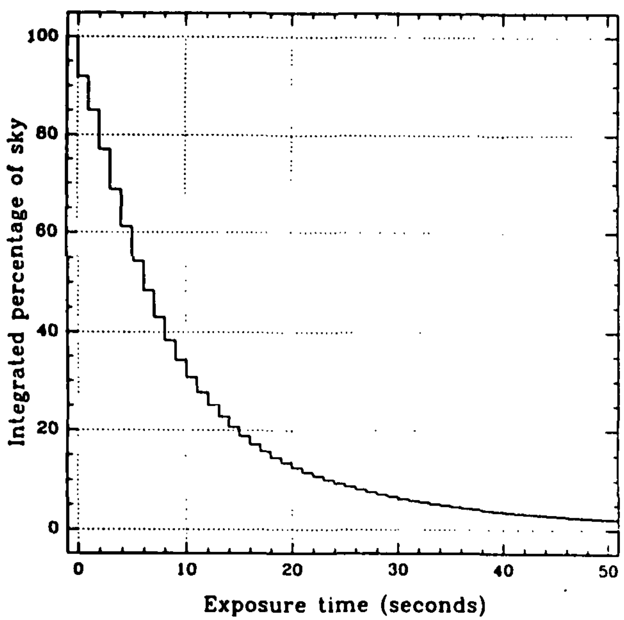

Figure 5

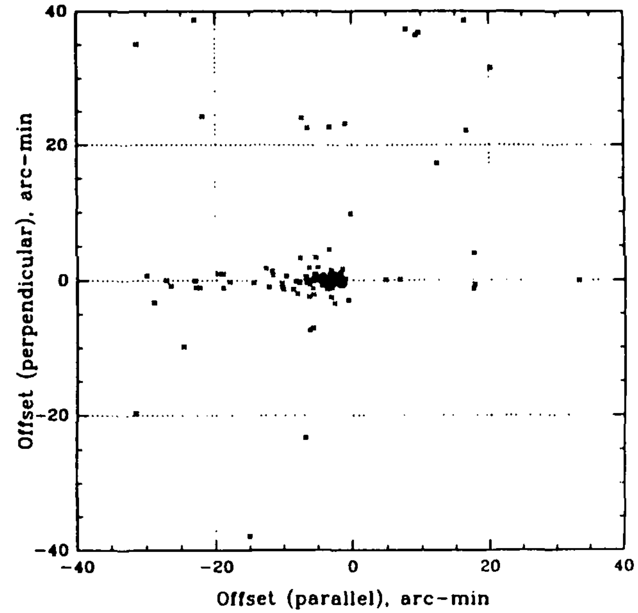

Figure 6a

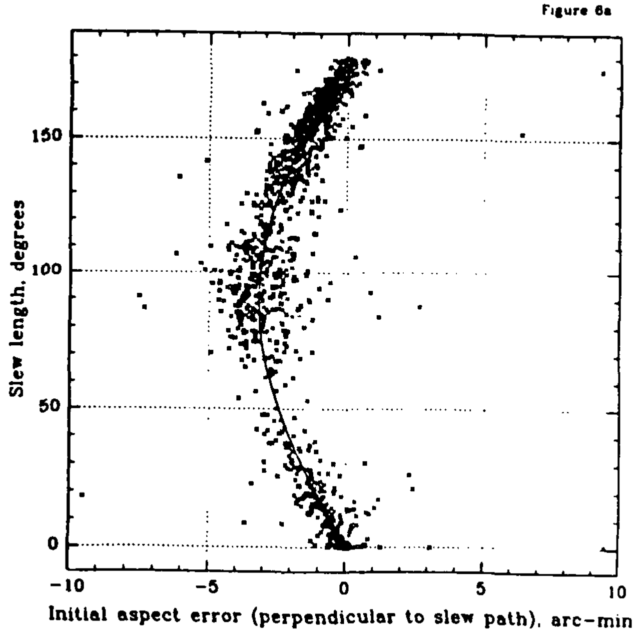

Figure 6b

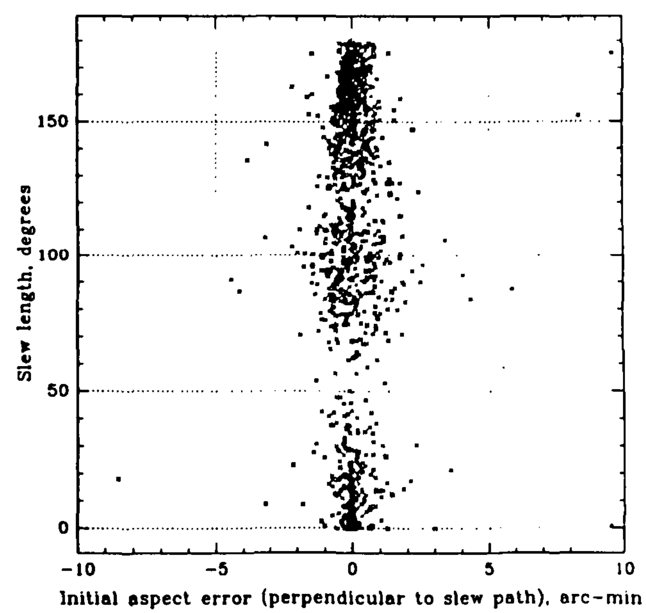

Figure 7a

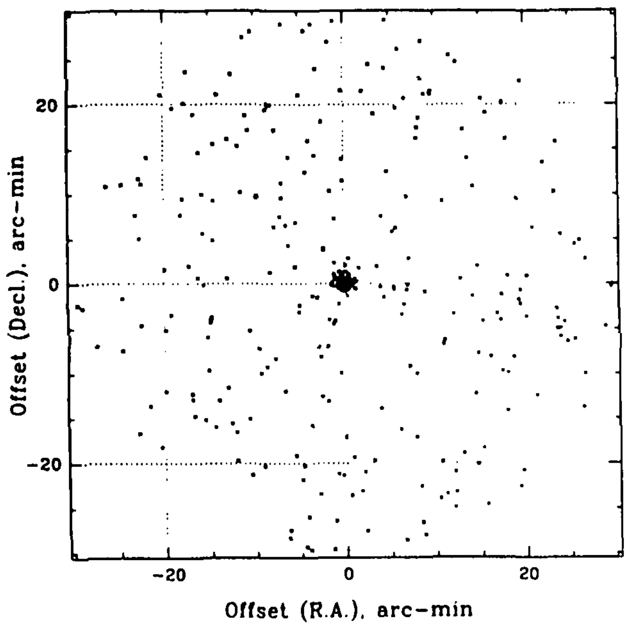

Figure 7b

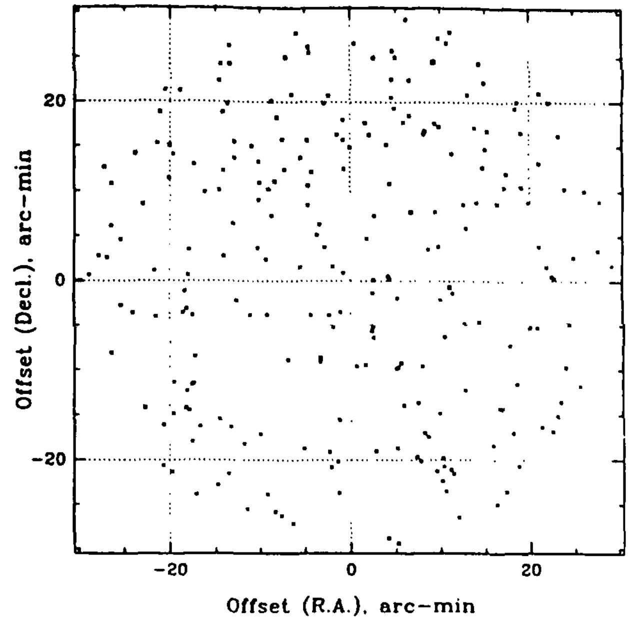

Figure 7c

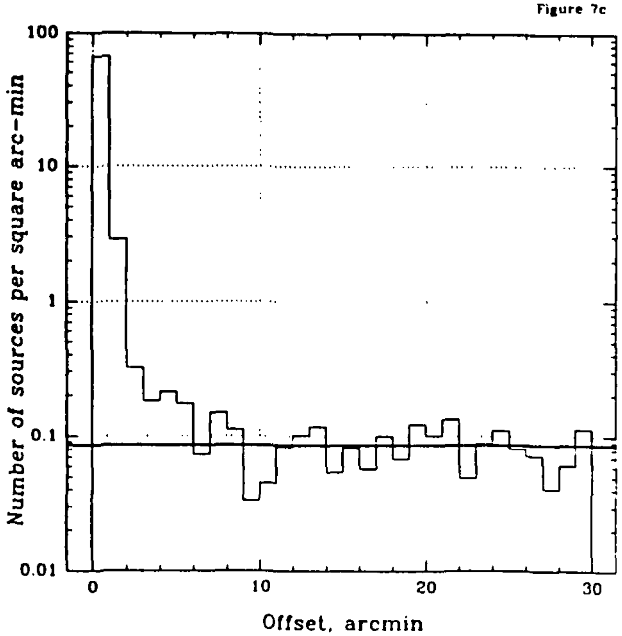

Figure 7d

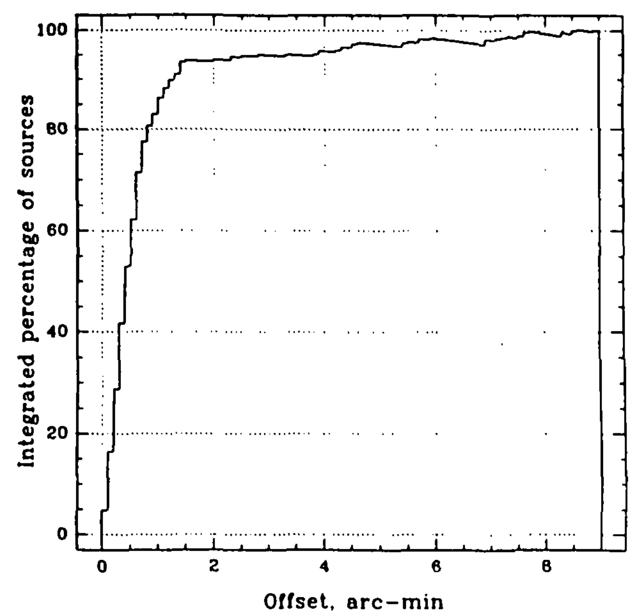

Figure 8

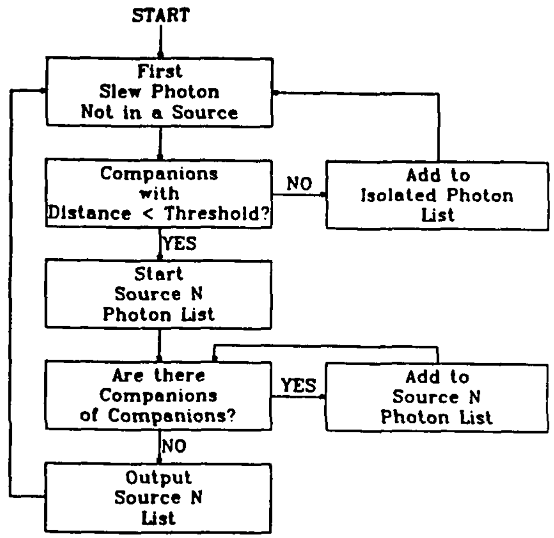

Figure 9

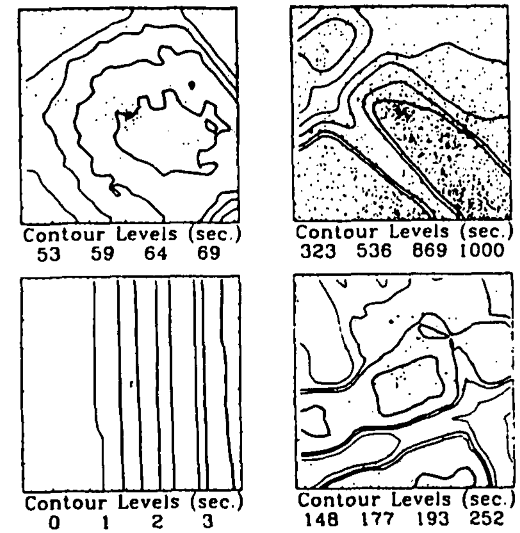

Figure 10

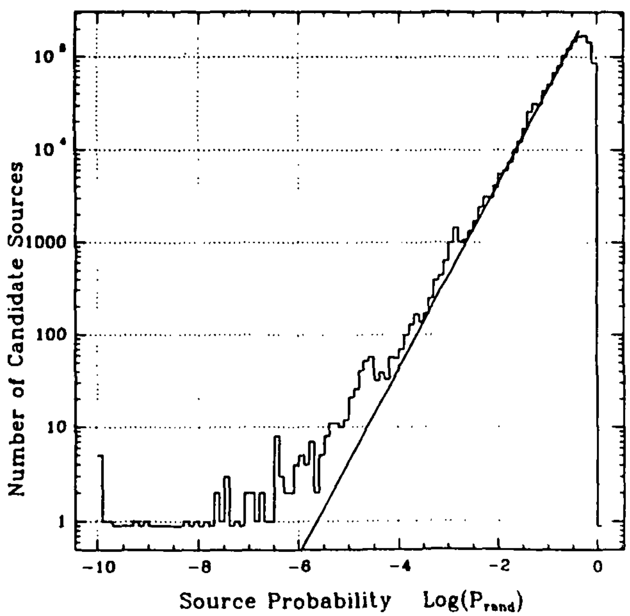

Figure 11

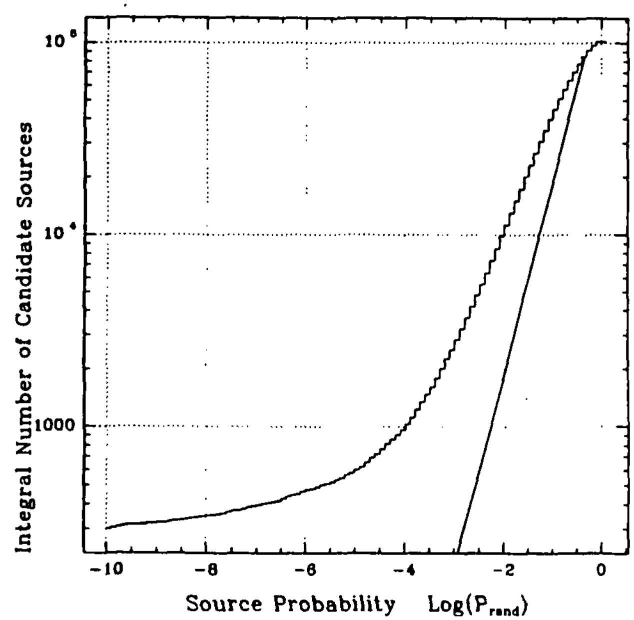

Figure 12

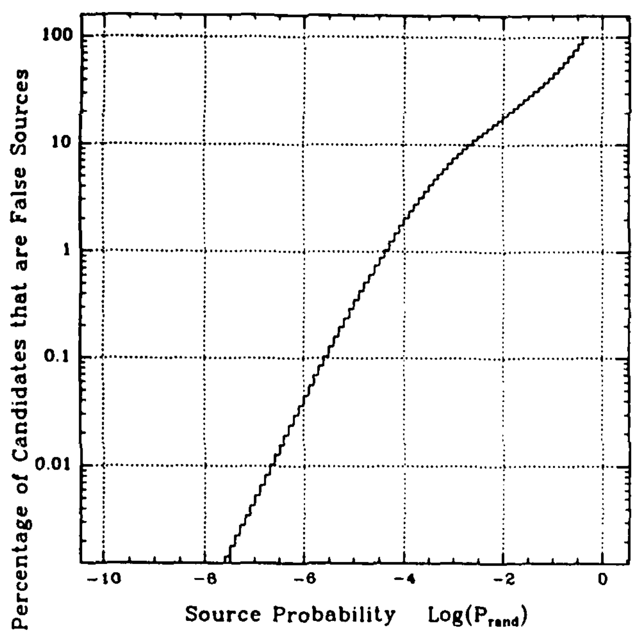

Figure 13

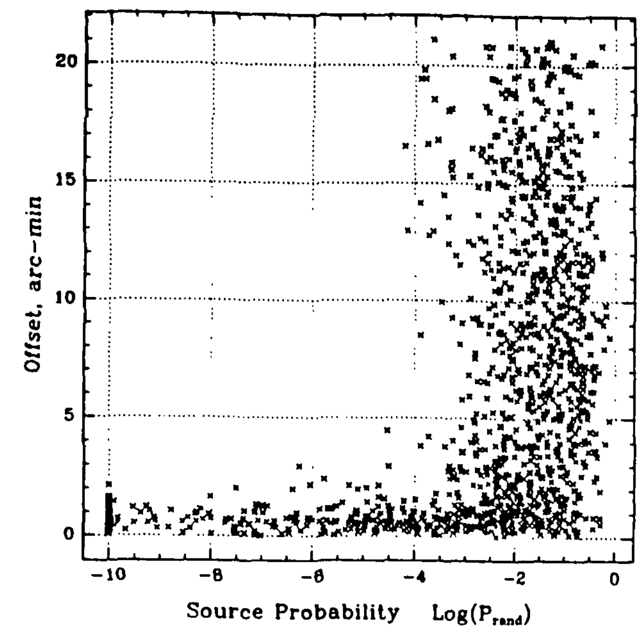

Figure 14

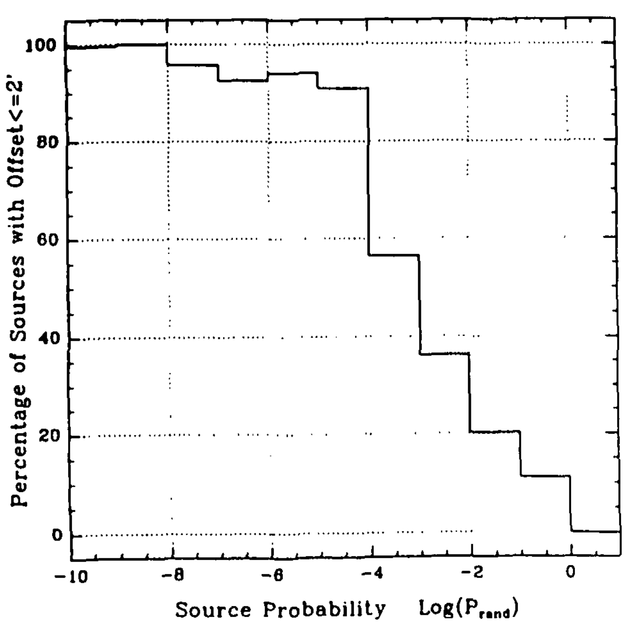

Figure 15

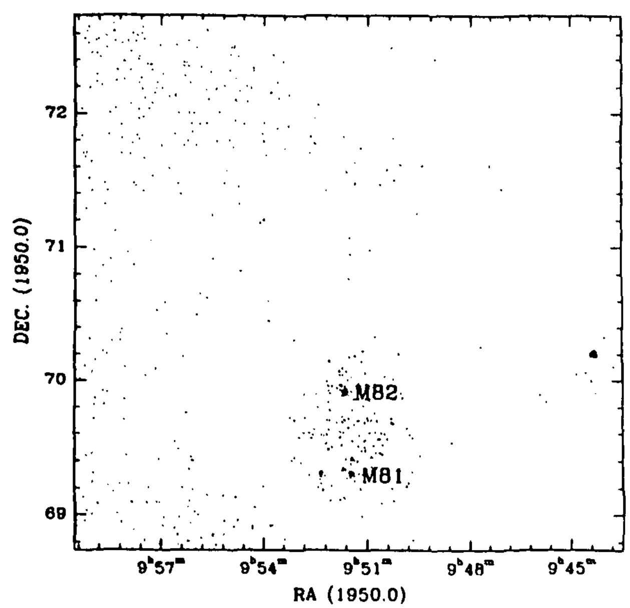

Figure 16a

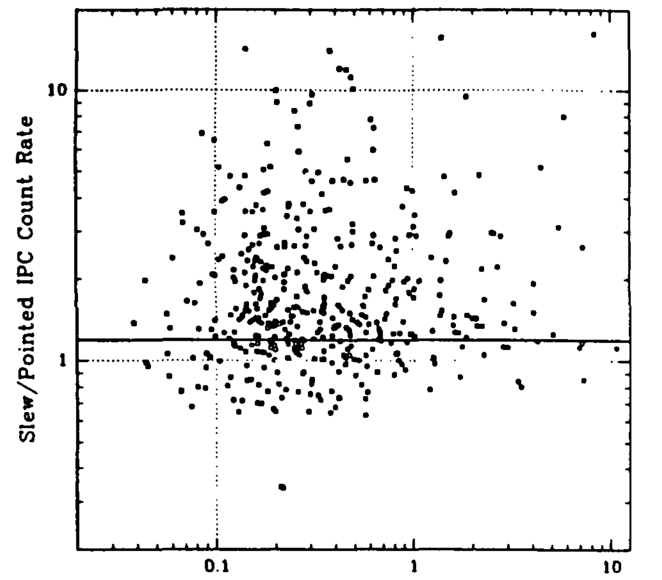

Figure 16b

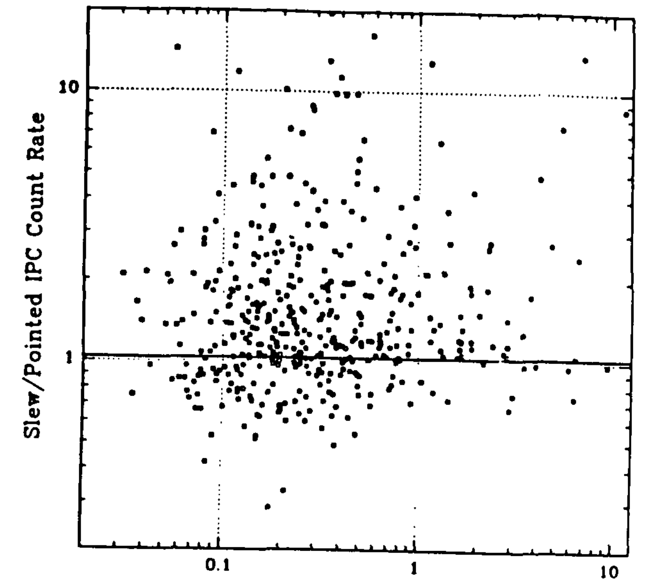

Figure 17

Slew Survey Source Distribution in Galactic Coordinates

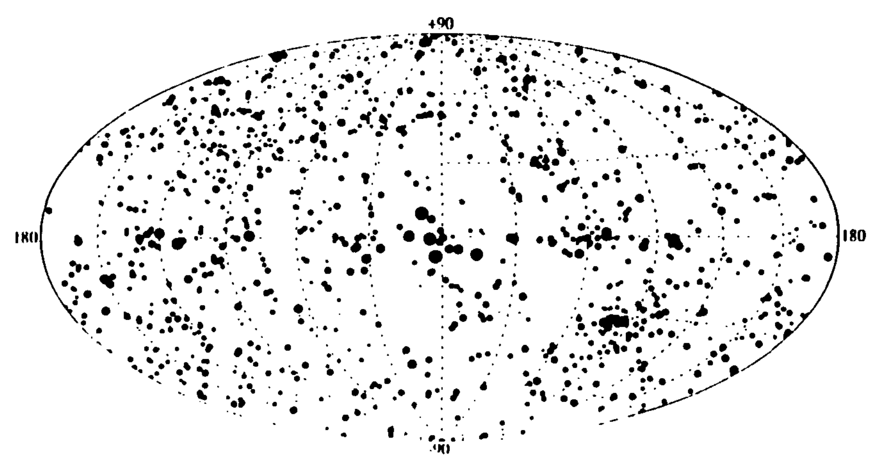

Figure 18

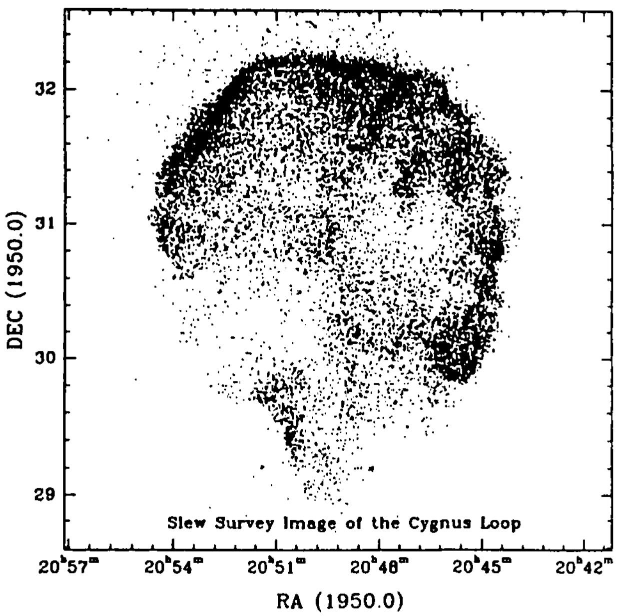

Figure 19

Slew Survey Image of the North Ecliptic Pole Region (10 Degree Radius)